UNIVERSITY POLITEHNICA of BUCHAREST

Doctoral School of Energy Engineering

ABSTRACT

DOCTORAL THESIS

Experimental studies on the operation and cavitational behaviour of parallel coupled, variable speed, centrifugal pumps

Author: ing. Petre-Ovidiu CIUC

PhD supervisor: Prof. dr. ing. habil. Sanda-Carmen GEORGESCU

Keywords:
cavitation, duty point, parallel coupling, pump shaft power,
pumping station, variable speed driven pump

2023

CONTENT

Preface	**1**
CAP. 1. Introduction	**3**
1.1. Structure of the doctoral thesis	3
1.2. The current state of research in the field of energy and cavitational operation of pumps	4
1.3. Problems in the operation of pumping stations caused by the hydraulic suction circuit of the pumps	9
1.3.1. Narrowing of the section of the suction line for connection to the pump suction flange	11
1.3.2. Existence of an elbow immediately upstream of the pump suction flange	14
1.4. Case study: Pumping station of the Seimenii Mici irrigation system (Constanța county)	18
1.4.1. Description of the studied system	18
1.4.2. Findings during the visit to SP Seimeni on 15 July 2016	23
1.4.3. Analysis of the operation of the Seimenii Mici irrigation system for the 2016 configuration	28
1.4.4. Findings during the visit to Seimeni SP on 20 September. 2017	29
1.4.5. Recommended measures to restore the Seimeni SP minimally invasive measures in relation to the initial configuration	32
1.4.6. Recommendations on how the Seimenii Mici irrigation system should work	34
1.4.7. Restoration of the Seimenii Mici pumping Station (May 2018)	35
CAP. 2. Design and execution of the experimental stand	**38**
2.1. Experimental stand in configuration from 2014-2017	38
2.1.1. Multi-stage centrifugal pump	42
2.1.2. Components and accessories of the Hydro-Unit Utility line pump station	43
2.1.3. Danfoss frequency converters (used in the period 2014÷2017)	45
2.1.4. Electric drive motor (three-phase asynchronous motor)	45
2.2. Description of the experimental stand designed and realized in 2018, within the doctoral thesis	47
CAP. 3. Automation and control of the experimental stand	**56**
3.1.Continuous adjustment of pump operation in pumping stations	56
3.2. Control and control of the pumping station	57
3.2.1. Pump station control	58
3.2.2. Components of the drive, measurement and control system	59
3.2.3. Automation control and control functions	62
3.2.4. Modes of operation of pumps	63
3.2.5. Automation panel operating interface	64
3.2.6. PLC specifications counting	67
CAP.4. Mathematical formulation of the studied problems	**71**
4.1. Measured parameters and calculated parameters	71
4.1.1. Measured parameters	71
4.1.2. Calculated parameters	76
4.2. Equation system describing system operation when prescribed pressure (PSP) refers to the	92

pressure indicated by the TR1 transducer on the discharge line in the pump station	
4.2.1. Where the monitoring node is TR1 and the stand operates without end consumers, with the VA and V1÷V3 valves in the normally open position	93
4.2.2. Where the monitoring node is TR1 and the stand operates without end-users, with the VA valve partially closed and the V1÷V3 valves in the normally open position	100
4.2.3. If the stand is operated without end-users, with the VA valve in the normally open position and the V1÷V3 valves partially closed	101
4.2.4. Where the monitoring node is TR1 and the stand operates without end consumers, with the VA and V1÷C3 valves partially closed	103
4.2.5. Where the monitoring node is TR1 and the stand operates with end consumers, WITH the VA and V1÷C3 valves partially closed	105
4.3. Equation system describing the operation of the system when prescribed pressure (PSP) refers to the pressure indicated by the TR2 transducer located on the discharge bus away from the pumping station, immediately downstream of the final consumers	108
4.3.1. Where the monitoring node is TR2 and the stand operates without final consumers	109
4.3.2. Where the monitoring node is TR2 and the stand operates with final consumers	111
4.4. Where the prescribed pressure (PSP) is set alternately, either in the TR1 monitoring node or TR2 monitoring node, for the same flow values (for the same positions of the VR valve and consumer taps)	116
4.4.1. Purpose of the study	116
4.4.2. Tandem operation with forced TR1 and calculated TR2	118
4.4.3. Tandem operation with forced TR2 and calculated TR1	119
CAP.5. Experimental study of the energetic and cavitational operation of pumps in the pumping station, without consumers, with prescribed pressure (PSP) at transducer TR1 in the pumping station	**121**
5.1. Types of experimental tests performed	121
5.2. Analysis and interpretation of the results obtained from the study, energy and cavitation operation of the pumps	123
CAP. 6. Comparative experimental study of the energy operation of pumps, controlled by prescribed pressure (PSP) maintained at discharge in the pump station (at TR1 pressure transducer) and away from the pump station (at TR2 pressure transducer)	**129**
6.1. Types of experimental tests carried out with prescribed pressure (PSP) set at TR1 and TR2 respectively	129
6.2. Analysis and interpretation of the results obtained from the study of the energy operation of pumps controlled by PSP set at TR1 and TR2 respectively	130
CAP.7. Conclusions	**137**
7.1. General conclusions on the results obtained	137
7.2. Original contributions	139
7.3. Research prospects	141
Bibliographic references	**142**
List of papers elaborated in the topic of the doctoral thesis	**158**
ANEXA A **ANEXA B**	

Preface

The doctoral thesis “Experimental studies on the energetic and cavitational functioning of variable speed centrifugal pumps coupled in parallel” contributes to improving the operation of pumping stations. The topic is of great interest in drinking water supply systems, as well as other hydraulic networks/systems in power plants and other industrial or irrigation objectives.

The chosen topic is not accidental: We identified the actuality of the topic and the opportunity to study it in the professional activity that I have been doing for over 15 years in energy engineering. I started my career in 2006, as an energy technician in the production and supply of electricity to a company in Câmpina, the main responsibility being the operation of micro hydropower plants. I then continued, until September 2010, as an electronics technician, in the manufacture of instruments and devices for measurement, verification and control at another company in Câmpina. After this first contact with the energy industry, in October 2010, I started my university studies at the Faculty of Energy at the University POLITEHNICA in Bucharest (UPB), where I graduated the Bachelor of Science in hydropower in July 2014. And in June 2016 I graduated from the Master’s degree program in Hydraulic technique and hydropower.

At the end of the third year of undergraduate studies, I did the 3-month internship at S.C. Multigama Tech s.r.l. in Bucharest, where I was initiated in the installation of pumps, revisions, repairs and maintenance of pumping equipment. After the internship, I continued the collaboration with the respective company, and since October 2014, I was hired as project manager at S.C. Multigama Tech. Since January 2016, I became a project manager at S.C. Multigama Service s.r.l. in Bucharest, a company where I still operate today, in the sector of pumping stations, water supply (drinking water, cooling water, technological water) and pumps in the energy and chemical industry. For more than 6 years, I have been responsible for maintenance contracts, I am in charge of organizing, planning and coordinating the entire process of commissioning and service/repair of pumps under warranty and post warranty, technical assistance and technical support, respectively I coordinate the work on the site.

Since October 2016, I became a PhD student at the UPB Doctoral School of Energy Engineering, under the guidance of prof. dr. eng. Sanda-Carmen Georgescu. In choosing the doctoral topic, I took into account the problems identified so far in the pumping stations in the country, namely the concrete situations encountered in situ, namely the fact that many pumping stations are misdesigned, the pumps do not operate at the designed capacity and/or cavitate, the pumps are incorrectly fitted and the electricity consumed for pumping is far too high. We have also encountered totally unfavorable situations in which the pumps are incorrectly mounted in the installation and, in addition, work with cavitation, which leads very quickly to vibration amplification and destruction of the bearings and rotors of the pumps.

Therefore, based on professional concerns at work, I chose to study at the PhD the energetic and cavitational operation of variable speed centrifugal pumps coupled in parallel, this coupling mode being the most used in pumping stations.

In order to justify the importance of the chosen theme, in the introductory part of the thesis, we presented in detail a case study, corresponding to the irrigation pumping station from Seimenii Mici (north of Cernavoda) – a modern pumping station, put into operation in 2015, respectively completely destroyed in 2017, due to poor design, but also to the ignorance of the operating staff.

For the study of the energetic and cavitational operation of pumps, we designed, built and commissioned an experimental stand in the Laboratory of Hydraulic machines (room Ela 022) in the Department of Hydraulics, Hydraulic machines and Environmental Engineering, UPB. The main components of the stand were obtained through sponsorship from companies, Multigama Tech, Multigama Service and Valrom.

I emphasize that I have conducted this experimental stand and have conducted all the experimental trial campaigns in collaboration with my colleague, PhD. Remus Alexandru Mădularea, who also completed his doctoral thesis [*Mădularea, 2023*] under the guidance of Professor Georgescu. The two doctoral theses were carried out in parallel and completed each other, so each thesis contains different sets of experimental trials, as appropriate, with or without the corresponding numerical modeling.

As I will show in this doctoral thesis, the experimental stand made allows the performance of the energy and cavitational tests of 3 multi-stage centrifugal pumps, driven with variable speed, coupled in parallel in a pumping station framed in a closed circuit hydraulic installation. In order to simulate the operation of the stand under a variable water requirement, we have provided and installed 3 final consumers on the discharge circuit of the pumping station. The experimental stand was equipped with measuring devices and an automation and control panel with HMI (Human Machine Interface). The stand control has been designed within the thesis to enable the operation of the pumps in the pump station (start/stop and change in their speed) to be controlled according to the pressure level recorded in one of the two monitoring nodes provided on the discharge bus, namely: a node located at the outlet of the pumping station, i.e. a node located at a distance from the pumping station, immediately downstream of the final consumers.

In the doctoral thesis, through the experimental study undertaken on the above-mentioned stand, I highlighted the influence of the suction circuit on the proper functioning of a pumping station that supplies a water supply network. Thus, we analyzed the problems that the energy and cavitational operation of variable speed turbo pumps puts in the operation of pumping stations and made conclusions about improving their operation.

1. Introduction

1.1. Structure of the doctoral thesis

The topic of this doctoral thesis is aimed at improving the operation of pumping stations, the focus being on avoiding cavitation (or diminishing the effects of cavitation), respectively on reducing the consumption of electricity for pumping. As will be shown below, the conclusions can be applied mainly in drinking water supply systems, but can also be extended to irrigation hydraulic circuits/systems, power plants, and other industrial objectives.

The thesis is structured in 5 chapters, the content of which is outlined in Figure 1.1. At the end of the thesis are the general conclusions and perspectives of the research, the list of original contributions, as well as the list of bibliographic references.

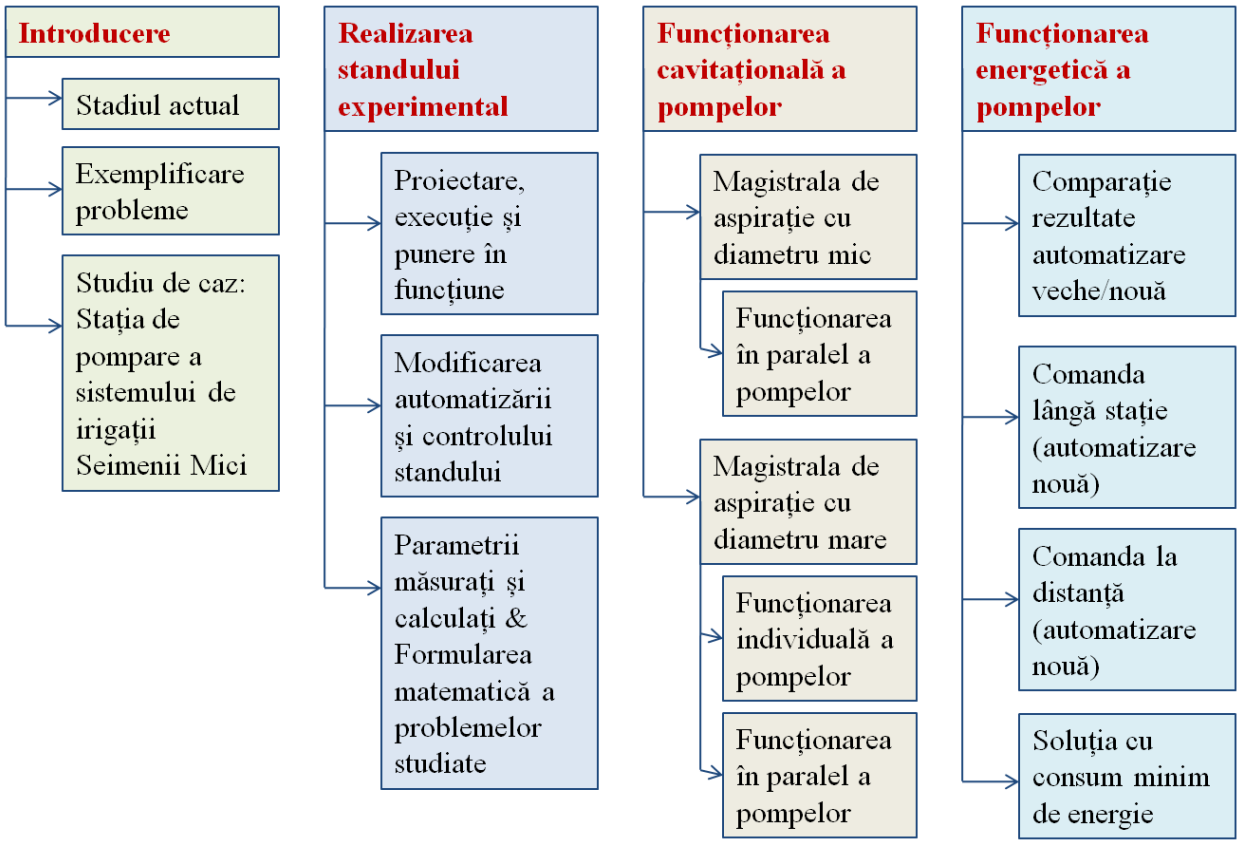

Fig. 1.1. Content of the doctoral thesis

1.2. The current state of research in the field of energy and cavitational operation of pumps

In this chapter we analyzed the current state of research in the field of energy and cavitational operation of pumps, according to the following 10 criteria of study differentiation:

- **A1**. Cavitation operation of the pump/pumps (blue background) | or operation with air in the installation (yellow background);
- **A2**. Cavitation-free operation of the pump/pumps;
- **A3**. The pump(s) operate at constant speed;
- **A4**. The pump(s) operate at variable speed;
- **A5**. Only one pump is installed in the installation;
- **A6**. The pumps are coupled in parallel;
- **A7**. The application refers to an experimental pumping installation;
- **A8**. The application refers to pumping stations from water supply systems or irrigation;
- **A9**. Theoretical study (mathematical modeling) and/or use of specialized software;
- **A10**. Method/strategy for regulating (controlling) the operation of the pumps.

Table 1.1 lists the relevant works that I have identified in the literature and which I have managed to access for each work, the met criteria are marked, among the ones listed above: **A1÷A10.**

Table 1.1. Summary of the content of selected bibliographic references

Nr. crt.	**Reference cited** [author, year of publication]	**A1**	**A2**	**A3**	**A4**	**A5**	**A6**	**A7**	**A8**	**A9**	**A10**
1	*Al-Arabi, 2010*	x	x	x		x		x			
2	*Al-Arabi & Alsalmi, 2017*	x		x			x	x			
3	*Al-Arabi & Selim, 2009*	x			x	x		x			
4	*Al-Hashmi, 2008*	x		x		x		x			
5	*Al-Hashmi et al., 2004*	x		x		x		x			
6	*Al-Obaidi, 2019*	x	x	x		x		x			
7	*Anton Alin et al., 2019*		x	x		x		x		x	
8	*Azizi et al., 2018*	x	x	x		x		x			
9	*Berardi et al., 2015a*		x	x	x		x		x	x	x
10	*Berardi et al., 2015b*		x	x	x		x		x	x	x
11	*Berardi et al., 2018*		x	x	x		x		x	x	x
12	*Birajdar et al., 2009*	x	x			x		x			
13	*Borges G., 2012*		x	x		x			x		
14	*Brennen, 2016*	x			x	x					
15	*Brennen & Braisted, 1980*	x						x			
16	*Briceño et al., 2019*		x	x	x		x		x	x	x
17	*Briceño-León et al, 2021*		x	x	x		x		x	x	x
Nr.	**Reference cited** [author,	**A1**	**A2**	**A3**	**A4**	**A5**	**A6**	**A7**	**A8**	**A9**	**A10**

crt.	year of publication]										
18	*Brogan et al, 2016*		x		x		x	x			x
19	*Capponi et al, 2014*		x		x		x		x		
20	*Chini et al, 2005*	x		x		x		x			
21	*Chudina, 2003*	x		x		x		x			
22	*Cimorelli et al, 2020*		x	x	x		x		x		
23	***Ciuc, 2014***		x	x	x	x	x	x			x
24	***Ciuc, 2016***		x	x	x	x	x	x		x	x
25	*Cowan et al, 2013*	x		x		x		x		x	
26	*Dadar et al, 2021*		x						x	x	
27	*Darweesh, 2018*		x	x	x	x		x		x	
28	*de Abreu Costa et al, 2018*		x		x	x		x		x	
29	*Dong et al, 2019*	x		x		x		x			
30	*Drăghici et al, 2017*	x			x	x		x			
31	*Drăghici et al, 2016*	x			x	x		x			
32	*Dunca et al, 2008*		x	x		x		x			
33	*Fu et al, 2015*	x		x		x		x		x	
34	*Georgescu A.-M., 2017*		x	x		x			x	x	
35	*Georgescu A.-M. et al, 2014a*		x		x	x	x	x		x	
36	*Georgescu A.-M. et al, 2015*		x	x	x	x				x	
37	*Georgescu A.-M. et al, 2007*		x		x		x		x	x	
38	*Georgescu A.-M. et al, 2014c*		x		x		x		x	x	x
39	*Georgescu A.-M. et al, 2017*		x		x		x		x	x	x
40	*Georgescu S.-C. & Georgescu A.-M., 2015*		x		x		x	x		x	
41	*Georgescu S.-C. et al, 2015*		x	x	x		x		x	x	x
42	*Georgescu S.-C. et al, 2010*		x	x			x	x		x	
43	*Giustolisi et al, 2016*		x	x			x		x	x	x
44	*Giustolisi et al, 2011*		x	x	x	x	x		x	x	
45	*Giustolisi et al, 2008*		x	x		x	x		x	x	
46	*Giustolisi & Walski, 2012*		x					x	x	x	
47	*Gomes et al, 2011*		x					x	x	x	
48	*Guo et al, 2021*	x	x	x		x		x			
49	*Guo et al, 2020*		x		x	x		x		x	
50	*Gupta et al, 2013*	x			x	x		x			
51	*Horowitz et al, 2006*		x	x	x	x	x	x		x	x
52	*Jensen & Dayton, 2000*	x		x		x		x			
53	*Kaya & Ayder, 2017*	x		x		x		x		x	
54	*Kotb & Abdulaziz, 2015*	x	x		x	x		x		x	
55	*Lamaddalena & Khila, 2012*		x		x		x		x		x
56	*Laucelli et al, 2016*		x	x	x		x		x	x	x
57	*Li & Baggett, 2007*		x		x		x		x	x	x
58	*Loucks & van Beek, 2017*		x							x	
59	*Mahaffey & van Vuuren, 2014*	x								x	
Nr.	**Reference cited** [author,	**A1**	**A2**	**A3**	**A4**	**A5**	**A6**	**A7**	**A8**	**A9**	**A10**

crt.	year of publication]										
60	*Maksimovic & Masry, 2009*		x						x	x	
61	*Marchi et al, 2012*		x	x	x	x			x	x	
62	*Menke et al, 2016*		x	x	x		x		x	x	x
63	*Mishra et al, 2020*								x	x	
64	*Moradi-Jalal et al, 2003*		x	x			x		x	x	
65	*Mousmoulis et al, 2019*	x		x		x		x			
66	*Muranho et al, 2014*		x	x			x		x	x	
67	*Ng & Brennen, 1978*	x	x	x		x		x			
68	*Oikonomou et al, 2018*		x						x	x	
69	*Page et al, 2017*		x		x	x			x	x	x
70	*Page et al, 2019*		x		x	x			x	x	x
71	*Pîrăianu et al, 2016*		x	x			x		x	x	
72	*Pothof & Clemens, 2011*	x		x		x		x		x	
73	*Pothof & Clemens, 2012*	x		x		x		x		x	
74	*Pothof & Karney, 2012*			x		x		x		x	
75	*Ross, 2023*		x						x		
76	*Rossman, 2000*		x	x	x	x	x	x	x	x	
77	*Rossman et al, 2020*		x	x	x	x	x	x	x	x	
78	*Salvadori et al, 2012*	x		x		x				x	
79	*Salvadori et al, 2015*	x		x		x		x		x	
80	*Sethi & Di Molfetta, 2019*		x						x	x	
81	*Shankar et al, 2021*		x		x		x	x		x	
82	*Shi, 2013*		x							x	x
83	*Sloteman, 2007*	x		x		x		x			
84	*Sreedhar et al, 2017*	x		x		x		x			
85	*Świętochowska & Bartkowska, 2022*		x						x	x	x
86	*Tanyimboh & Templeman, 2004*		x	x		x				x	
87	*Thornton & Lambert, 2006*		x							x	x
88	*Todini, 2011*		x							x	
89	*Todini et al, 2007*		x		x		x		x	x	
90	*Trifunović, 2006*		x							x	
91	*Van Bennekom et al, 2001*		x			x					
92	*Zhang L. & Zhuan, 2019*		x		x		x		x		
93	*Zhang Z. et al, 2020*	x		x		x		x			
94	*Wagner et al, 1988*		x			x				x	
95	*Wu et al, 2009*		x	x	x	x	x		x	x	x
	Total work on criteria	**32**	**70**	**55**	**41**	**53**	**35**	**47**	**40**	**62**	**23**
	Percentage [%] per criterion of the total of 91 works	**34**	**74**	**58**	**43**	**56**	**37**	**49**	**42**	**65**	**24**

Table 1.1. it contains 95 scientific papers, which we have selected and analyzed, the subjects treated in them being directly or related to the topic of the doctoral thesis.

A number of 32 works correspond to criterion **A1** (pump/pump cavitation operation | air operation in the installation), of which,

- **21 works strictly treat the cavitation operation of the turbopomps, and of these:**
  - Only 5 works refer to variable speed pumps (criterion A4) [Al-Arabi & Selim, 2009; Gupta et al, 2013; Brennen, 2016; Drăghici et al, 2016; Drăghici et al, 2017], The remaining 16 works addressing strictly the case of constant speed pumps (criterion A3);
  - Only one paper studies the cavitation operation of parallel coupled pumps (criterion A6) [Al-Arabi & Alsalmi, 2017], i.e. with constant pump speed (A3) drive; The remaining 20 works refer strictly to the isolated operation of the studied pump (criterion A5), and 5 of these 20 studies correspond to the variable speed pumps (A4) cited above;
  - 20 of the 21 works refer to the cavitational operation of pumps in experimental pumping facilities (criterion A7), and 4 of the 20 also contain theoretical study (criterion A9); a single work (Salvadori et al, 2012) is strictly theoretical (A9);
- **7 works deal with the energetic and cavitational functioning of the turbopomps**, with an emphasis on cavitation operation (Ng & Brennen, 1978; Birajdar et al., 2009; Al-Arabi, 2010; Kotb & Abdulaziz, 2015; Azizi et al., 2018; Al-Obaidi, 2019; Guo et al, 2021]; all these 7 studies refer to the isolated operation of pumps (criterion A5) in experimental pumping facilities (A7); One work (Kotb & Abdulaziz, 2015) refers to variable speed driven pumps (A4), and the other 6 works refer to constant speed driven pumps (A3); a single work (Kotb & Abdulaziz, 2015) also contains a theoretical part (criterion A9);
- **4 works deal with air operation in the installation,** namely: A theoretical study (criterion A9) is related to air accumulation on the pipe section connected to the pump suction flange (Mahaffey & van Vuuren, 2014), 2 studies address both theoretical (A9) and experimental air accumulation (Air bags) in sloping pipes (water supply, wastewater transport) and in soda pipes (Pothof & Clemens, 2011; Pothof & Clemens, 2012], respectively, a study experimentally treats the air drive in vertical axis pumps, through the vortex formed between the free surface of the water in the tank and the pump suction (Zhang Z. Et al, 2020]; the 3 experimental studies cited were conducted in experimental pumping facilities (criterion A7), equipped with a single pump (A5) operated with constant speed (A3).

A number of 70 works correspond to criterion **A2** (pump/pump cavitation-free operation), of which 63 works strictly treat the energy operation of the turbopomps, and 7 works also contain cavitational operation, corresponding to criterion **A1** (these have been analyzed and cited previously). **Of the 59 remaining works,**

- 41 works refer to **variable speed** pumps (criterion **A4**) and 19 of them consider the case of constant speed pumps (criterion **A3**); 12 works strictly address the case of constant speed pumps (**A3**); 12 of the 59 works do not mention anything about the pump/pump speed, so it can be added (by default) to criterion **A3**;
- 35 works study the energy operation of parallel coupled pumps (criterion **A6**), and 9 of them also refer to the isolated operation of the studied pump (criterion **A5**); 15 works refer strictly to the isolated operation of the studied pump (**A5**); 14 of the 63 works do not mention the operation of the pump/pumps;

- 40 works refer to the operation of pumps in **pumping stations** (criterion **A8**), and 4 of them also refer to experimental pumping plants (**A7**); 14 works refer strictly to the operation of pumps in experimental pumping plants (**A7**); From a hydraulic system point of view, 9 of the 63 works do not comply with criteria **A7**|**A8**;
- Of the 18 works based on **experimental pumping installations** (**A7**), 15 works also contain mathematical modeling (criterion **A9**), and 4 of them also mention the **method of regulating the operation of pumps** (criterion **A10**);
- Of the 36 works based on **pumping stations** (**A8**), 31 works also contain mathematical modeling (**A9**), and 16 of the 36 also mention the **method of regulating pumps** (**A10**).

Among the 63 works analyzed above, which correspond to criterion **A2** (pump/pump cavitation-free operation), we identified **28 studies related to the energy operation of parallel coupled pumps** (criterion **A6**) and **variable speed driven pumps** (criterion **A4**). **Of these 28 studies,**

- 16 studies consider the **constant speed pump drive** (**A3**);
- 21 studies refer to **pumping stations** (**A8**), and of these, 2 studies also contain experimental installation (**A7**); 19 of the 21 studies corresponding to criterion **A8** also contain mathematical modeling (**A9**); 13 out of the 21 studies corresponding to criterion **A8** also mention the **method of regulating the operation of pumps** (**A10**); the 2 studies attached to criterion **A7** do not correspond to criterion **A10**;
- 7 studies refer strictly to **experimental pumping installations** (**A7**), and of these, 5 studies also contain mathematical modeling (**A9**); 2 of the last 5 studies also mention the **method of regulating the operation of pumps** (**A10**).

In this thesis, the chosen topic mainly covers the following combination of criteria: Cavitational (criterion **A1**) and/or energetic operation (criterion **A2**) of parallel coupled turbopomps (criterion **A6**), variable speed driven (criterion **A4**), mounted in experimental pumping facilities (criterion **A7**) or in pumping stations (criterion **A8**), studied including theoretically (Criterion **A9**) or ordered based on a method/strategy of regulation (criterion **A10**). **The combination of the above criteria** can be expressed using the logical operators as follows: **A1**|**A2** & **A4** & **A6** & **A7**|**A8** & **A9** & **A10**.

Among the 32 jobs that correspond to criterion **A1**, we have **not identified any studies related to cavitation operation of parallel coupled** (**A6**) variable speed (**A4**) pumps. We have identified **only one work** [Al-Arabi & Alsalmi, 2017] in which the pumps operate **parallel coupled** (**A6**) **with constant speed** (**A3**). Moreover, none of the work in criterion **A1 refers to pumping stations** (**A8**), respectively **none mentions any method/strategy for regulating the operation of pumps** (**A10**).

Among the 63 works that strictly deal with the energy operation of the turbopomps (criterion A2), we identified 17 works in which the pumps are coupled in parallel (A6) and are driven with variable speed (A4) based on a method/strategy of regulation (A10), of which,

- **13 works** [*Li & Baggett, 2007; Wu et al, 2009; Lamaddalena & Khila, 2012; Georgescu A.-M. et al, 2014c; Georgescu S.-C. et al, 2015; Berardi et al., 2015a; Berardi et al., 2015b;*

Laucelli et al, 2016; Menke et al, 2016; Georgescu A.-M. et al, 2017; Berardi et al., 2018; Briceño et al., 2019; Briceño-León et al, 2021] it refers to **pumping stations** (**A8**);

- **4 works** [*Horowitz et al, 2006;* ***Ciuc, 2014****; Brogan et al, 2016;* ***Ciuc, 2016***] it refers to **experimental pumping facilities** (**A7**).

Of the total of 17 works cited above, **12 works consider both variable speed drive** (A4) **and constant speed pump drive** (A3), so only 5 works [*Li & Baggett, 2007; Lamaddalena & Khila, 2012; Georgescu A.-M. et al, 2014c; Brogan et al, 2016; Georgescu A.-M. et al, 2017*] falls strictly to criterion A4.

I would like to mention that 2 of the above mentioned works belong to me **[*Ciuc, 2014 & 2016*].** These are the projects for completing the studies, which we have carried out for the bachelor's degree (in 2014) and for the dissertation (in 2016). Both projects were based on an experimental stand that we made and put into operation in 2014, in the Laboratory of Hydraulic machines in UPB, which we upgraded later, in April 2016.

Following the bibliographic analysis undertaken on the basis of the 95 papers cited in Table 1.1, **it appears that the topic addressed in this doctoral thesis is not covered in these specialized works on the cavitational operation of parallel coupled pumps, the theme is insufficiently covered on the energy operation of parallel coupled pumps, ordered based on a method or strategy for regulating their operation** (17 works represent less than **19%** of the total of 91 works analyzed).

Moreover, **none of the 95 works analyzed simultaneously deals with both aspects of the operation of parallel coupled pumps, namely energy and cavitation operation**. It is clear that both aspects must be taken into account simultaneously in order to achieve the correct operation of the existing pumping stations in water supply systems, irrigation, cooling water, technological water circuits, etc. in industry. From this point of view, I believe that this thesis makes a positive contribution in the field studied.

1.4. Case study: Pumping station of the Seimenii Mici irrigation system (Constanța county)

In this section, the incorrect design of a pumping station was exemplified by a case study, both on the suction and discharge side, which led to the destruction of the pumping station less than a year and a half after its commissioning **[*Georgescu S.-C. et al (Ciuc), 2017b*]**. The case study presented below refers to the pumping station of the Seimenii Mici irrigation system in Constanta County (about 6 km north of Cernavoda town), a semi-buried pumping station with a dry chamber, equipped with 4 single-stage centrifugal pumps, coupled in parallel, driven with variable speed. The pumping station (hereinafter SP Seimeni) is part of the irrigation system of agricultural land in the area: The station is supplied with water from the Danube through a suction line of about 2.5 km; the discharge bus leads the water to an irrigation system (branched network) with 10 central pivots, arranged so as to cover as large an irrigable area as possible.

The total (cumulative) length of the sections of the branched network between the Seimeni SP and the central pivots is about 13.4 km. A maximum of 3 of the 10 pivots can operate simultaneously [***Georgescu A.-M. et al (Ciuc), 2018***; *Mădulărea, 2022*].

2. Design and execution of the experimental stand

2.1. The experimental stand in the configuration from 2014÷2017

In the spring of 2014, at the Laboratory of Hydraulic machines (room ELA022) in UPB, we made and put into operation the experimental stand in figure 2.1 [Ciuc, 2014]. The basic component of the experimental stand in Figure 2.1 was the pressure lift system called Hydro-Unit Utility line [DP pumps, 2012], produced by DP Pumps of the Netherlands (part of KSB Germany). This pumping station (hereinafter: SP) is equipped with 3 variable speed driven pumps coupled in parallel by steel pipes and fittings. The cold water supply was made in a closed circuit from a constant level tank, open at atmospheric pressure. In the stand in Figure 2.1, the water tank was connected to the SP by pipes and fittings made of white PPR (pipes were very short in length); a flow control valve was mounted on the discharge pipe before entering the tank; there was also an insulation valve on the suction line, kept in the normally open position.

Fig. 2.1. The experimental stand configuration during the period 2014÷2017

In 2016, we modernized the experimental stand in Figure 2.1 [Ciuc, 2016]: More specifically, we installed display interfaces on the Danfoss frequency converters [Danfoss, 2012], which allowed the development of the research [Dunca, Ciuc et al, 2017]. From 2014 to 2017, the Hydro-Unit Utility line pump station remained connected to the hydraulic system with the very short suction/discharge route in Figure 2.1.

As will be shown in section 2.2, starting with 2018, the pumping station has been connected to a new closed-circuit hydraulic installation (designed and carried out within the doctoral thesis), with a long length of the suction/discharge route - a downstream installation with three final consumers.

The supply tank, designed and made in 2014 (Ciuc, 2014) (figure 2.2), was also used in the new experimental stand, made in 2018 within the doctoral thesis (section 2.2). The design of the fuel tank in Figure 2.2 corresponds to a cylindrical tank with a total volume of 75 liters, made of glass fiber. The tank is open at atmospheric pressure is covered with a cover, but it is not sealed at all (it only serves to cover, so that dust or objects do not fall into the water).

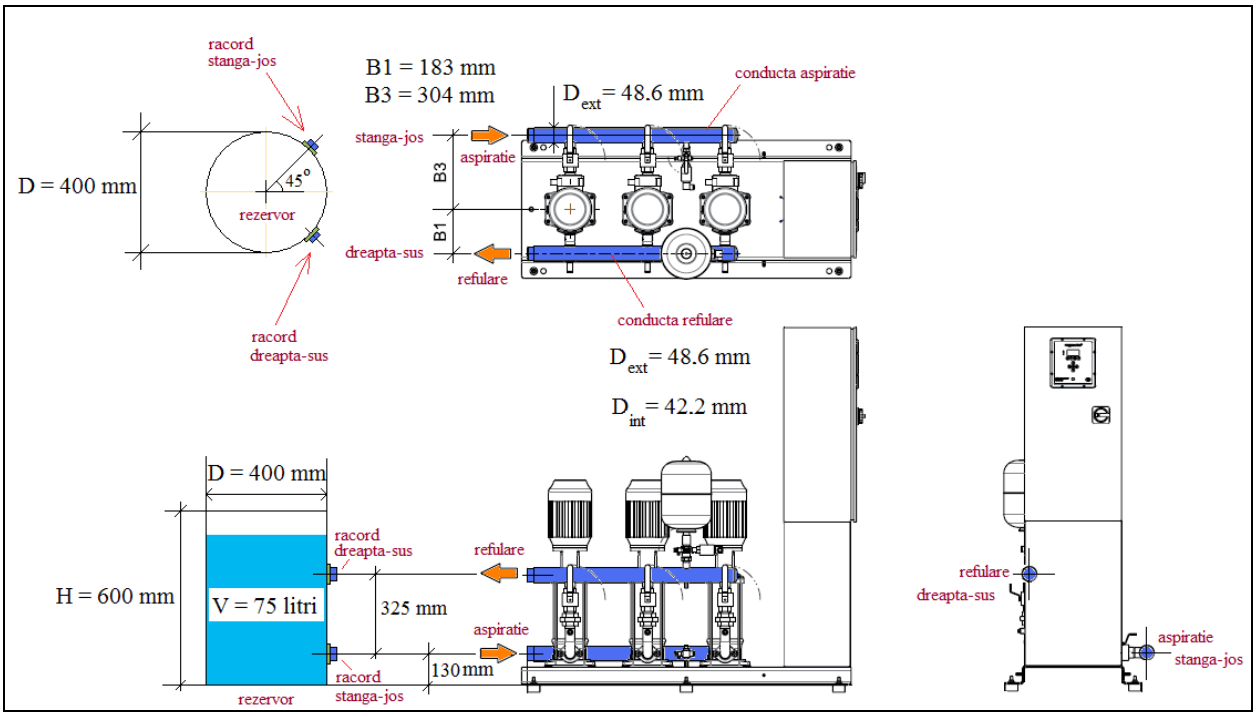

Fig. 2.2. Diagram of the connection of the supply tank in relation to the pump station

The Hydro-Unit Utility line pumping station has been made in accordance with European standards (CE European marking System and EAS European acceptance scheme) [*DP Pumps, 2012*]:

Hydro-Unit Utility line pumping systems can be used for high-rise buildings and blocks, residential complexes, industry, hospitals, hotels, commercial buildings, etc. and customized according to the requirements of the beneficiaries.

The system is controlled from an automation and control panel via a panel called Megacontrol [DP pumps, 2012], a simple to use and equipped with the most advanced settings. The panel is mounted in a cabinet on the motherboard, integrated into the pumping system; the Megacontrol panel is mounted on the cabinet door, the graphical control interface (with buttons and display) being accessible to users. It has high flexibility if the operating data of the pump station changes. DP-Pumps has equipped the Megacontrol panel for optimal pump operation by:

• energy savings due to intelligent control;
• starting the pumps can be done by softstarter, star-triangle switch or frequency converter;
• LEDs indicating the status of the system;
• multiple functions and simple operation;
• Setting through human-panel interface, PDA or laptop;
• system data available through display;
• equalization and optimization of operating hours;
• low pressure protection by pressure transducer;
• failure warning through self-protected contacts.

Table 2.1. – Capabilities of the utility-line pumping system

Number of pumps	2-6 (in this case, 3 pumps)
Maximum pumping height	120 m
Maximum operating pressure [PN]	16 bar (PN16)
Maximum flow rate	660 m^3/h
Connections	G6/4” up to NW 250
Liquid circulated	clean/aggressive liquids
Fluid temperature circulated	from -15°C to 60°C

Utility-line pressure lifting systems have advanced communication functions for management and control. Information from Megacontrol can be converted into different management systems. The following parameters can be found: System pressure; pump status; suction pressure; errors/defects; system status. The operating parameters are shown in Table 2.1.

The pumping station is energy efficient thanks to the optimization of the operation of the pumps through frequency converters mounted in the control panel. At commissioning (PIF), the SP was equipped with Danfoss frequency converters [Danfoss, 2012]. The control of the pumps (start/stop and the variation in their speed) was carried out via the Megacontrol control panel, from the PIF in 2014 to the end of 2019, first by 2017 on the short-line hydraulic installation (figure 2.1), then between 2018 and October 2019 on the new installation (section 2.2).

The most important components of the Utility line pressure lifting systems are the high-quality DPV vertical electropump units (Figure 2.3). The installation is standard, with the size of the G2” fittings (starting with NW 65, they are flanged).

Fig. 2.3. Multi-stage centrifugal pump DPV2/3 B [*DP Pumps, 2013b*]

The Hydro-Unit Utility line pumping station in the Hydraulic Machine Laboratory (room ELA022) in UPB consists of the following components:

• 3 identical, multi-stage centrifugal pumps with vertical axis (figure 2.3);
• direction flap and two valves (ball valves) mounted upstream and downstream of each pump;
• pressure transducer on the suction bus and on the discharge bus of the group;
• automation and control panel;
• 3 frequency converters;
• air cushion tank;
• connection pipes.

After the modification of the hydraulic installation, namely **after the connection of the pumping station**, in 2018, to the new hydraulic installation designed and carried out under this thesis, the Danfoss frequency converters [Danfoss, 2012] and the Megacontrol control panel [DP pumps, 2012] were used for the first part of the measurements made for the thesis – measurements made between september 2018 and october 2019. Following the modernization of the experimental stand, by changing the automation (Chapter 3), Mitsubishi frequency converters and the Mitsubishi FX5U-32M PLC were used as of November 2019 [Mitsubishi Electric, 2021].

This chapter presents the components of the Hydro-Unit Utility line pump station that originally equipped the stand (until October 2019). In chapter 3, the new automation is described and the upgrades to the stand are presented as of November 2019.

2.2. Description of the experimental stand designed and realized in 2018, within the doctoral thesis

At the beginning of 2018, we designed, executed (Figure 2.11) and commissioned a new hydraulic installation (figures 2.12÷2.14), with my colleague, eng. Remus Alexandru Mădulărea [Mădulărea, 2022]: We changed the lengths of the suction and discharge buses and implicitly the position of the supply tank, then we added 3 final consumers (3 taps) away from the pumping station. We connected this installation to the Hydro-Unit Utility line pumping station, keeping the automation existing in 2018 (the "initial" automation).

Fig. 2.11. Execution of hydraulic installation – bonding of pipe sections from PPR

Fig. 2.12. The new configuration of the experimental stand executed within the doctoral thesis

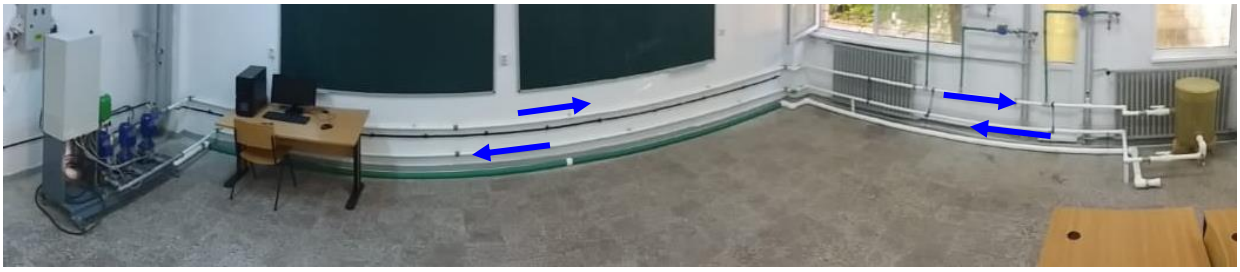

Fig. 2.13. Panoramic view of the experimental stand in the Laboratory of Hydraulic machines (ELA 022) here the suction bus has DN40, so small diameter (to study the operation of the pumps mainly with cavitation)

Fig. 2.14. Panoramic view of the experimental stand in the Laboratory of Hydraulic machines (ELA 022) here the suction bus has DN63, so large diameter (to study the operation of pumps with or without cavitation)

For the doctoral thesis, we executed the hydraulic installation with interchangeable suction lines, executed in two dimensional variants: Small diameter, DN40 (figures 2.13 and 2.15), for testing the pumps mainly in cavitation mode, respectively large diameter, DN63 (figures 2.14 and 2.16), for testing pumps with or without cavitation.

Fig.2.15. Suction line DN40

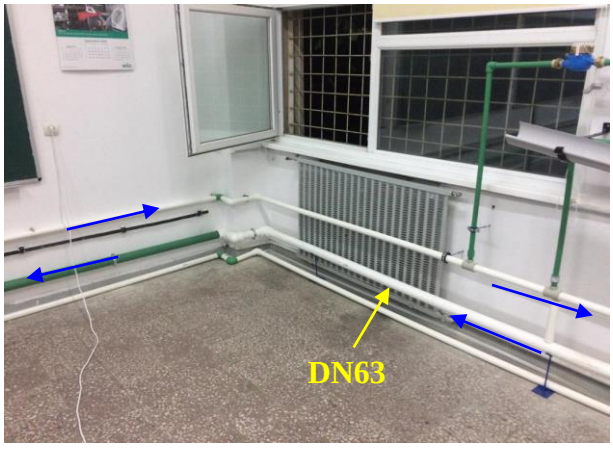

Fig.2.16. Suction line DN63

In the diagram in Figure 2.17, the experimental stand from 2018 is shown, the electropump are marked P1, P2 and P3. All components of the stand are detailed in the legend of figure 2.17.

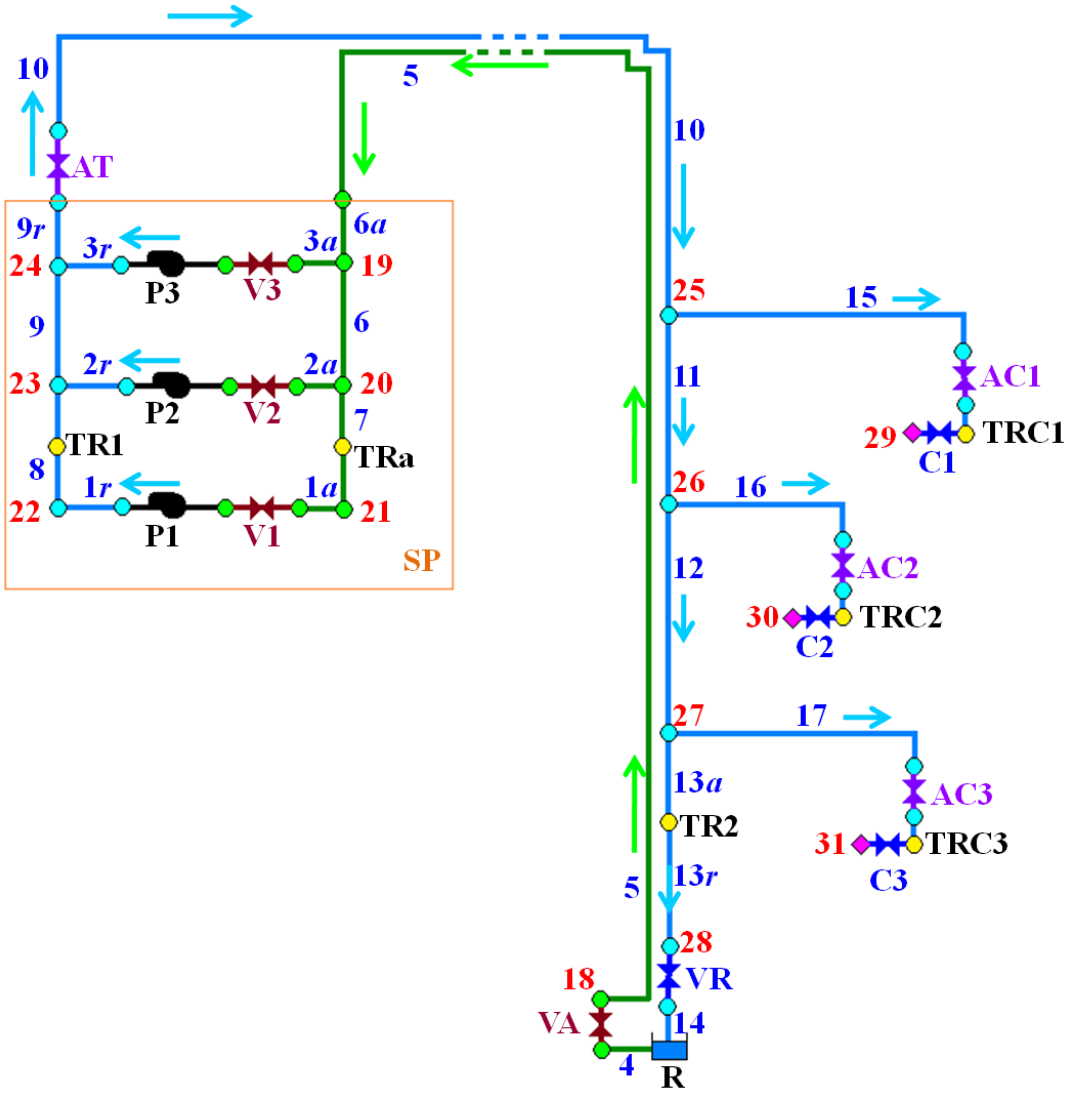

Fig. 2.17. ***Experimental stand scheme: R tank open at atmospheric pressure; P1÷P3 pumps in the SP pumping station; hydraulic suction circuit is green and discharge circuit blue****; 17 main pipes (j = 1÷17) and 14 calculation knots (j = 18÷31); pipes in SP (j ∈ {1÷3; 6; 6a; 7÷9; 9r}) they are made of stainless steel; the rest of the pipes (j ∈ {4÷5; 10÷17}) they are from PPR and belong to the hydraulic installation; on the suction pipe j = 4, the VA valve is in the normally open position; in SP, the pumps are connected between the suction pipes (with j = 1a÷3a) and the discharge (j = 1r÷3r); upstream of the pumps are insulation valves* ***V1÷ V3*** *in the normally open position; when each pump is rolled back, there is a return flap and an insulation valve in the normally open position (not shown in the diagram); in the SP, on the pipe j = 7 the TRA pressure transducer is located on the suctio, and on the pipe j = 8 the TR1 pressure transducer is located on the discharge; on the discharge line j = 10, Immediately after SP, it is the AT watermeter that measures the total volume of water pumped (at is symbolized as a general purpose valve); nodes j = 2931 are the end consumers (the outlet holes in the 3 taps* ***C1÷C3****); Upstream of each tap* ***C1÷C3*** *there is a pressure transducer* ***TRC1÷TRC3****, and each transducer is preceded by a noted watermeter* ***AC1÷AC3****; on the pipe j = 13 (between the sections 13a and 13r) the pressure transducer is located* ***TR2****; valve VR* ***flow regulation is at the***

downstream end of the discharge bus, near the tank (mounted on the pipe *j = 14, after node 28).*

Tables 2.2 and 2.3 show the geometrical data of the network: The length of the pipes L_j and the inner diameter of the pipes D_j, respectively the odds z_j nodes.

Table 2.2. Length of the pipe L_j (in metres), Nominal diameter (DN in inches for steel and in mm for PPR) and inner diameter D_j (in mm), where j is the pipeline index

ID pipeline, *j*	L_j [m]	DN and D_j [mm]	ID pipeline, *j*	L_j [m]	DN and D_j [mm]
1a	0.15	DN 1¼″ 36.6	*8*	0.16+0.16 (Upstream + downstream of TR1)	DN 1¾″ 42.3
1r	0.37	DN 1″ 27.9	*9*	0.32	DN 1¾″ 42.3
2a	0.15	DN 1¼″ 36.6	*9r*	0.16	DN 1¾″ 42.3
2r	0.37	DN 1″ 27.9	*10*	10.845	DN 40 29
3a	0.15	DN 1¼″ 36.6	*11*	0.44	DN 40 29
3r	0.37	DN 1″ 27.9	*12*	0.92	DN 40 29
4	0.825	DN 50 36.2	*13* *13a*	0.45 (amonte de TR2)	DN 40 29
			13r	0.775	
5	13.44	DN 40 / DN 63 29 / 45.8	*14*	0.28	DN 50 36.2
6a	0.16	DN 1¾″ 42.3	*15*	1.84+0.2 (Upstream + downstream of AC1)	DN 20 14.4
6	0.32	DN 1¾″ 42.3	*16*	1.555+0.2 (Upstream + downstream of AC2)	DN 20 14.4
7	0.16+0.16 (Upstream + downstream of TRa)	DN 1¾″ 42.3	*17*	1.77+0.2 (Upstream + downstream of AC3)	DN 20 14.4

Table 2.3. The elevation of the knot z_j (in meters above the floor), where j is the index of the knot

ID *knot* (*knots*), *j*	z_j [m]	ID *knot* (*knots*), *j*	z_j [m]
18÷21 and pressure transducer	0.23	upstream 30: connection knots	1.27

connection knots TRa		AC2 & TRC2	
22÷28 and connection knots TR1, AT & TR2	0.53	30 (Outlet from the C2 tap)	1.055
Upstream 29: connection knots AC1 & TRC1	1.57	upstream 31: connection knots AC3 & TRC3	1.5
29 (Outlet from the C1 tap)	1.355	31 (Outlet from the C3 tap)	1.285

On the discharge pipes were installed 4 watermeters [*Bmeters, 2021a & 2021b*], to measure the volume of water pumped. One of them is mounted on the discharge bus, in the vicinity of the outlet of the pumping station, to measure the total volume of water (this watermeter is noted AT in figures 2.17 and 2.18); The other three watermeter are fitted one at each consumer (watermeters AC1, AC2 and AC3), as shown in Figure 2.19.

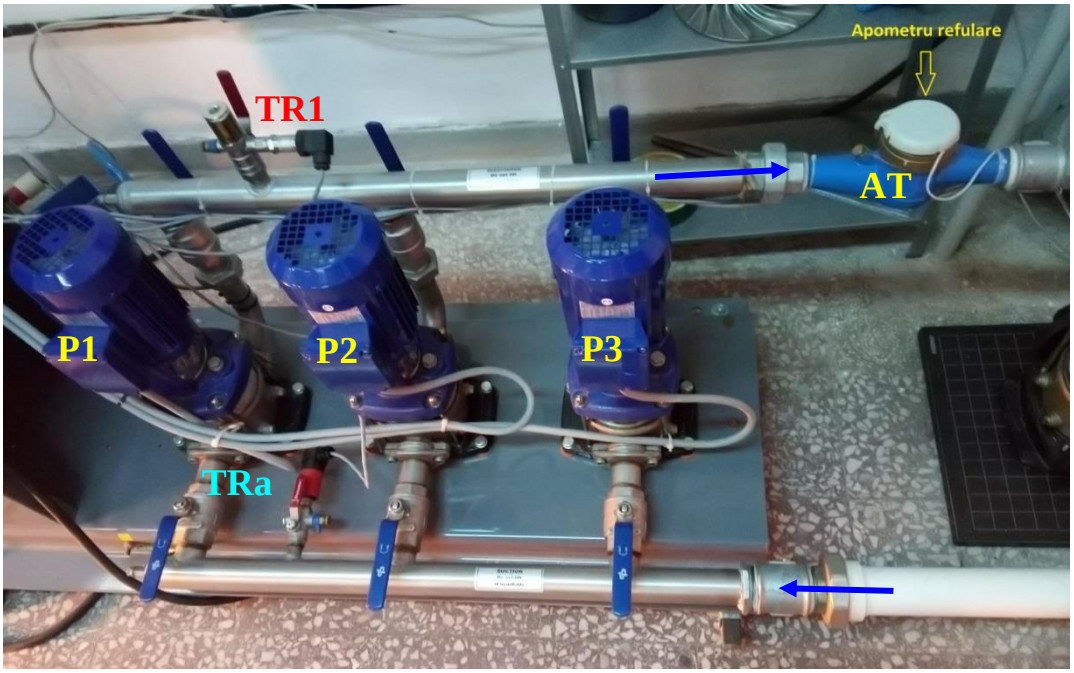

Fig. 2.18. Layout of the general watermeter (pulse counter) at on the discharge bus; P1÷P3 pumps and TRa and TR1 pressure transducers in the pump station

Fig. 2.19. Layout of watermeters (pulse counter) ***AC1÷AC3*** *to consumers*

The pump station (SP) is supplied from the open tank R (with a capacity of 75 liters): At the exit from R, the water enters the pipe with j = 4 (provided with THE VA valve in the normally open position), then is passed through the suction bus j = 5 until the entry into the SP (upstream of node 19, figure 2.17). There are 3 C1÷C3 end consumers (immediately upstream of nodes 29÷31) each of the three consumers is supplied by a pipe connected perpendicularly to the discharge line (through separation tees). The C1÷C3 control valves allow the flow rate to be adjusted for each individual consumer. To maintain a constant water level in the tank, the water jets from the three consumers are taken over by an inclined trough (figure 2.20), which directs the water back into the tank. The difference in flow between the pumped flow rate and the consumer outputs goes directly into the tank through the pipe *j = 14* (according to the diagram in Figure 2.17). The VR adjustment valve upstream of the tank, placed on the line *j = 14* is used to control the flow in the hydraulic system.

Fig. 2.20. Water jets from end consumers collected in the gutter channel

Fig.2.21. Frequency converters Mitsubishi FR-CS82-025-60

In November 2019, improvements were made to the experimental stand, by upgrading the automation part. The new automation has many advantages over the old one:

- Latest generation Mitsubishi frequency converters (Figure 2.21), series FR-CS82S-025-60 [*Mitsubishi Electric, 2021*];

- Allows quick switching of the prescribed pressure between the transducer in the pumping station, denoted by TR1 and the transducer next to the tank, denoted by TR2 (figure 2.22);
- pressure transducers **TRC1÷TRC3** for each individual consumer, whose signal is picked up and displayed in real time on the counting PLC (Figure 2.23);
- *PLC metering ensures the display of relative pressures (measured with* **TRC1÷TRC3**), counting and displaying volumes from the watermeter **AC1÷AC3** near consumers **C1÷C3**;
- *PLC metering ensures* the metering and display of the total volume of water related to the general apometer noted AT.

On the old automation we could not automatically record the water volumes: The one delivered by the pumping station, respectively those consumed by the C1÷C3 taps; We could not record the relative pressures from the three consumer pressure transducers either, and the TR2 pressure transducer had to be connected to the Megacontrol panel via a long cable.

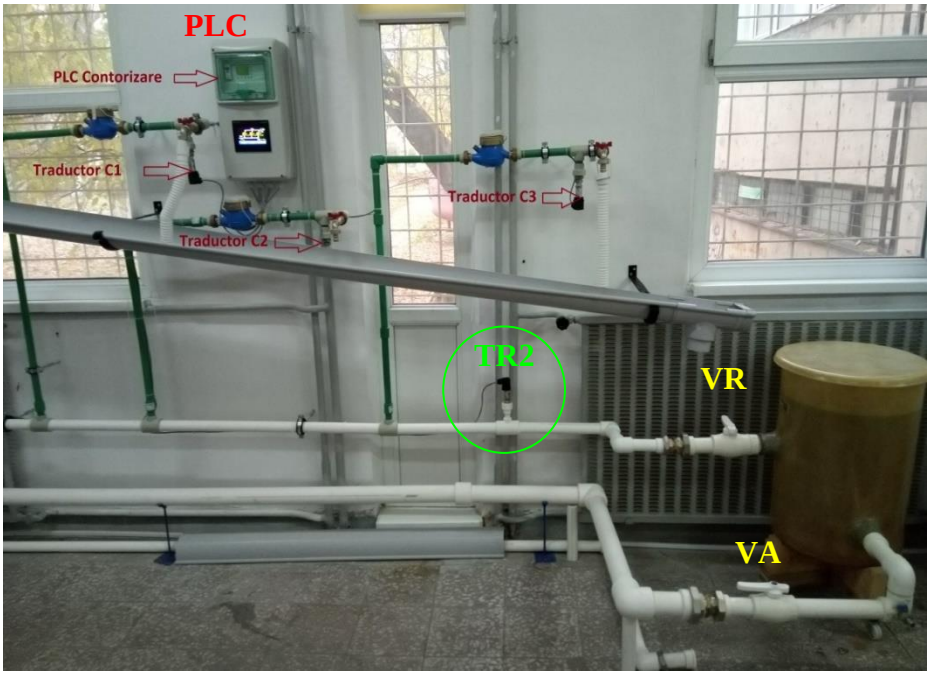

*Fig.2.22. The three pressure transducers for each individual consumer **TRC1÷TRC3**, pressure transducer **TR2**; **PLC metering; adjustment valve on discharge (VR) and suction valve (VA - normally open)***

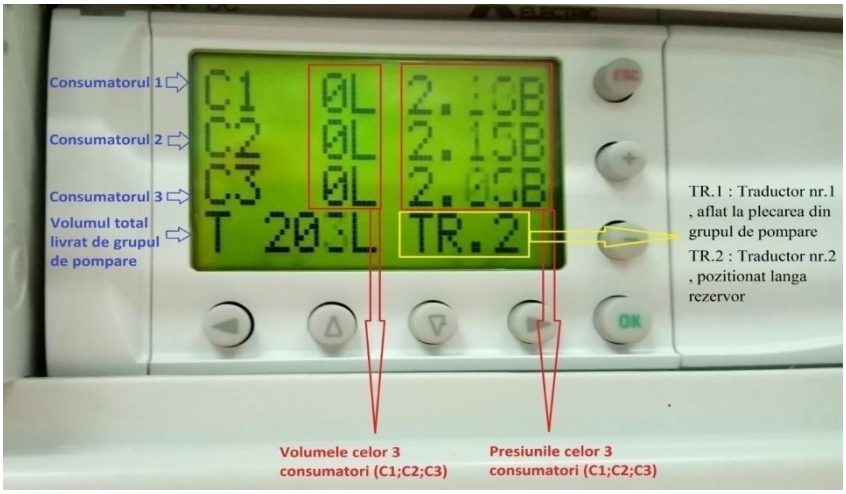

Fig. 2.23 PLC metering – displayed information

The minimum suction pressure can be changed from the touch screen (Human Panel Interface, **HMI** - Human Machine Interface). If the suction pressure falls below the set pressure (means cavitation or no water), the group stops to protect the pumps, with warning message as shown in Figure 2.24.

Fig. 2.24. Touch screen: Warning message - minimum suction pressure

Fig. 2.25. Touch screen: Minimum and maximum frequency setting

The minimum and maximum operating frequency of the frequency converters can be set, as shown in Figure 2.25, where the maximum frequency is the nominal one (i.e. 60 Hz) and **the minimum frequency is 25 Hz** and corresponds to a pump speed equal to **41.7% of the rated speed** (Thus, if the frequency drops **below 25 Hz, the pump is automatically switched off**).

The menu accessible on the HMI touch screen can provide information on the number of connections and operating hours for each pump (Figure 2.26).

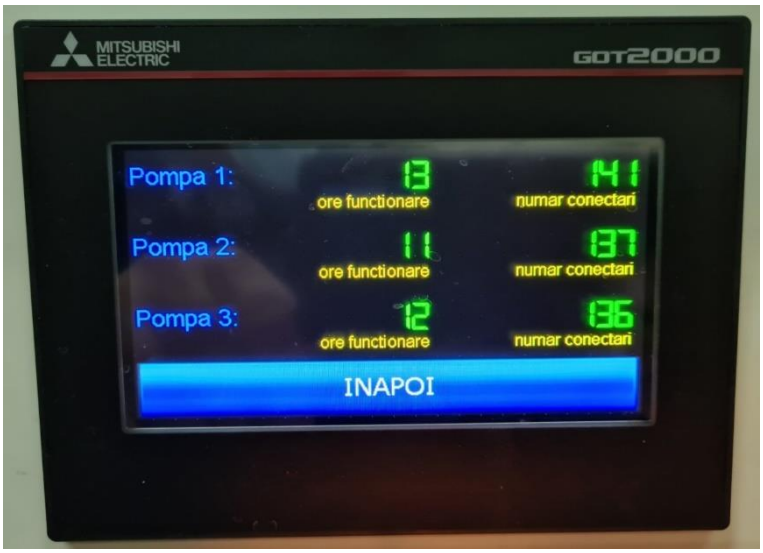

Fig. 2.26. Touch screen: Number of connections and operating hours for each pump

All information about the operation of the pump station is displayed in real time on the main screen (Figure 2.27). Also from here you can change the desired pressure in the system (prescribed pressure), also called pressure set point (PSP), respectively you can order the operation of the pumps manually (with imposed frequency with constant value) or automatically (with variable frequency).

Fig. 2.27. Main screen with information about the operation of the pump station

It is possible to check for any damage that may occur in operation. In Figure 2.28, a few damage was simulated to check the functionality of the program and whether the damage corresponds to the existing one. These damages remain in history and can be checked at any time.

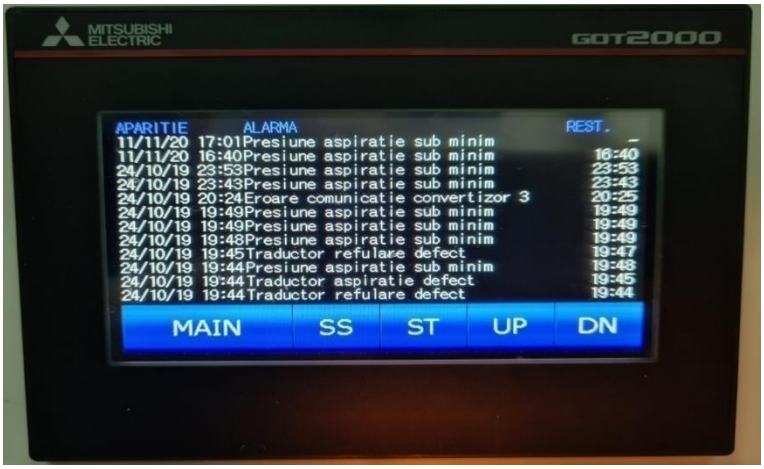

Fig. 2.28. Damage message screen

In the system, a PLC FX5U-32M programmable automatic was fitted, which controls the pumps and pressure adjustment. In chapter 3, dedicated to automation, the operation of this programmable automatic is described.

4. Mathematical formulation of the studied problems

4.1. Measured parameters and calculated parameters

4.1.1. Measured parameters

In the closed-circuit experimental stand described in Chapter 2, the *Hydro-Unit Utility* line *(DP pumps, 2012)* is the pumping station (SP) and the hydraulic circuit outside the pumping station is the pumping-supplied hydraulic system (water distribution network).

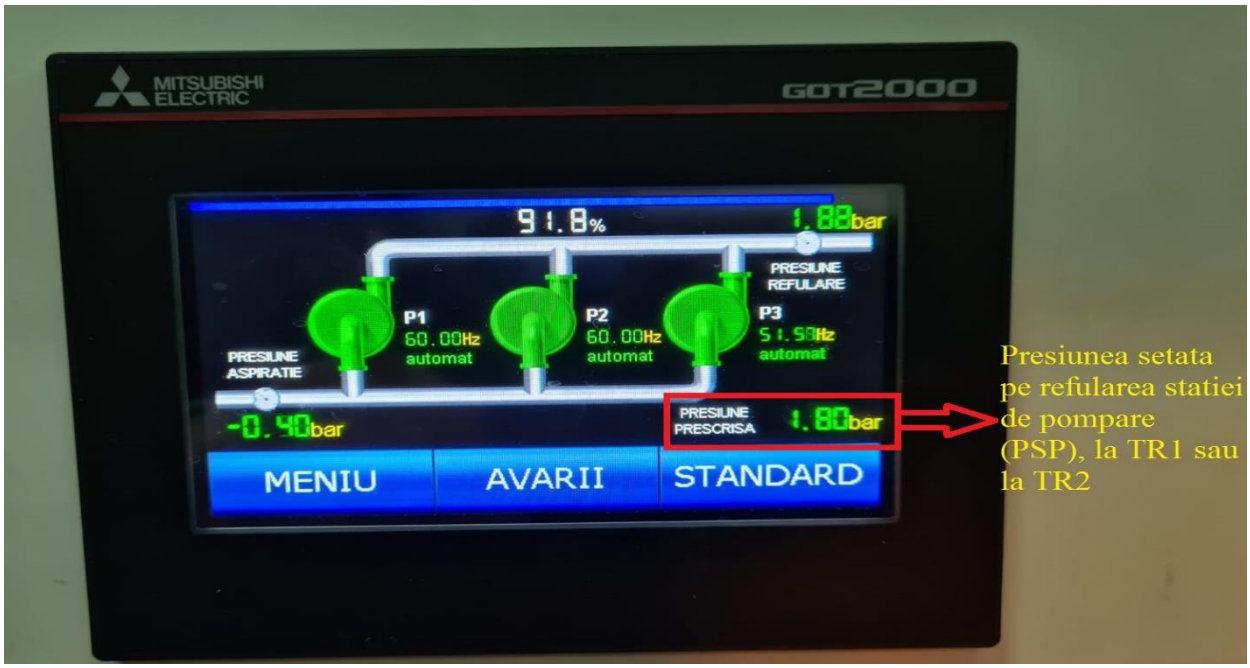

Fig. 4.1. HMI touch screen: display of prescribed pressure (PSP), set to TR1 pressure transducer or TR2 transducer (here $p_{PSP} = 1.8\,bar$*) and relative pressure display* p_{ref} *measured at discharge by that transducer* $p_{ref} = p_{TR1}$ *or* $p_{ref} = p_{TR2}$ *(see "discharge pressure" with value* $p_{ref} = 1.88$ *bar); the relative pressure is also displayed* p_{TRa} *On the SP suction line, measured with* ***TRa*** *the pressure transducer (see "suction pressure":* $p_{TRa} = -0.4\,bar$*)*

The pump station does not have flow meters to record flow through each pump and does not have pressure transducers at the inlet and outlet of each pump. In the absence of flow meters inside the SP, the flow rate pumped with each pump will be determined based on the characteristic curves provided by the manufacturer (Figure 2.4) and similarity relationships.

The following parameters were set and measured in the experimental stand:

- **PSP** noted [bar] - **Pressure Set Point** - represents the prescribed pressure, more precisely the relative set pressure (desired/preset value, as in Figure 4.1), to be maintained at one of the following monitoring nodes in the system:

  - at the **TR1** node located on the SP discharge line, where the pressure p_{TR1} is indicated by the **TR1 pressure transducer** mounted in the SP on the discharge line with index *j=8* (see Figures 2.7 and 2.17);

  - at node **TR2** located on the **discharge main away from the pumping station**, where the pressure p_{TR2} is indicated by the pressure transducer **TR2** (mounted away from the SP, on the pipe with *j = 13*, in the vicinity of reservoir **R**, upstream of the flow control valve **VR** (see Figures 2.17 and 2.18).

  The chosen monitoring node (represented by **TR1** or **TR2**) is also displayed on the *PLC metering* screen (Figure 4.2);

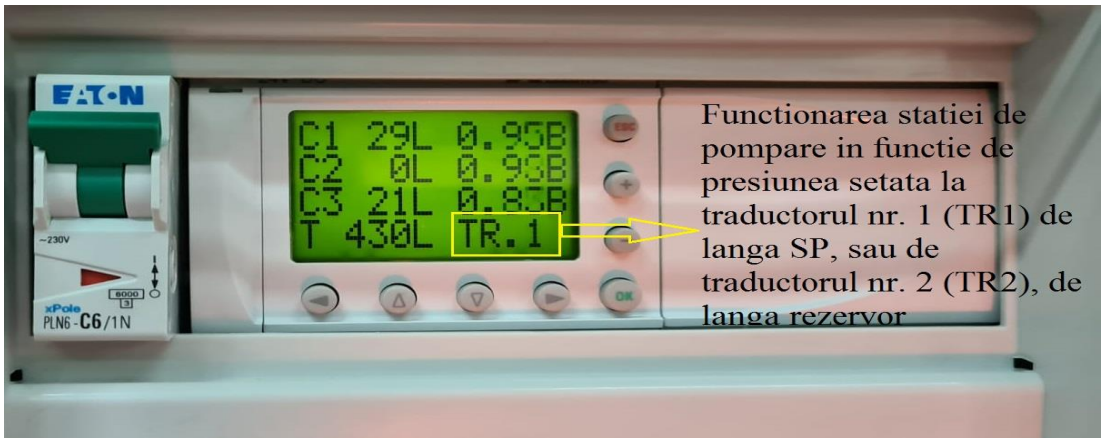

Fig. 4.2. PLC metering screen: the selected monitoring node is displayed in the lower-right corner of the screen: ***TR1*** *or* ***TR2*** *(TR1 is displayed here); the left column of the screen displays the water volume values in [litres], measured with the* ***AC1÷AC3*** *water meters on consumers* ***C1÷C3*** *(water volumes consumed), respectively with the* ***AT*** *water meter located immediately downstream of the SP outlet which measures the total volume pumped ; the first 3 positions of the right column of the screen display the relative pressures indicated by the* ***TRC1÷TRC3*** *transducers of the consumers in [bar].*

- p_{ref} **[bar]** – the relative pressure measured (recorded) at discharge by the TR1 transducer or the TR2 transducer as appropriate; the p_{ref} pressure value is displayed on the HMI - Human Machine Interface - sensor screen (Figures 4.1 and 4.3). The automation and control system (Chapter 3) implements the pump station's operating algorithm, which consists of switching the pumps on/off and varying the speed of the pumps in operation (including switching the operation of the pumps), so that the prescribed PSP pressure value is reached for certain values of the total flow rate Q_T through the plant. Basically, the operation of the pumps in SP is controlled so that a p_{ref} pressure equal to (or as close as possible to) the prescribed PSP pressure is ensured (achieved) at the chosen monitoring node (TR1 or

TR2): $p_{ref} = p_{TR1} \cong p_{PSP}$ or $p_{ref} = p_{TR2} \cong p_{PSP}$; there are also situations when the pumps are fully loaded (all running at rated speed) and the system cannot provide the prescribed pressure, namely. $p_{ref} << p_{PSP}$ (as in figure 4.3);

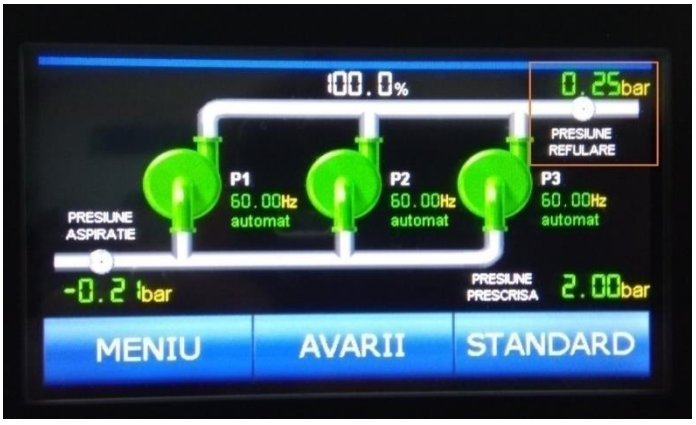

Fig. 4.3. HMI touch screen: Display of the relative discharge pressure, measured with one of the TR1 or TR2 pressure transducers ("discharge pressure", here $p_{ref} = 0.25\,bar$); in the situation shown, all pumps are operating at rated speed and the system cannot provide the prescribed pressure value ($p_{PSP} = 2$ bar), so in this case, $p_{ref} << p_{PSP}$

- p_{TRa} **[bar]** – **the relative pressure on the suction line in the pumping station**, recorded by the pressure transducer **TRa** (Figure 2.7), mounted on the pipe with index j = 7 in Figure 2.17; the value of this pressure is displayed on the HMI screen (as in Figure 4.4);

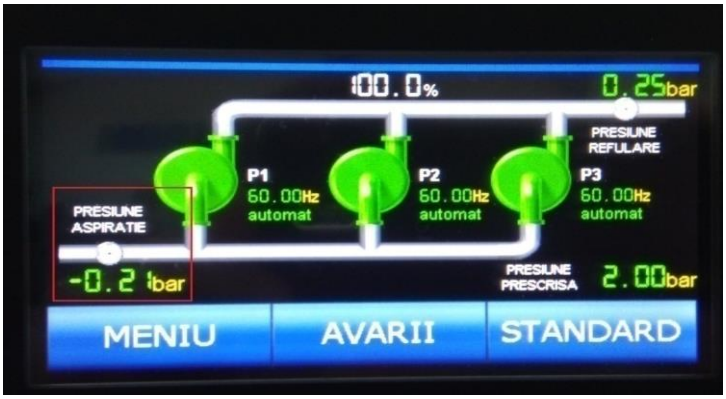

*Fig. 4.4. HMI touch screen: display of relative pressure on the suction line in SP, measured with the pressure transducer **TRa** ("suction pressure", here $p_{TRa} = -0.21\,bar$)*

- ***f*** **[Hz]** – the operating frequency of the electric motors, which is modified by the frequency converters in order to be able to maintain the prescribed p_{PSP} pressure on the discharge; for the 3 pumps **P1**÷**P3**, the measured frequencies will be noted $f_1 \div f_3$; their values are displayed on the HMI *touch screen* (figure 4.5); they are also displayed on the display of each frequency converter (figure 2.21);

- P_{elmas} **[kW] – the electrical power absorbed by the pump motor, measured** and displayed for each individual motor according to its load; for the 3 pumps **P1÷P3**, the electrical powers absorbed by the motors will be noted $P_{elmas1} \div P_{elmas3}$; their measured values are displayed on the HMI sensor screen (figure 4.6); they can also be displayed in the menu of each frequency converter display;

Fig. 4.5. HMI touch screen: display of frequencies $f_1 \div f_3$ in [Hz]; green RUN indicator shows that the pumps are running; the switches (grey circles) are set to AUT (automatic), so the speed of the pumps is adjusted by the automation system; if MAN (manual) is chosen, then the pumps will run at a fixed frequency set/selected by the operator; for position 0, the pump will be taken out of operation (disconnected) by the operator

Fig. 4.6. HMI screen: electrical powers absorbed by motors, $P_{elmas1} \div P_{elmas3}$ [kW]

- V **[litres] – volume of water,** recorded with the pulse apometer, calibrated with 1 pulse/litre [*Bmeters, 2021a și 2021b*]; we checked the apometers with the volumetric method, and the volumetric measured flow rate values correspond to the values calculated from the apometer readings (ratio between the volume counted by the apometer and the time duration in seconds); the volumes of water measured with the water meters **AC1÷AC3** at consumers **C1÷C3** (**volumes of water consumed**) are noted $V_{C1} \div V_{C3}$; the total volume pumped is noted V_T and corresponds to the indication of the water meter **AT**, located immediately downstream of the SP outlet; the values of the volumes of water measured are displayed in litres on the PLC metering screen (Figures 4. 2 and 4.7);

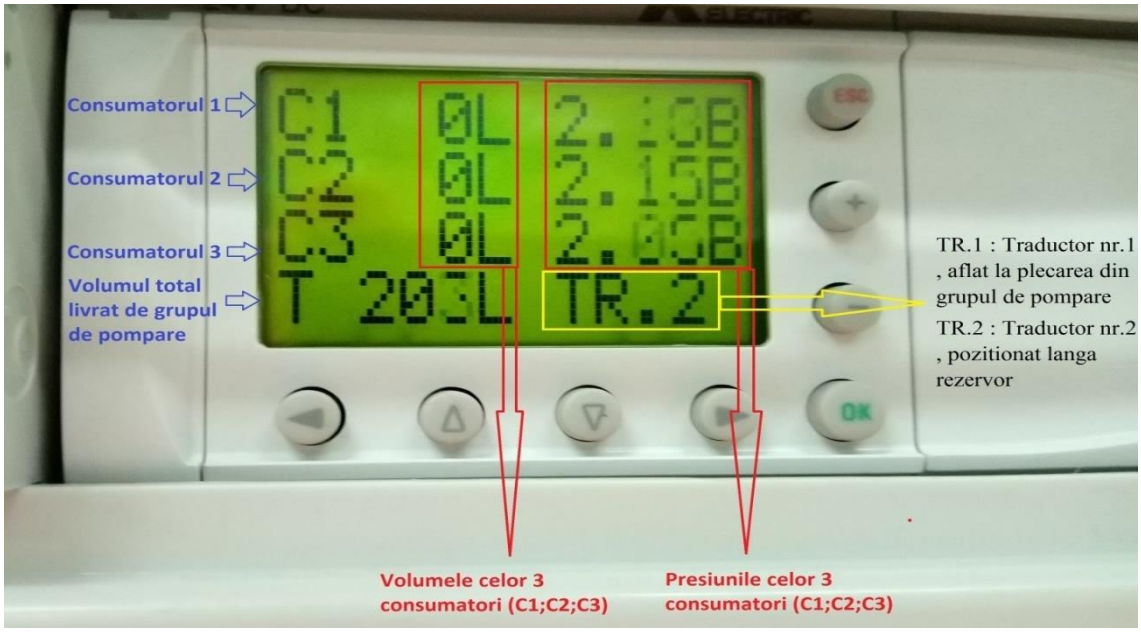

*Fig. 4.7. PLC metering screen: in the lower-right corner of the screen TR1 or TR2 is displayed (here TR2 is displayed), depending on the chosen monitoring node; in the left column of the screen the water volume values $V_{C1} \div V_{C3}$ are displayed in [litres], measured at consumers **C1÷C3** (here the values are null, the consumers' taps are closed); the lower left corner of the screen shows the total volume pumped V_T; the relative pressures $p_{C1} \div p_{C3}$ indicated by the pressure transducers **TRC1÷TRC3** near the consumers **C1÷C3** are displayed in [bar] in the first 3 positions of the column on the right of the screen*

- p_C **[bar] – the relative pressure at the consumer,** measured with the **TRC1÷TRC3** pressure transducer mounted immediately upstream of the final consumer valve; for the 3 consumers **C1÷C3**, these pressures are noted $p_{C1} \div p_{C3}$; the values of these pressures are displayed in bar on the PLC metering screen (figures 4.2 and 4.7);

- t **[seconds] – the time measured** by means of a stopwatch, which is necessary to calculate the water flow; the time measured at the **AT** meter is noted t_T , and the times measured at the **AC1÷AC3** meters for **C1÷C3,** consumers are noted $t_{C1} \div t_{C3}$;

- v_v **[mm/s] – vibration speed**, measured with an analogue vibrometer with digital display (model *Viber X1*), whose technical characteristics are: accelerometer with sensitivity 100 mV/*g*±15% and precision ±3% of the maximum scale, which is 20g for acceleration [*VMI, 2021*].

4.1.2. Calculated parameters

Based on the parameters measured during the tests on the experimental stand, the **following parameters were calculated:**

- r [dimensionless size] – **relative speed** (or relative frequency), refined as the ratio of pump speed n to rated speed n_0 (or as the ratio of displayed frequency f to rated frequency $f_0 = 60$ Hz); for **P1÷P3** pumps, operating at speeds $n_1 \div n_3$; relative speeds (relative frequencies) are denoted $r_1 \div r_3$, where

$$r_1 = \frac{n_1}{n_0} = \frac{f_1}{f_0};\ \ r_2 = \frac{n_2}{n_0} = \frac{f_2}{f_0};\ \ r_3 = \frac{n_3}{n_0} = \frac{f_3}{f_0} \tag{4.1}$$

- Q **[m³/s]** – **the water flow rate,** conveniently converted into litres/s or **m³/h**, as appropriate (flow rates determined from water meter records are directly calculated in litres/s; pump characteristic curves are provided by the manufacturer in **m³/h**); it is considered:

  - **total pumped flow rate** Q_T (at the pump station outlet), respectively the water flows consumed $Q_{C1} \div Q_{C3}$ (to final consumers **C1÷C3**), calculated in [**liters/s**], then converted to [m³/s] and [m³/h]; determined by water meters, based on the volume of water V [liters] recorded at each water meter and the time recorded t [s], such:

$$Q_T = \frac{V_T}{t_T};\ Q_{C1} = \frac{V_{C1}}{t_{C1}};\ Q_{C2} = \frac{V_{C2}}{t_{C2}};\ Q_{C3} = \frac{V_{C3}}{t_{C3}} \tag{4.2}$$

  - **pumped flow (the flow rate through each pump),** noted as appropriate Q_1, Q_2, respectively Q_3; at the exit of the SP at junction 24 upstream of the main pipeline *j* = 10 in Figure 2.17 (or at the inlet to the SP at Node 19 at the downstream end of the suction line *j* = 5), the **continuity equation applies**:

$$Q_T = Q_1 + Q_2 + Q_3 \tag{4.3}$$

  - **at pump energy operating points F1÷F3**, the pumped flows $Q_1 \div Q_3$ are denoted $Q_{F1} \div Q_{F3}$; their values are calculated from the system of equations defining the operation of the hydraulic system, presented in **section 4.2**;

  - at the energy operating point F related to the parallel coupling of the pumps (i.e. at node 24 at the SP outlet), the flow rate is equal to the total pumped flow rate: $Q_F \equiv Q_T$;

  - at points **FC1÷FC3** of cavitational operation of the pumps, the limit flows are noted $Q_{\lim 1} \div Q_{\lim 3}$ [*Georgescu S.-C. & Georgescu A.-M., 2014a*]; their values are difficult to

determine for pumps coupled in parallel; the operating condition of pumps without cavitations can be written: $Q_{F_i} < 0.97\, Q_{\lim i}$ with the index $i = 1 \div 3$;

- $\boldsymbol{H_{p_j}}$ **[m] – piezometric load in a node *j***, defined by the relation:

$$H_{p_j} = \frac{p_j}{\rho g} + z_j \tag{4.4}$$

where p_j is the relative pressure [Pa] in the node j and z_j is the node elevation [m] (for the experimental stand, the values of the node dimensions are given in Table 2.3); term $p_j/(\rho g)$ is called pressure load [metres];

- $\boldsymbol{H_{h_j}}$ **[m] – hydrodynamic load at a node *j*** located at the upstream or downstream end of a pipeline, defined by the relation:

$$H_{h_j} = \frac{v_j^2}{2g} + \frac{p_j}{\rho g} + z_j = M_{c_j} Q_j^2 + \left(\frac{p_j}{\rho g} + z_j \right) = M_{c_j} Q_j^2 + H_{p_j} \tag{4.5}$$

where v_j [m/s] is the velocity of the water at that end of the pipe (at the node *j*) and M_{c_j} [s^2/m^5] is the kinetic modulus, which is defined $M_{c_j} = 0.0826/D_j^4$ for pipe diameter D_j [m] (for the experimental stand, the pipe diameter values are given in Table 2.2);

For hydraulically long pipelines (pipelines with ratio $L_j/D_j > 200$, between the length L_j [m] and pipe diameter D_j [m]), the kinetic modulus can be neglected, in which case the hydrodynamic load can be considered equal to the piezometric load: $H_{h_j} \cong H_{p_j}$;

- $\boldsymbol{H}$ **[m] – pumping head (pump load),** noted as appropriate H_1, H_2, respectively H_3 for **P1÷P3** pumps; the load characteristic curves of the pumps are approximated by the following 2nd order polynomial regression curves **[*Ciuc et al, 2019a*]**, for any value of relative speed $r_1 \div r_3$ (4.1):

$$\begin{aligned} H_1 &= H_1(Q_1) = a \cdot r_1^2 - b \cdot Q_1^2, \quad r_1 \le 1 \\ H_2 &= H_2(Q_2) = a \cdot r_2^2 - b \cdot Q_2^2, \quad r_2 \le 1 \\ H_3 &= H_3(Q_3) = a \cdot r_3^2 - b \cdot Q_3^2, \quad r_3 \le 1 \end{aligned} \tag{4.6}$$

where $a = 31.62$ și $b = 17.625 \cdot 10^6$; pump loads H_i (with $i = 1 \div 3$) results in meters, **for flow values in m3/s.** Pump load characteristic curves, defined by relations (4.6), were determined **based on similarity relations** [*Georgescu S.-C. & Georgescu A.-M., 2014a*], applied to pairs of values {flow rate - pumping head} corresponding to the load curve provided by the manufacturer for the rated speed (Figure 2.4(a)).

The load curves (4.6) are plotted in Figure 4.8 for 5 values of relative speed: $r \in \{1;\ 55/60;\ 50/60;\ 45/60;\ 40/60\} = \{1; 0.9167; 0.8333; 0.7500; 0.6667\}$.

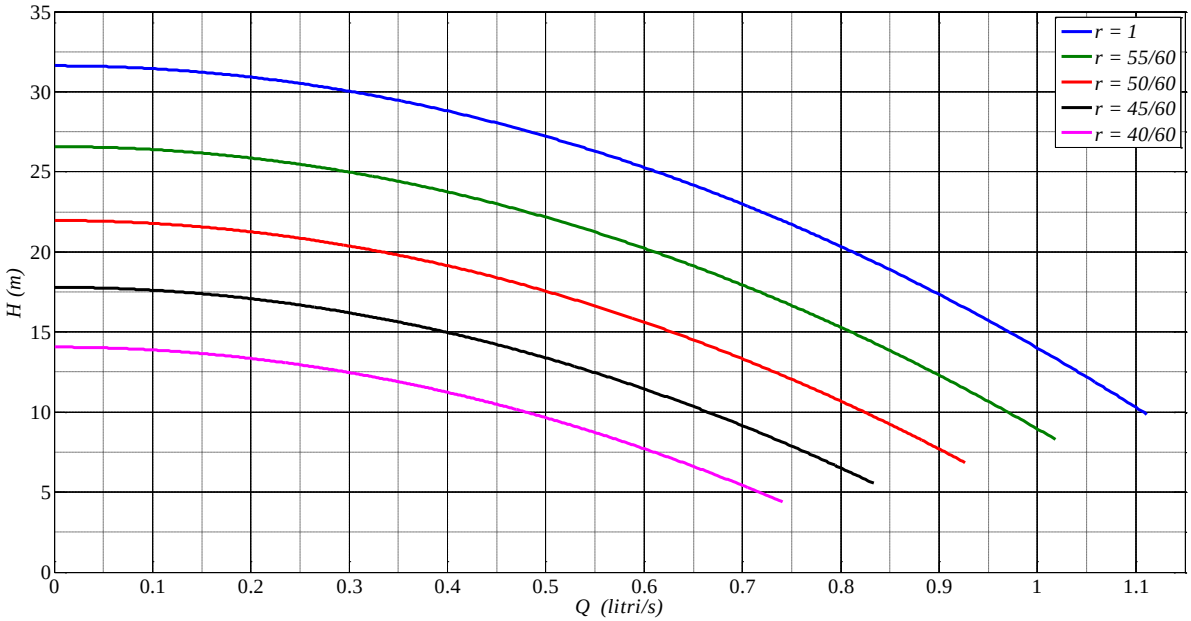

Fig. 4.8. Load characteristic curves (4.6) of pumps for different values of relative speed: $r \in \{1;\ 55/60;\ 50/60;\ 45/60;\ 40/60\}$

At **the F1÷F3 energy operating points of the pumps**, the pumping heads are $H_{F1} \div H_{F3}$, and their values result from (4.6), for pumped flows $Q_{F1} \div Q_{F3}$:

$$\begin{aligned} H_{F1} &= a \cdot r_1^2 - b \cdot Q_{F1}^2 \\ H_{F2} &= a \cdot r_2^2 - b \cdot Q_{F2}^2 \\ H_{F3} &= a \cdot r_3^2 - b \cdot Q_{F3}^2 \end{aligned} \tag{4.7}$$

- $\boldsymbol{H_F}$ **[m] – the load at the energy operating point F for the parallel coupling of the pumps**, corresponding to node **24** at the outlet of the pumping station (Figure 2.17); its value is calculated on the basis of the system of equations defining the operation of the hydraulic system, presented in **Section 4.2**;

- **η** [dimensionless size] – **pump efficiency, noted as appropriate** η_1, η_2, respectively η_3 for pumps **P1÷P3**; **Pump efficiency characteristic curves** are approximated by the following 2nd order polynomial regression curves **[*Ciuc et al, 2019a*],** for any value of relative speed (4.1):

$$\begin{aligned} \eta_1 &= \eta_1(Q_1) = 1647 Q_1/r_1 - 1.28 \cdot 10^6 (Q_1/r_1)^2, \quad r_1 \le 1 \\ \eta_2 &= \eta_2(Q_2) = 1647 Q_2/r_2 - 1.28 \cdot 10^6 (Q_2/r_2)^2, \ r_2 \le 1 \\ \eta_3 &= \eta_3(Q_3) = 1647 Q_3/r_3 - 1.28 \cdot 10^6 (Q_3/r_3)^2, \quad r_3 \le 1 \end{aligned} \tag{4.8}$$

where the yield results in dimensionless (subunit) values, for flow values in **m3/s**; for ease of reading, yield values will be expressed **in percentages [%].**

The characteristic efficiency curves of the pumps, defined by the relations (4.8), were determined based on the **parabola of the homologous operating points** [*Georgescu S.-C. & Georgescu A.-M., 2014a*]) and the pairs of values {flow - efficiency} corresponding to the efficiency curve provided by the manufacturer for the rated speed in Figure 2.4(b).

Efficiency curves (4.8) are plotted in Figure 4.9 for 5 values of relative speed: $r \in \{1;\ 55/60;\ 50/60;\ 45/60;\ 40/60\} = \{1; 0.9167; 0.8333; 0.7500; 0.6667\}$.

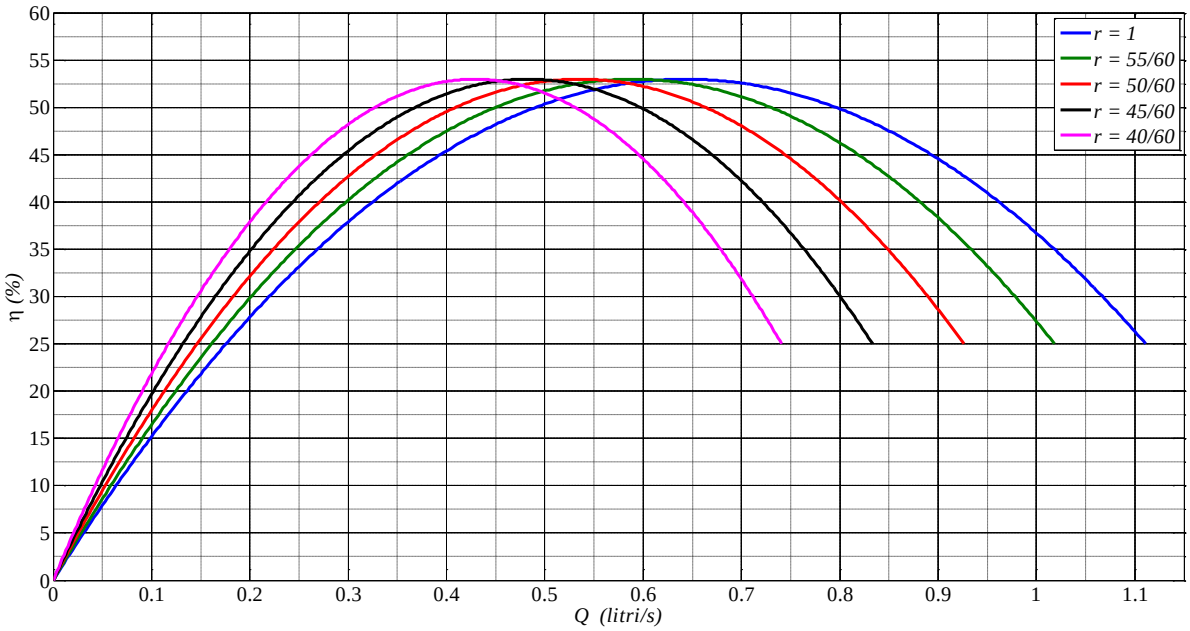

Fig. 4.9. Efficiency characteristic curves (4.8) of pumps for different values of relative speed: $r \in \{1;\ 55/60;\ 50/60;\ 45/60;\ 40/60\}$*; the efficiency is in percentages*

In the **F1÷F3 energy operating points of the pumps,** pump efficiencies are noted $\eta_{F1} \div \eta_{F3}$, and their values result from (4.8), for pumped flows $Q_{F1} \div Q_{F3}$:

$$\begin{aligned} \eta_{F1} &= 1647 Q_{F1}/r_1 - 1.28 \cdot 10^6 (Q_{F1}/r_1)^2 \\ \eta_{F2} &= 1647 Q_{F2}/r_2 - 1.28 \cdot 10^6 (Q_{F2}/r_2)^2 \\ \eta_{F3} &= 1647 Q_{F3}/r_3 - 1.28 \cdot 10^6 (Q_{F3}/r_3)^2 \end{aligned} \qquad (4.9)$$

- $\boldsymbol{\eta_{agr}}$ [dimensionless size] – **aggregate efficiency, pump - drive motor**; is calculated as the product of pump efficiency η and electric motor efficiency η_{me};

- ***P*** **[W]** – **pump power,** noted as appropriate P_{F1}, P_{F2}, respectively P_{F3} for pumps **P1÷P3**, calculated with the relations:

$$P_{F1}=\frac{\rho g Q_{F1} H_{F1}}{\eta_{F1}};\quad P_{F2}=\frac{\rho g Q_{F2} H_{F2}}{\eta_{F2}};\quad P_{F3}=\frac{\rho g Q_{F3} H_{F3}}{\eta_{F3}} \tag{4.10}$$

where $\rho=1000\,\text{kg/m}^3$ is the density of water and $g=9.81$ m/s^2 is the gravitational acceleration;

- ***P_{el}* [W] – the electric power absorbed by the electric motor,** calculated; between the electric power P_{el} and the pump power (4.10) there is the relationship:

$$P_{el_i}=P_{Fi}/\eta_{me} \qquad \text{where } i=1\div 3 \tag{4.11}$$

where η_{me} is the efficiency of the electric motor; for the pump drive motors equipping the stand, the manufacturer's technical specifications indicate the value $\eta_{me}=0.76$ [*DP Pumps, 2013a*];

- ***P_T* [W] – total power consumed for pumping -** is the sum of the powers of the 3 pumps:

$$P_T=P_{F1}+P_{F2}+P_{F3} \tag{4.12}$$

- ***P_{elT}* [W] – total electrical power absorbed in the pumping station, calculated -** is the sum of the electrical powers absorbed by the motors of the 3 pumps:

$$P_{elT}=P_{el_1}+P_{el_2}+P_{el_3} \tag{4.13}$$

- ***n* [rot/min] – pump speed,** usually expressed in [rpm] and defined as the number of revolutions executed by the shaft per unit time; if there is a rigid or elastic coupling between the pump and the electric motor, the pump speed is considered to be equal to the motor speed; when driving pumps with three-phase motors (the most common case - this is also the case for the electric pumps studied), the asynchronous speed n is lower than the synchronous speed n_{si} namely:
  $n=s\cdot n_{si}$, due to slippage $s<1$; the synchronous speed is calculated with the relation $n_{si}=60\,f/p$, where $f=50$ Hz is the frequency of the supply current, and p is the number of pairs of magnetic poles resulting from the winding of the electric motor;

- ***NPSH* [m] – net positive suction load required by the pump, noted** $NPSH_1$, $NPSH_2$, respectively $NPSH_3$ for pumps **P1÷P3**; **The required NPSH curve** (Figure 2.4(c)) provided by the manufacturer **for rated speed** [*DP Pumps, 2013b*] is approximated by a 3rd order polynomial regression curve **[*Ciuc et al, 2019a*]**, as follows:

$$NPSH_i=5.04-1.27\cdot 10^4 Q_i+8\cdot 10^6 Q_i^2+7.5\cdot 10^9 Q_i^3,\quad i=1\div 3,\ \text{for } r_i=1 \tag{4.14}$$

where the NPSH value required by the pump results in meters, for flow values in m3/s.

Similarity relations indicate that the ratio of pumped flow rates (flow rate at speed n and flow rate at rated speed n_0) is proportional to the relative speed $r = n/n_0$, respectively that the **ratio of pump loads** (pumping head at speed n and pumping head at rated speed n_0) is proportional to the square of the relative speed: r^2 [*Georgescu S.-C. & Georgescu A.-M., 2014a*].

By extension, the ratio of the net positive suction loads required by the pump (NPSH required at speed n and NPSH required at rated speed n_0) is also proportional to the square of the relative speed: r^2 .

As a result, **based on the similarity relations applied to the required NPSH curve at rated speed** (4.14), **the characteristic curves of the required NPSH of the pumps** will be defined **for any value of relative speed** by the following polynomial regression curves of degree 3:

$$\begin{aligned} NPSH_1 &= 5.04\, r_1^2 - 1.27\cdot 10^4 r_1\, Q_1 + 8\cdot 10^6 Q_1^2 + 7.5\cdot 10^9 Q_1^3 / r_1, \quad r_1 \le 1 \\ NPSH_2 &= 5.04\, r_2^2 - 1.27\cdot 10^4 r_2 Q_2 + 8\cdot 10^6 Q_2^2 + 7.5\cdot 10^9 Q_2^3 / r_2, \quad r_2 \le 1 \\ NPSH_3 &= 5.04\, r_3^2 - 1.27\cdot 10^4 r_3 Q_3 + 8\cdot 10^6 Q_3^2 + 7.5\cdot 10^9 Q_3^3 / r_3, \quad r_3 \le 1 \end{aligned} \tag{4.15}$$

The NPSH curves (4.15) are plotted in Figure 4.10 for 5 values of relative speed: $r \in \{1;\ 55/60;\ 50/60;\ 45/60;\ 40/60\} = \{1; 0.9167; 0.8333; 0.7500; 0.6667\}$.

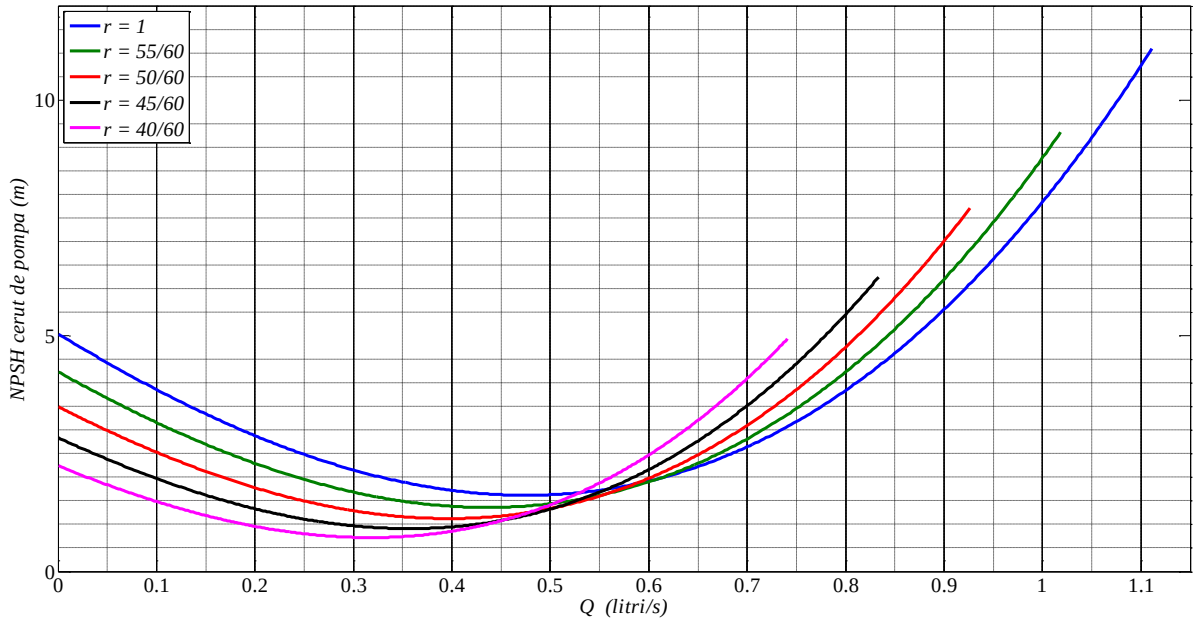

Fig. 4.10. Characteristic curves of NPSH required by pumps (4.15) for different values of relative speed: $r \in \{1;\ 55/60;\ 50/60;\ 45/60;\ 40/60\}$

At **pump energy operating points F1÷F3**, the values of the $NPSH$ required by the pump are denoted $NPSH_{F1} \div NPSH_{F3}$ and their values result from (4.15), for pumped flows $Q_{F1} \div Q_{F3}$

$$NPSH_{F1} = 5.04\, r_1^2 - 1.27 \cdot 10^4 r_1\, Q_{F1} + 8 \cdot 10^6 Q_{F1}^2 + 7.5 \cdot 10^9 Q_{F1}^3 / r_1, \quad r_1 \le 1$$
$$NPSH_{F2} = 5.04\, r_2^2 - 1.27 \cdot 10^4 r_2 Q_{F2} + 8 \cdot 10^6 Q_{F2}^2 + 7.5 \cdot 10^9 Q_{F2}^3 / r_2, \quad r_2 \le 1 \qquad (4.16)$$
$$NPSH_{F3} = 5.04\, r_3^2 - 1.27 \cdot 10^4 r_3 Q_{F3} + 8 \cdot 10^6 Q_{F3}^2 + 7.5 \cdot 10^9 Q_{F3}^3 / r_3, \quad r_3 \le 1$$

- $\boldsymbol{M_j}$ **[s²/m⁵] – the hydraulic resistance modulus** can be defined for any pipe of the installation (with index $j = 1 \div 17$) in the form:

$$M_j = M_{dj} + M_{lj} = 0.0826\, \lambda_j \frac{L_j}{D_j^5} + 0.0826 \frac{\sum \zeta_j}{D_j^4} = 0.0826 \left(\lambda_j \frac{L_j}{D_j} + \sum \zeta_j \right) \frac{1}{D_j^4} \qquad (4.17)$$

where M_{dj} is the distributed hydraulic resistance modulus and M_{lj} is the local hydraulic resistance module;

- $\boldsymbol{M_{dj}}$ **[s²/m⁵] – the distributed hydraulic resistance modulus** of the pipe with index *j* depends on the Darcy coefficient λ_j, coefficient that can be calculated with the Swamee-Jain formula *[Swamee & Jain, 1976]* for the entire turbulent flow regime:

$$\lambda_j = 0.25 \left[\lg \left(\frac{5.74}{Re_j^{0.9}} + \frac{k_j}{3.7 D_j} \right) \right]^{-2} \qquad (4.18)$$

where k_j is the absolute roughness of the pipe walls with index *j*; it is considered value $k_j = 0.05$ mm for all steel pipes [*Drăghici, 1971*; pag. 246] with index $j \in \{1 \div 3; 6 \div 9\}$ and $k_j = 0.005$ mm for all pipes in PPR, with $j \in \{4; 5; 10 \div 17\}$; numărul Reynolds Re_j according to the flow on the pipe with the index *j* is defined as follows:

$$Re_j = \frac{4 Q_j}{\pi D_j \upsilon} \qquad (4.19)$$

where $\upsilon = 10^{-6}$ m²/s is the kinematic viscosity of water at 20°C;

For **the rusty turbulent regime**, defined for $Re_j \ge 560 D_j / k_j$, Darcy's coefficient λ_j can be calculated **with the Prandtl-Nikuradse formula** [*Georgescu A.-M. & Georgescu S.-C., 2007*] a formula that does not depend on flow:

$$\lambda_j = \left(2 \lg \left(\frac{D_j}{k_j} \right) + 1.14 \right)^{-2} \qquad (4.20)$$

- $\boldsymbol{M_{lj}}$ **[s²/m⁵] – local hydraulic resistance modulus** depends on local hydraulic head loss coefficients ζ_j.

For hydraulically long pipelines (pipelines with ratio $L_j/D_j > 200$, between the length L_j and diameter D_j), local hydraulic head losses can be neglected, so $M_{l_j} \to 0$; based on this assumption, in the studied plant, the local hydraulic head loss coefficients ζ_j can only be considered negligible **along two pipelines**: the suction line with j = 5, respectively, the backflow pipe with j = 10.

As a result, **the hydraulic calculation for the whole installation will be carried out under the assumption of hydraulically short pipelines**, namely with consideration of all local hydraulic head losses and kinetic terms at the pipeline ends.

ζ_j coefficients **will be determined by numerical calculation for the valves/valves operated (partially closed or fully open) during the experiments**, namely:

- VR flow control valve located on the discharge line j = 14 downstream (where the coefficient ζ_j is noted ζ_{VR}) – **VR** control valve is used in all experiments;
- taps of end consumers **C1÷C3** (with coefficients ζ_j note $\zeta_{C1}; \zeta_{C2}; \zeta_{C3}$) – these taps are only opened in certain experiments;
- **V1÷V3** valves on the suction lines of pumps, pipes with indexes j = 1*a*; 2*a*; 3*a* (coefficients ζ_j are noted $\zeta_{V1}; \zeta_{V2}; \zeta_{V3}$) – these valves are only partially closed for certain cavitating tests; for the normally open position, the value of $\zeta_{V1}; \zeta_{V2}; \zeta_{V3}$ are given in table 4.1;
- **VA** valve located upstream on the suction line j = 4 (where the coefficient ζ_j is noted ζ_{VA}) – this valve is only partially closed for certain cavitation tests; for the normally open position, the ζ_{VA} value is given in Table 4.1.

For other types of fittings, namely for 90° bends, sudden section flares/shorts, tees with separation, tees with jointing, non-return valves, as well as when flowing through isolation valves in the normally open position, the values of the ζ_j coefficients are given in table 4.1– these ζ_j values are taken/processed from [*Drăghici, 1971*; pages 249-253]. The determination of the ζ_A coefficients at passage through the **AT** and **AC1÷AC3** water meters is inserted after table 4.1.

Table 4.1. Values of ζ_j coefficients on j-index pipelines for 90°, bends, sudden section flares/shorts, splitting/dividing tees, fully open valves

j	ζ_j	$\sum\zeta_j$	Description of the type of singularity, pipe and/or corresponding node

1*a*	1.15		tee with separation at node 21, upstream on pipe *j = 1a*
V1	0.4		the isolating valve **V1** in the normally open position on pipe *j = 1a* (unless **V1** is operated for cavitational testing, where ζ_{V1} is determined by numerical calculation)
2*a*	1.15		tee with separation at node 20, upstream on pipe j = 2a
V2	0.4		isolating valve **V2** in normally open position on pipe *j = 2a* (unless **V2** is operated for cavitational testing, where ζ_{V2} is determined by numerical calculation)
3*a*	1.15		tee with separation at node 19, upstream on pipe j = 3a
V3	0.4		isolating valve **V3** in normally open position on pipe *j = 3a* (unless **V3** is operated for cavitational testing, where ζ_{V3} is determined by numerical calculation)
1*r*	0.8	$\Sigma\zeta_{1r}$ =2.06	check valve on pipe *j = 1r*
1*r*	0.4		isolation valve in normally open position on pipe *j = 1r*
1*r*	0.3		elbow 90° in vertical plane on pipe with *j = 1r*
1*r*	0.56		tee with joint in node 22, downstream on pipe *j = 1r*
2*r*	0.8	$\Sigma\zeta_{2r}$ =2.06	non-return valve on pipe *j = 2r*
2*r*	0.4		isolation valve in normally open position on pipe *j = 2r*
2*r*	0.3		elbow 90° in vertical plane on pipe with *j = 2r*
2*r*	0.56		tee with joint in node 23, downstream on pipe *j = 2r*
3*r*	0.8	$\Sigma\zeta_{3r}$ =2.06	non-return valve on pipe *j = 3r*
3*r*	0.4		isolation valve in normally open position on pipe *j = 3r*
3*r*	0.3		elbow 90° in vertical plane on pipe with *j = 3r*
3*r*	0.56		tee with joint in node 24, downstream on pipe *j = 3r*
4	0.35	$\Sigma\zeta_4$ = 0.99 (0.95 when *j*=5 is DN40)	outlet from reservoir (sharp narrowing section), upstream pipe *j = 4*
4	2 × 0.3		two bends 90° vertically on pipe *j = 4*
4	0.04		DN50 / DN63 abruptly flared at junction 18, downstream on pipe *j = 4* (except experimental tests with pipe *j = 5* with DN40)
VA	0.4		**VA** valve in normally open position on pipe *j = 4* (except when **VA** is operated for cavitational testing, where ζ_{VA} is determined by numerical calculation)
5	6 × 0.3	$\Sigma\zeta_5$ = 1.8 (1.95 when *j*=5 is DN40)	6 bends 90° in horizontal plane on pipe *j = 5*
5	0.05		sudden narrowing DN50 / DN40 in node 18, upstream of pipe j = 5 (only for experimental tests with pipe *j = 5* with DN40)
5	0.1		suction line connection to pumping station, upstream of node 19: DN40 / DN1¾″ sharp flaring, ζ coefficient downstream on pipe j = 5 with DN40 (only for tests with *j = 5* with DN40)
6*a*	0.01	0.01	suction line connection to pumping station, upstream of node 19:

		(0 when *j*=5 is DN40)	DN63 / DN1¾″ sharp flaring, ζ coefficient downstream on pipe *j* = 6*a* with DN40 (only for tests with *j* = 5 with DN40)
6	0.25		tee with separation at node 19, on pipe *j* = 6 immediately downstream of node 19
7	0.25		tee with separation in node 20, upstream on pipe *j* = 7
8	0.44		tee with join in node 23, downstream on pipe *j* = 8
9	0.44		tee with join in node 24, on pipe *j* = 9 upstream of node 24
9*r*	0		no local hydraulic head losses on this section
10	0.1	$\Sigma\zeta_{10}$ =1.3	connection of the discharge main to the pumping station, downstream of node 24: abrupt narrowing DN1¾″ / DN 40, ζ upstream on pipe *j* = 10
10	4 × 0.3		4 bends 90° in horizontal plane on pipe j = 10
AT	ζ_{AT}		passage through the **AT** gauge: the variation of ζ_{AT} as a function of flow is plotted in Figure 4.11(b); the local hydraulic head loss $h_{l\,AT}$ through the **AT** gauge is described below in relation (4.22); although **AT** is mounted on pipe *j* = 10, $h_{l\,AT}$ will be considered separately in the energy law expression - so $\Sigma\zeta_{10}$ in M_{l10} (4.17) does not include the coefficient ζ_{AT}
11	0.06		tee with separation at node 25, upstream on pipe *j* = 11
12	0.06		tee with separation in node 26, upstream on pipe *j* = 12
13	0.06	$\Sigma\zeta_{13}$ = 0.06+ 0.64	tee with separation in node 27, on pipe *j* = 13 upstream of TR2
13	2 × 0.3		two bends 90° in horizontal plane on pipe with *j* = 13
13	0.04		abrupt section flare in node 28, downstream on pipe *j* = 13
VR	ζ_{VR}		flow control valve VR mounted on pipe j = 14 (ζ_{VR} is determined by numerical calculation)
14	1		inlet to reservoir (sudden section deflection), downstream on pipe *j*=14
15	0.92	$\Sigma\zeta_{15}$ = 1.22+ 0.3	tee with separation in node 25, upstream on pipe j = 15
15	0.3		elbow 90° in vertical plane on pipe with *j* = 15, upstream of AC1
15	0.3		elbow 90° in horizontal plane on pipe with *j* = 15, downstream of AC1
C1	ζ_{C1}		tap at consumer **C1** at the downstream end of pipe j = 15 (ζ_{C1} is determined by numerical calculation)
AC1	ζ_{AC1}		passage through gauge **AC1**: the variation of ζ_{AC1} as a function of flow is plotted in Figure 4.12(b); the local hydraulic head loss $h_{l\,AC1}$ through gauge **AC1** is described in relation (4.23);

			although **AC1** is mounted on pipe $j = 15$, $h_{l\,AC1}$ will be considered separately in the energy law expression - so $\Sigma\zeta_{15}$ in M_{l15} (4.17) does not include the coefficient ζ_{AC1}
16	0.92	$\Sigma\zeta_{16}$ = 1.22+ 0.3	tee with separation at node 26, upstream on pipe $j = 16$
16	0.3		elbow 90° vertically on pipe with $j = 16$, upstream of AC2
16	0.3		elbow 90° in horizontal plane on pipe with $j = 16$, downstream of AC2
C2	ζ_{C2}		tap at consumer C2 at the downstream end of pipe $j = 16$ (ζ_{C2} is determined by numerical calculation)
AC2	ζ_{AC2}		passage through gauge **AC2**: the variation of ζ_{AC2} as a function of flow is plotted in Figure 4.12(b); the local hydraulic head loss $h_{l\,AC2}$ through gauge **AC2** is described in relation (4.23); although **AC2** is mounted on pipe $j = 16$, $h_{l\,AC2}$ will be considered separately in the energy law expression - so $\Sigma\zeta_{16}$ in M_{l16} (4.17) does not include the coefficient ζ_{AC2}
17	0.92	$\Sigma\zeta_{17}$ = 1.22+ 0.3	tee with separation at node 27, upstream on pipe $j = 17$
17	0.3		elbow 90° vertically on pipe with $j = 17$, upstream of AC3
17	0.3		elbow 90° in horizontal plane on pipe with $j = 17$, downstream of AC3
C3	ζ_{C3}		tap at consumer C3 at the downstream end of pipe $j = 17$ (ζ_{C3} is determined by numerical calculation)
AC3	ζ_{AC3}		passage through gauge **AC3**: the variation of ζ_{AC3} as a function of flow is plotted in Figure 4.12(b); the local hydraulic head loss $h_{l\,AC3}$ through gauge **AC3** is described in relation (4.23); although **AC3** is mounted on pipe $j = 17$, $h_{l\,AC3}$ will be considered separately in the energy law expression - so $\Sigma\zeta_{17}$ in M_{l17} (4.17) does not include the coefficient ζ_{AC3}

- $\boldsymbol{h_{l\,A}}$ **[m] – loss of local hydraulic load when passing through the water meter**; the $h_{l\,A}$ value as a function of flow can be estimated by processing data available in the literature [*Pressure Loss, 2022*]. For the 2 types of water meters mounted on DN40 and DN20 pipes in the experimental stand, the available $h_{l\,A}$ values are plotted in Figures 4.11(a) and 4.12(a).

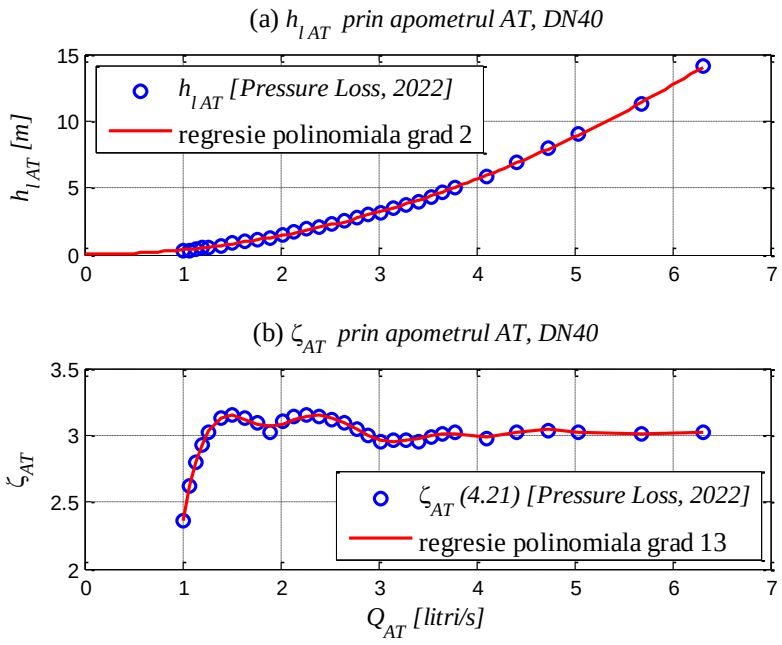

*Fig. 4.11. Local hydraulic head losses $h_{l\,AT}$ (in meters) and the coefficient ζ_{AT} calculated with (4.21) as a function of the flow rate Q_T (in litres/s) for the **AT** general water meter (mounted on the pipe j = 10 with DN40): available processed data [Pressure Loss, 2022] and polynomial regression curves proposed in thesis*

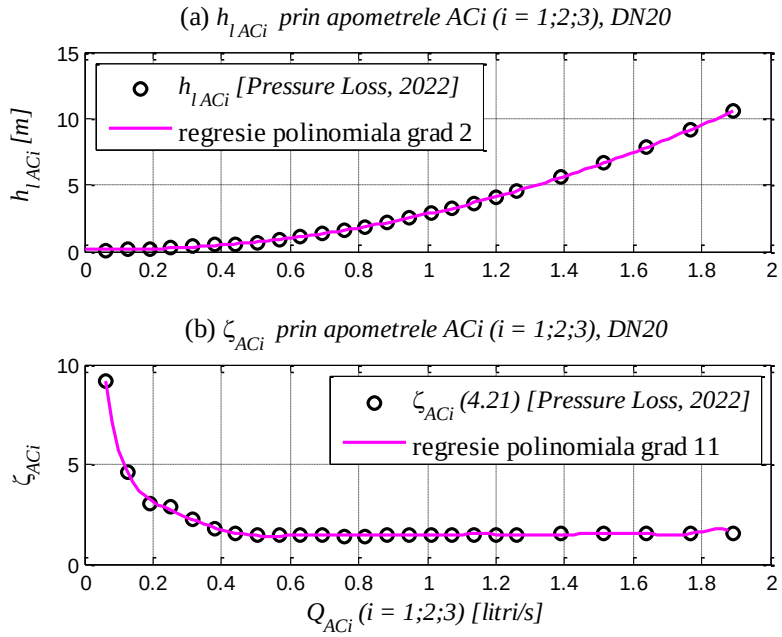

*Fig. 4.12. Local hydraulic head losses $h_{l\,ACi}$ (in meters) and the coefficient ζ_{ACi} calculated with (4.21) as a function of the flow rate Q_{Ci} (in litres/s), with i = 1÷3, for **AC1÷AC3** water meters from **C1÷C3** consumers, mounted on DN20 pipes: available processed data [Pressure Loss, 2022] and polynomial regression curves proposed in the thesis*

The values of the ζ_A coefficient can be calculated as follows:

$$h_{l\,A} = 0.0826\,\frac{\zeta_A}{D_j^4}\,Q_j^2 \;\Rightarrow\; \zeta_A = \frac{h_{l\,A}\,D_j^4}{0.0826\,Q_j^2} \tag{4.21}$$

where the index *j* is:

- *j* = 10 for the **AT** general water meter mounted on pipe *j* = *10* with DN40, diameter equivalent to DN 1½″; it follows $h_{l\,AT} = h_{l\,AT}(Q_T)$ and ζ_{AT} ;

- *j* = 15÷17 for **AC1÷AC3** meters from **C1÷C3** consumers, on DN20 pipes, diameter equivalent to DN ¾″; it follows $h_{l\,ACi} = h_{l\,ACi}(Q_{Ci})$ and ζ_{ACi} (written for *i* = 1÷3).

The pairs of available $h_{l\,AT} = h_{l\,AT}(Q_T)$ and $h_{l\,ACi} = h_{l\,ACi}(Q_{Ci})$ values can be approximated by the following 2nd order polynomial regression curves:

$$h_{l\,AT} = 0.3523\,Q_T^2 - 0.0011\,Q_T + 0.0055 \tag{4.22}$$

$$h_{l\,ACi} = 3.189\,Q_{Ci}^2 - 0.5656\,Q_{Ci} + 0.1968\,; \quad i = 1 \div 3 \tag{4.23}$$

where $h_{l\,AT}$ and $h_{l\,AC1} \div h_{l\,AC3}$ results in meters for flow values Q_T and $Q_{C1} \div Q_{C3}$ in litres/s. The proposed regression curves (4.22) and (4.23) are plotted in Figures 4.11(a) and 4.12(a).

The ζ_{AT} and ζ_{ACi} values calculated with (4.21) flow function can be approximated by higher degree polynomial regression curves, i.e. $\zeta_{AT} = \zeta_{AT}(Q_T)$ values by a polynomial of degree 13 and $\zeta_{ACi} = \zeta_{ACi}(Q_{Ci})$ values by a polynomial of degree 11, respectively; the calculated ζ values and the proposed regression curves are plotted graphically in Figures 4.11(b) and 4.12(b);

- ζ_{VR} [dimensionless size] – **the local hydraulic head loss coefficient at the flow control valve VR,** mounted downstream on the discharge main near the reservoir (on the pipe with index j = 14 in Figure 2.17); the value of the coefficient ζ_{VR} is obtained as the solution of the system of nonlinear equations defining the operation of the hydraulic system.

Given the data in Table 4.1, for pipe with $j = 14$, the hydraulic resistance modulus (4.17) is written as follows:

$$M_{14} = 0.0826\left(\lambda_{14}\,\frac{L_{14}}{D_{14}} + (\zeta_{14} + \zeta_{VR})\right)\frac{1}{D_{14}^4} \tag{4.24}$$

I mention that, for a set of **experimental tests performed without consumers** (with the taps of the final consumers **C1÷C3** in the fully closed position, i.e. for $Q_{C1} = Q_{C2} = Q_{C3} = 0$), i.e. for $Q_{14} \equiv Q_T$, in a previous study **[*Ciuc et al, 2019b*]** we established that the value of the

coefficient ζ_{VR} can be determined using polynomial regression curves $\zeta_{VR} = \zeta_{VR}(Q_{14})$ of higher degree, defined in portions according to the critical value $Q_{14} \equiv Q_T = 0.83 \cdot 10^{-3}\,\mathrm{m^3/s} = 3\,\mathrm{m^3/h}$ of the total pumped flow (namely a polynomial of degree 3 for $Q_{14} < 3\,\mathrm{m^3/h}$, respectively of degree 5 for $Q_{14} \geq 3\,\mathrm{m^3/h}$);

- $\zeta_{C1}, \zeta_{C2}, \zeta_{C3}$ [dimensionless sizes] – **local hydraulic head loss coefficients at consumer valves C1÷C3** mounted on pipes with index *j* = 15÷17; these coefficients are obtained as the **solution of the system of nonlinear equations** defining the operation of the hydraulic system.

  Given the data in Table 4.1, for pipes with *j* = 15÷17, the hydraulic resistance moduli (4.17) are written as follows:

$$\begin{cases} M_{15} = 0.0826\left(\lambda_{15}\dfrac{L_{15}}{D_{15}} + \left(\Sigma\zeta_{15} + \zeta_{C1}\right)\right)\dfrac{1}{D_{15}^4} \\ M_{16} = 0.0826\left(\lambda_{16}\dfrac{L_{16}}{D_{16}} + \left(\Sigma\zeta_{16} + \zeta_{C2}\right)\right)\dfrac{1}{D_{16}^4} \\ M_{17} = 0.0826\left(\lambda_{17}\dfrac{L_{17}}{D_{17}} + \left(\Sigma\zeta_{17} + \zeta_{C3}\right)\right)\dfrac{1}{D_{17}^4} \end{cases} \tag{4.25}$$

- $\zeta_{V1}, \zeta_{V2}, \zeta_{V3}$ [dimensionless sizes] – **local hydraulic head loss coefficients at V1÷V3 valves mounted on pump suction lines -** lines with index *j* = 1*a*÷3*a* (Figure 4.13).

  The isolation valves V1÷V3 are usually in the normally open position (in which case, $\zeta_{V1} = \zeta_{V2} = \zeta_{V3} = 0.4$, as in Table 4.1); these valves were partially closed only **for some experimental tests where the cavitational operation of the pumps was studied**, in which case the coefficients $\zeta_{V1}; \zeta_{V2}; \zeta_{V3}$ are obtained as the **solution of the system of nonlinear equations** defining the operation of the hydraulic system.

  Given the data in Table 4.1, for pipes with $j = 1 \div 3$, the hydraulic resistance moduli (4.17) are written as follows:

$$\begin{cases} M_1 = M_{1a} + M_{1r} = 0.0826\left(\lambda_{1a}\dfrac{L_{1a}}{D_{1a}^5} + \dfrac{\left(\zeta_{1a} + \zeta_{V1}\right)}{D_{1a}^4}\right) + 0.0826\left(\lambda_{1r}\dfrac{L_{1r}}{D_{1r}^5} + \dfrac{\Sigma\zeta_{1r}}{D_{1r}^4}\right) \\ M_2 = M_{2a} + M_{2r} = 0.0826\left(\lambda_{2a}\dfrac{L_{2a}}{D_{2a}^5} + \dfrac{\left(\zeta_{2a} + \zeta_{V2}\right)}{D_{2a}^4}\right) + 0.0826\left(\lambda_{2r}\dfrac{L_{2r}}{D_{2r}^5} + \dfrac{\Sigma\zeta_{2r}}{D_{2r}^4}\right) \\ M_3 = M_{3a} + M_{3r} = 0.0826\left(\lambda_{3a}\dfrac{L_{3a}}{D_{3a}^5} + \dfrac{\left(\zeta_{3a} + \zeta_{V3}\right)}{D_{3a}^4}\right) + 0.0826\left(\lambda_{3r}\dfrac{L_{3r}}{D_{3r}^5} + \dfrac{\Sigma\zeta_{3r}}{D_{3r}^4}\right) \end{cases} \tag{4.26}$$

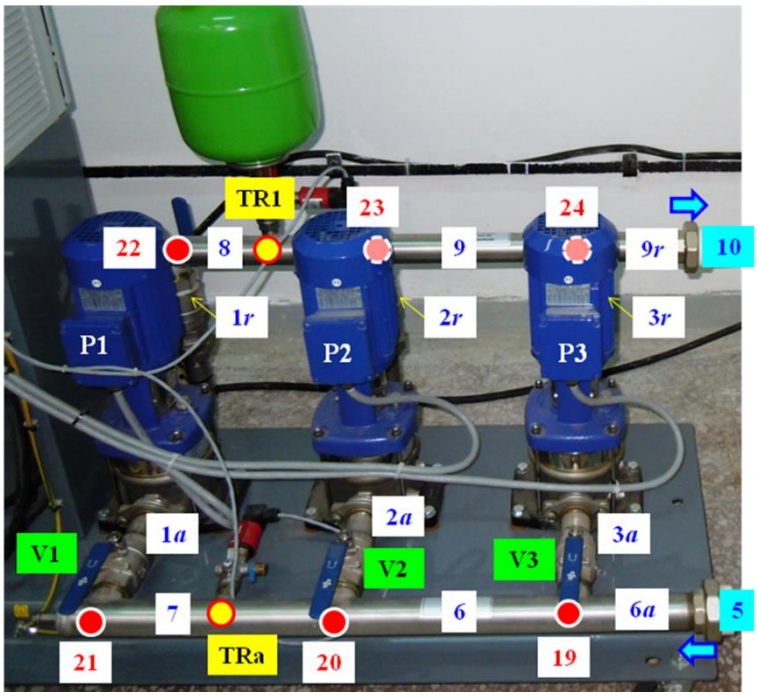

*Fig. 4.13. Pumping station (SP):pumps **P1÷P3**; index pipes j ∈{1a÷3a; 1r÷3r; 5; 6; 6a; 7÷9; 9r; 10}, index nodes j = 19÷24, wherej=19 is near the entrance to SP, and j=24 is at the exit of the SP; the valves **V1÷V3** on pump suction lines (j = 1a÷3a) – isolating valves in normally open position; pressure transducer **TRa** on the suction line from SP (in the middle of line j = 7); pressure transducer **TR1** on the discharge line from SP (in the middle of line j = 8)*

- ζ_{VA} [dimensionless sizes] – **the local hydraulic head loss coefficient at the VA valve at the upstream end of the suction main**, immediately after the outlet of the reservoir (on the pipe with index j = 4 in Figure 2.17); **the VA valve is usually in the normally open position (in which case,** $\zeta_{VA} = 0.4$); this valve was **partially closed only for some experimental tests studying the cavitational operation of the pumps**, in which case $\zeta_{VA} > 0.4$ and its value is obtained as the **solution of the system of nonlinear equations** defining the operation of the hydraulic system.

  Given the data in Table 4.1, for pipe with $j = 4$, the hydraulic resistance modulus (4.17) is written as follows:

$$M_4 = 0.0826\left(\lambda_4 \frac{L_4}{D_4} + (\Sigma\zeta_4 + \zeta_{VA})\right)\frac{1}{D_4^4} \qquad (4.27)$$

- $NPSH_a$ **[m] – net positive suction load available in the installation**, noted as appropriate $NPSH_{a1}$, $NPSH_{a2}$, respectively $NPSH_{a3}$ for pumps **P1÷P3**; the calculation relation for $NPSH_{a_i}$ with the index $i = 1 \div 3$, is applied to the suction circuit of the pump, between the free surface of the water in the tank R (where the speed is neglected, the pressure is equal to

the atmospheric pressure, whose absolute value is $p_{atm} = 10.328$ m.c.a., and the dimension of the free surface is z_R) and the suction flange of the pump considered, whose axis is at the dimension $z_a = 0.23$ m (according to Table 2.2, where $z_a = z_{19} = z_{20} = z_{21} = 0.23$ m):

$$NPSH_{a_i} = \frac{p_{atm} - p_v}{\rho g} - H_{ga} - h_{r\,R-a_i} \text{ pentru } i = 1 \div 3 \qquad (4.28)$$

where p_v is the vaporization pressure of water ($p_v = 0.238$ m.c.a., for water at a temperature of 20°C); $H_{ga} = (z_a - z_R)$ is the geometric suction head, the value of which is negative (**providing a counterpressure on pump suction**) because $z_R > z_a$; **height z_R of the free surface of the water in the tank is kept constant during the experimental tests**; this rating varied from one set of measurements to another between $z_R = 0.67$ m and $z_R = 0.77$ m (**most measurements** were made with $z_R = 0.73$ m); term $h_{r\,R-a_i}$ is the sum of the hydraulic load losses on the suction circuit and is defined **for each pump** as follows (Figure 4.14):

$$\begin{aligned} h_{r\,R-a1} &= (M_4 + M_5)Q_5^2 + M_6 Q_6^2 + (M_7 + M_{1a})Q_1^2, \text{ pentru pompa P1} \\ h_{r\,R-a2} &= (M_4 + M_5)Q_5^2 + M_6 Q_6^2 + M_{2a} Q_2^2, \quad \text{pentru pompa P2} \\ h_{r\,R-a3} &= (M_4 + M_5)Q_5^2 + M_{3a} Q_3^2, \quad \text{pentru pompa P3} \end{aligned} \qquad (4.29)$$

where the hydraulic resistance moduli are defined in (4.17); $M_{1a} \div M_{3a}$ are extracted from (4.26), and M_4 is explained in (4.27).

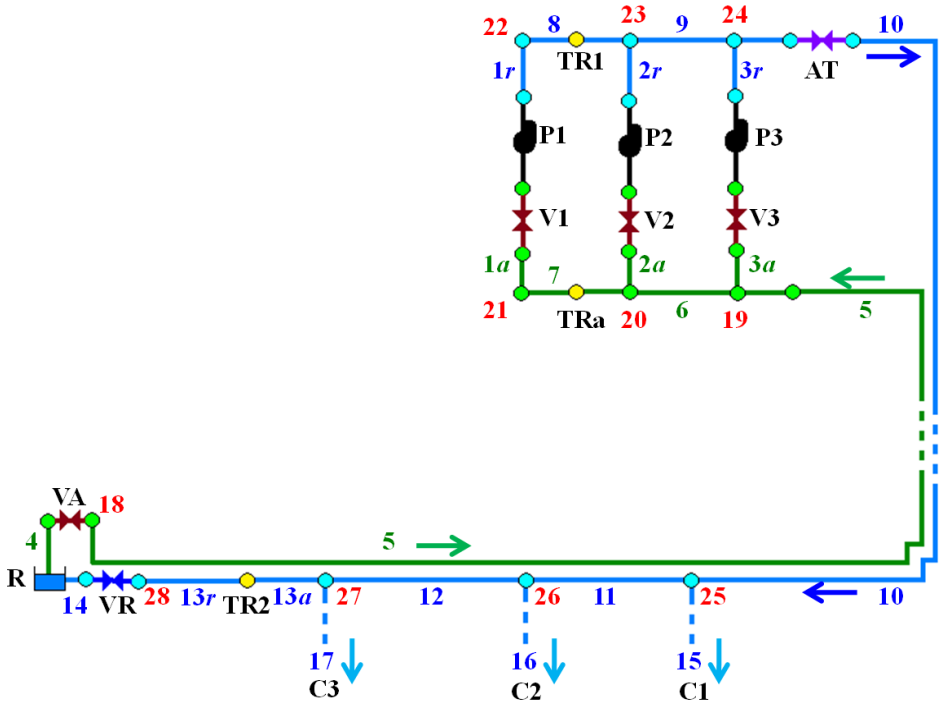

Fig. 4.14. Simplified hydraulic circuit diagram in Figure 2.17

According to the scheme in Figure 4.14 and taking into account the **continuity equation in nodes**, the relations (4.29), related to the **hydraulic load losses on the suction circuit**, become:

$$\begin{cases} h_{rR-a1} = (M_4 + M_5)Q_T^2 + M_6(Q_2 + Q_3)^2 + (M_7 + M_{1a})Q_1^2, & \text{pentru pompa P1} \\ h_{rR-a2} = (M_4 + M_5)Q_T^2 + M_6(Q_2 + Q_3)^2 + M_{2a}Q_2^2, & \text{pentru pompa P2} \\ h_{rR-a3} = (M_4 + M_5)Q_T^2 + M_{3a}Q_3^2, & \text{pentru pompa P3} \\ Q_T = Q_1 + Q_2 + Q_3 \end{cases} \tag{4.30}$$

Inserting then in (4.30) the calculated values of the pumped flow rates $Q_{F1} \div Q_{F3}$ (corresponding to the **F1÷F3 energy operating points of the pumps),** the hydraulic head losses on suction are written as follows:

$$\begin{aligned} h_{rR-a1} &= (M_4 + M_5)(Q_{F1} + Q_{F2} + Q_{F3})^2 + M_6(Q_{F2} + Q_{F3})^2 + (M_7 + M_{1a})Q_{F1}^2 \\ h_{rR-a2} &= (M_4 + M_5)(Q_{F1} + Q_{F2} + Q_{F3})^2 + M_6(Q_{F2} + Q_{F3})^2 + M_{2a}Q_{F2}^2 \\ h_{rR-a3} &= (M_4 + M_5)(Q_{F1} + Q_{F2} + Q_{F3})^2 + M_{3a}Q_{F3}^2 \end{aligned} \tag{4.31}$$

Inserting the results given by (4.31) into the expression (4.28) gives the values of the net **positive suction load available in the system for each pump** as a function of the three pumped flows:

$$NPSH_{a_i} = NPSH_{a_i}(Q_{F1}, Q_{F2}, Q_{F3}), \quad i = 1 \div 3 \tag{4.32}$$

The operating condition of non-cavitating pumps is based on the values calculated with the relations (4.16) for the **NPSH required by each pump**, respectively with the relation (4.32) for the **NPSH available in the plant**, the condition being expressed as:

$$NPSH_{F_i} < NPSH_{a_i}(Q_{F1}, Q_{F2}, Q_{F3}), \quad i = 1 \div 3 \tag{4.33}$$

4.2. Equation system describing system operation when prescribed pressure (PSP) refers to the pressure indicated by the TR1 transducer on the discharge line in the pump station

In this chapter, it is assumed that the **prescribed pressure** (set/desired), denoted p_{PSP} (where **PSP** = Pressure Set Point), **is to be maintained at the TR1 monitoring node located on the discharge line from the pumping station,** where the discharge pressure p_{ref} is indicated by the **TR1 pressure transducer** (positioned in SP as in Figures 2.6 and 2.17): $p_{ref} = p_{TR1}$.

In this thesis, **all experimental cavitational tests were performed only for the TR1 monitoring node.** Since in the tests **VA** and **V1÷V3** valves on the suction circuit were used in turn or simultaneously in different combinations of positions (open or partially closed), in this chapter we have **analysed separately different cases corresponding to the operation of the experimental stand,** namely:

- operation without final consumers, with the **VA** and **V1÷V3** valves on the suction circuit in the normally open position (subsection 4.2.1);
- operation without final consumers, with the **VA** valve partially closed and the **V1÷V3** valves in the normally open position (subchapter 4.2.2);
- operation without final consumers, with the **VA** valve in the normally open position and the **V1÷V3** valves partially closed (subsection 4.2.3);
- operation without end-users, with **VA** and **V1÷V3** partially closed (subsection 4.2.4);
- operation with end-users, with **VA** and **V1÷V3** partially closed (subchapter 4.2.5).

4.2.1. Case where the monitoring node is TR1 and the stand operates without end-users, with the VA and V1÷V3 valves in the normally open position

Here's how the experimental stand works:

- **no end-users -** with consumers' taps **C1÷C3** turned off, in which case the flow consumed is zero: $Q_{C1} = Q_{C2} = Q_{C3} = 0$;

- **with valves VA and V1÷V3 in the normally open position,** in which case the local hydraulic head loss coefficients have the values in Table 4.1: $\zeta_{VA} = 0.4$ and $\zeta_{V1} = \zeta_{V2} = \zeta_{V3} = 0.4$.

In this case, the operation of the stand depends on **4 unknown quantities**, namely: the pumped flow rates $Q_1 \div Q_3$ and the local hydraulic pressure drop coefficient ζ_{VR} at the regulating valve **VR -** to determine their values, **4 equations are needed**.

Pressure transducers **TR1** and **TRa**, mounted in the pumping station (SP) in the middle of the pipes with index $j = 8$ on the delivery side and $j = 7$ on the suction side of the SP (Figure 4.14), allow the measurement (determination) of the **differential pressure** Δp:

$$\Delta p = \left(p_{TR1} - p_{TRa} \right) \tag{4.34}$$

Between the two pipelines (therefore between the two pressure transducers) there is the difference in dimension $\Delta z = 0.3\,\text{m}$ (table 2.3). With the notations in **Section 4.1** and Figure 4.13, **the continuity equation in nodes**, together with **Bernoulli's relation** applied between node 19 (near the entrance to SP) and the node where **TRa** is located, respectively between the node where **TR1** is located and node 24 (at the exit from SP), form the following system of nonlinear equations:

$$\begin{cases} H_{h19} = H_{hTRa} + M_6(Q_1+Q_2)^2 + 0.5M_7Q_1^2 \\ H_{hTR1} = H_{h24} + 0.5M_8Q_1^2 + M_9(Q_1+Q_2)^2 \end{cases} \quad (4.35)$$

The difference of the hydrodynamic loads in nodes TR1 and TRa is equal to the difference of the piezometric loads in the same nodes (TR1 and TRa are mounted on pipes of the same diameter, through which flows the same flow, namely Q_1):

$$H_{hTR1} - H_{hTRa} = H_{pTR1} - H_{pTRa} = \frac{(p_{TR1} - p_{TRa})}{\rho g} + (z_{TR1} - z_{TRa}) = \frac{\Delta p}{\rho g} + \Delta z \quad (4.36)$$

Given (4.36), the difference of the hydrodynamic loads at nodes 24 and 19 in the system (4.35), equal to the difference of the piezometric loads between the same nodes - located on pipes of the same diameter, through which flows the same total flow Q_T defined by (4.3), is written:

$$H_{h24} - H_{h19} = H_{p24} - H_{p19} = \left(\frac{\Delta p}{\rho g} + \Delta z\right) - (M_6 + M_9)(Q_1+Q_2)^2 - 0.5(M_7+M_8)Q_1^2 \quad (4.37)$$

where, according to the data in Tables 2.2 and 4.1, the hydraulic resistance moduls $M_6 \div M_9$ have different values, although the pipes with index j = 6÷9 have the same dimensions.

In a previous experimental study **[*Dunca, Ciuc et al, 2017*]**, conducted on the same pumping station (SP), the simplifying assumption was adopted that the pumping heads H_{Fi} of the **P1**÷**P3** pumps (with index i = 1÷3) at the energy operating points **F1**÷**F3**, can be considered approximately equal to the load at point **F** of the parallel coupling - load found at node 24, immediately upstream of the SP outlet (Figure 4.13). **Such an assumption corresponds to neglecting hydraulic head losses on the pipelines inside the pumping station.** The graphical representation of the load curve of the pumps coupled in parallel corresponds to the graph in Figure 3.1, in which the "continuous regulation" of pump operation has been exemplified for the parallel coupling of one, two or three pumps equipping the experimental stand, for relative speeds between a minimum (chosen $r_m = 40/60 \cong 0.67$) and nominal value: $r = 1$.

Although the above assumption is acceptable, **in this PhD thesis, the hydraulic head losses on the pipelines inside the pumping station will be considered and explained** for each energy law written on the hydraulic path passing through any pump **P1**÷**P3**. **As a result, the law of energies is applied between node 19** (SP inlet) **and node 24** (SP outlet), passing through each pump, from P1, to P3, and the following 3 equations result:

$$H_{h19} + H_1 = H_{h24} + (M_6 + M_9)(Q_1+Q_2)^2 + (M_7 + M_1 + M_8)Q_1^2 \quad (4.38)$$

$$H_{h19} + H_2 = H_{h24} + (M_6 + M_9)(Q_1+Q_2)^2 + M_2Q_2^2 \quad (4.39)$$

$$H_{h19} + H_3 = H_{h24} + M_3Q_3^2 \quad (4.40)$$

In the energy laws (4.38)÷(4.40), the following compact notations were used for the hydraulic resistance moduli of the suction/backflow pipes between which the pumps are connected **P1÷P3**: $M_1 = (M_{1a} + M_{1r})$, $M_2 = (M_{2a} + M_{2r})$ and $M_3 = (M_{3a} + M_{3r})$. The resistance modules $M_1 \div M_3$ are explained by the relations (4.26) - these resistance modules depend on the flow rates Q_i (which are **unknowns of the system of equations**): $M_i = M_i(Q_i)$, with $i = 1 \div 3$. The values of the local hydraulic head loss coefficients ζ_j are given in Table 4.1.

Given the relation (4.37), the laws of energies (4.38)÷(4.40) can be compacted and rewritten by highlighting the **pumping heads** H_i (with $i = 1 \div 3$) as functions dependent on the pumped flows, as follows:

- for **P1 pump:**

$$H_1 = \left(\frac{\Delta p}{\rho g} + \Delta z \right) + 0.5\,(M_7 + M_8)Q_1^2 + M_1 Q_1^2 \tag{4.41}$$

- for **P2 pump**:

$$H_2 = \left(\frac{\Delta p}{\rho g} + \Delta z \right) - 0.5\,(M_7 + M_8)Q_1^2 + M_2 Q_2^2 \tag{4.42}$$

- for **P3 pump**:

$$H_3 = \left(\frac{\Delta p}{\rho g} + \Delta z \right) - (M_6 + M_9)(Q_1 + Q_2)^2 - 0.5\,(M_7 + M_8)Q_1^2 + M_3 Q_3^2 \tag{4.43}$$

At the outlet of the SP, on the discharge main with index j = 10, there is the **AT** gauge with the help of which the total pumped flow, noted Q_T (by the volume V_T recorded in a given period of time t_T), can be determined. The **continuity equation** at the outlet of the SP (4.3) can be rewritten as:

$$Q_1 + Q_2 = Q_T - Q_3 \tag{4.44}$$

Inserting (4.44) and the $H_i = H_i(Q_i)$ expressions from (4.6) into equations (4.41)÷(4.43), the following functions result $f_1 = 0$, $f_2 = 0$ and $f_3 = 0$ **[*Ciuc et al, 2019a*]**, where $a = 31.62$ and $b = 17.625 \cdot 10^6$:

- for **P1 pump**:

$$f_1 = \left(a \cdot r_1^2 - b \cdot Q_1^2 \right) - \left(\frac{\Delta p}{\rho g} + \Delta z \right) - 0.5\,(M_7 + M_8)Q_1^2 - M_1 Q_1^2 = 0 \tag{4.45}$$

- for **P2 pump**:

$$f_2 = \left(a \cdot r_2^2 - b \cdot Q_2^2 \right) - \left(\frac{\Delta p}{\rho g} + \Delta z \right) + 0.5\,(M_7 + M_8)Q_1^2 - M_2 Q_2^2 = 0 \tag{4.46}$$

- for **P3 pump**:

$$f_3 = \left(a \cdot r_3^2 - b \cdot Q_3^2\right) - \left(\frac{\Delta p}{\rho g} + \Delta z\right) + (M_6 + M_9)(Q_T - Q_3)^2 + \\ + 0.5\,(M_7 + M_8)Q_1^2 - M_3 Q_3^2 = 0 \tag{4.47}$$

The system of 3 nonlinear equations formed by the functions $f_i = 0$ (4.45)÷(4.47) has 3 unknowns, namely the pumped flows Q_i (with $i = 1 \div 3$).

Due to the flow dependence of Darcy's coefficients λ_j defined by the Swamee-Jain formula (4.18), coefficients which are found in the expression of the hydraulic resistance modules M_j (4.17), functions (4.45)÷(4.47) forms a system of strongly nonlinear equations, which can be solved numerically *[Mădulărea, 2022],* using the specialized function called **fsolve** in MATLAB ® [*MATLAB, 2022*] and GNU Octave [*Eaton et al, 2022*].

Range of flow rates corresponding to experimental stand tests **[*Ciuc et al, 2019a*]**, [*Mădulărea, 2022*] shows that on pipes inside the SP (on pipes with index $j \in \{1a \div 3a; 1r \div 3r; 6a; 6 \div 9; 9a\}$) **the flow is turbulent pre-flow,** and on the PPR pipes of the hydraulic installation (on pipes with index $j \in \{4; 5; 10 \div 14\}$), **the flow is turbulently smooth,** so **use of the Swamee-Jain formula (4.18) is indicated.**

We also checked the solutions (flow values) under the assumption of a **rough turbulent flow on the pipes** inside the SP - regime for which the Darcy coefficient λ_j can be calculated with the Prandtl-Nikuradse formula (4.20) – formula that does not depend on flow. Based on this assumption, the degree of nonlinearity of the system of equations (4.45) ÷ (4.47) is reduced and the solution of the system can be easily determined in this way: extract (by radical) the flow rate Q_1 from (4.45), and then enter into (4.46) and (4.47), from where the values Q_2 and Q_3 are extracted (by radical). **We verified this assumption by calculation** with both the Swamee-Jain formula (4.18) and the Prandtl-Nikuradse formula (4.20), and the difference between the calculated pumped flow values varies in the range $[-0.00023\ldots+0.00011]$ in **litres/s (!),** so the difference is negligible, being well below the accuracy class of the **AT** apometer. As a result, the assumption of rough turbulent flow can be adopted to more easily calculate pumped flows in some particular cases, such as the simple case, discussed in this subchapter 4.2.1.

However, in order to cover all the cases studied, **the thesis will strictly consider the Swamee-Jain formula.**

Based on the relations (4.6) describing the load curves $H_i = H_i(Q_i)$ of the pumps at any relative speed $r_i = n_i / n_0 = f_i / f_0$ (with $i = 1 \div 3$) and based on the continuity equations that apply at each node of the system, the **law of energies on the closed hydraulic circuit, starting from the reservoir R, passing through each pump P1÷P3 and returning back to the reservoir**,

leads to the following nonlinear equations, written in turn as functions $f_4 = 0$, $f_5 = 0$ and $f_6 = 0$, namely:

$$f_4 = a \cdot r_1^2 - b \cdot Q_1^2 - \left(M_4 + M_5 + M_{6a} + M_{9r} + \sum_{j=10}^{13} M_j + M_{14} \right) Q_T^2 - \\ - h_{l\,AT} - (M_6 + M_9)(Q_1 + Q_2)^2 - (M_7 + M_1 + M_8) Q_1^2 = 0 \tag{4.48}$$

$$f_5 = a \cdot r_2^2 - b \cdot Q_2^2 - \left(M_4 + M_5 + M_{6a} + M_{9r} + \sum_{j=10}^{13} M_j + M_{14} \right) Q_T^2 - \\ - h_{l\,AT} - (M_6 + M_9)(Q_1 + Q_2)^2 - M_2 Q_2^2 = 0 \tag{4.49}$$

$$f_6 = a \cdot r_3^2 - b \cdot Q_3^2 - \left(M_4 + M_5 + M_{6a} + M_{9r} + \sum_{j=10}^{13} M_j + M_{14} \right) Q_T^2 - \\ - h_{l\,AT} - M_3 Q_3^2 = 0 \tag{4.50}$$

where the local hydraulic head loss $h_{l\,AT}$ through the **AT** gauge mounted on the pipe with j = 10 is defined in (4.22) by a polynomial regression curve: $h_{l\,AT} = h_{l\,AT}(Q_T)$. The hydraulic resistance modul M_j of the $f_4 \div f_6$ functions are defined in (4.17) with the values of the local hydraulic head loss coefficients ζ_j given in Table 4.1 (where the values ζ_{VA} and $\zeta_{V1} \div \zeta_{V3}$ correspond to the valves **VA** and **V1÷V3** in the open position); the value ζ_{VR} of the control valve **VR** has to be calculated. The hydraulic resistance moduli M_4 and M_{14} incorporating also the component due to local hydraulic head losses in valve **VA** (from pipe *j = 4*) and in valve **VR** (from pipe *j = 14*), respectively, are written:

$$\begin{cases} M_4 = 0.0826 \left(\lambda_4 \dfrac{L_4}{D_4^5} + \dfrac{(\zeta_4 + \zeta_{VA})}{D_4^4} \right) \\ M_{14} = 0.0826 \left(\lambda_{14} \dfrac{L_{14}}{D_{14}^5} + \dfrac{(\zeta_{14} + \zeta_{VR})}{D_{14}^4} \right) \end{cases} \tag{4.51}$$

In (4.51), the coefficient ζ_{VR} is unknown and depends on the flow through, i.e. the flow Q_{14} entering the reservoir through the pipe *j* = 14: $\zeta_{VR} = \zeta_{VR}(Q_{14})$.

The regulating valve VR was used in different positions from fully closed to fully open **in all experimental tests**, so for any non-zero value of flow entering the tank through pipe j = 14, the coefficient ζ_{VR} is **non-zero:** $\zeta_{VR} > 0$. Knowing the values of the pumped flow rates $Q_1 \div Q_3$, **calculated as the solution of the system** (4.45)÷(4.47), **the unknown value** of the ζ_{VR} coefficient corresponding to the **control valve VR can be calculated** using one of the functions

(4.48)÷(4.50) - **any of these 3 functions**. The solution ζ_{VR} of any equation (4.48)÷(4.50) can be obtained using the specialised function ***fsolve*** in MATLAB.

For all experimental tests conducted without consumers, with the prescribed pressure (PSP) set at the TR1 pressure transducer, during which the VA and V1÷V3 valves are held fully open, for each set of recorded values: $\Delta p = \left(p_{TR1} - p_{TRa}\right)$, $Q_T = V_T / t_T$ and $r_1 \div r_3$ (given by the displayed frequencies $f_1 \div f_3$), the calculated values of pumped flow rates $Q_1 \div Q_3$ correspond to the flow rates $Q_{F1} \div Q_{F3}$ at the **energy operating points F1÷F3**. Inserting values $Q_{F1} \div Q_{F3}$ in relations (4.7), (4.9) and (4.16), respectively, gives the pumping heads $H_{F1} \div H_{F3}$, performance $\eta_{F1} \div \eta_{F3}$ and values $NPSH_{F1} \div NPSH_{F3}$ of the NPSH required by the pumps at **F1÷F3**. Inserting values $Q_{F1} \div Q_{F3}$ in relation (4.32), based on relations (4.28) and (4.31), we obtain the values $NPSH_{a1} \div NPSH_{a3}$ of the NPSH available in the plant, then check the inequality (4.33) to determine the operating mode: no cavitations, incipient cavitations or developed cavitations. Based on the relations (4.10) and (4.11) the values of the pump power $P_{F1} \div P_{F3}$, respectively the electric power $P_{el1} \div P_{el3}$ absorbed by the electric motor of each pump can be calculated. This then gives the total power consumed for pumping P_T (4.12) and the total electrical power absorbed in the pumping station, denoted P_{elT} (4.13).

The methodology described in this chapter allows the calculation of the parameters that define the energy and cavitation operation of P1÷P3 pumps, according to the scheme in Figure 4.15.

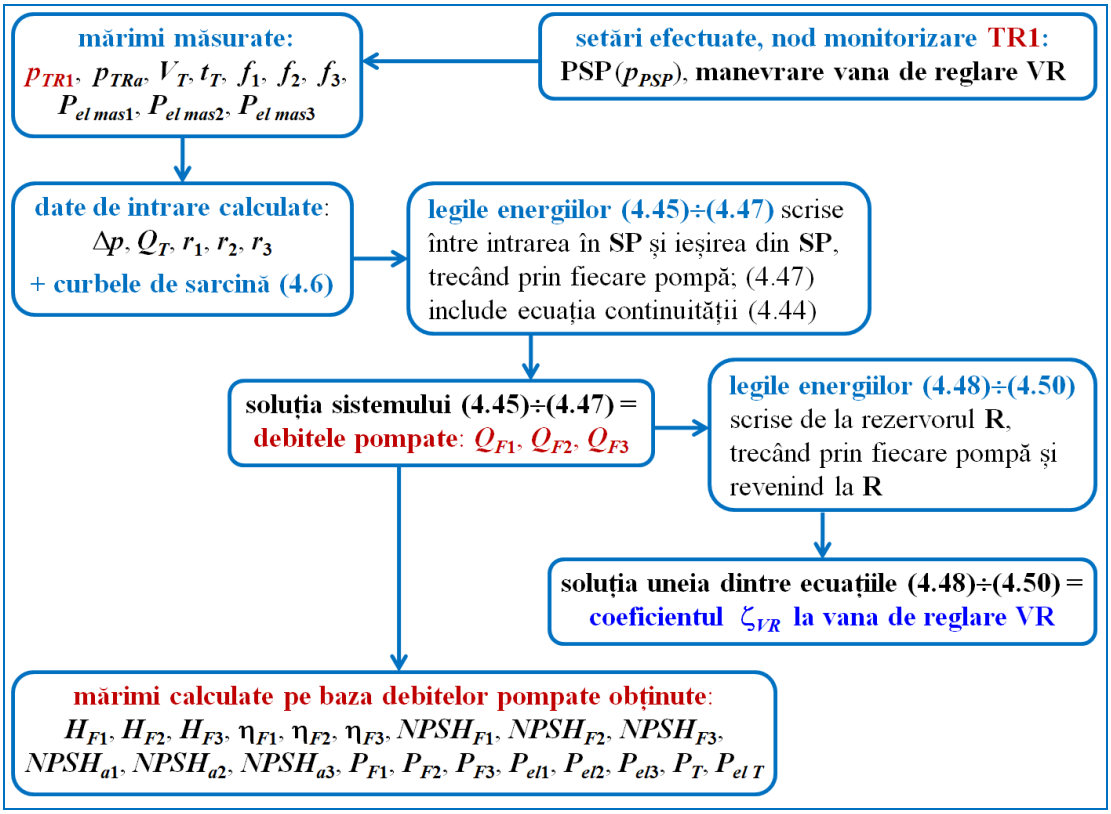

Fig. 4.15. Logic diagram of solution determination - TR1 monitoring node, operation without final consumers, with VA and V1÷V3 valves on suction circuit in normally open position

This calculation methodology corresponds to a **sensorless control approach in the pumping station [*Ciuc et al, 2019a*]** - an approach considered acceptable when working with insufficient measuring instruments (as mentioned, the experimental stand is not equipped with flow meters, and inside the pumping station, neither the flow pumped with each pump nor the pressure jump between suction and discharge of each pump can be measured).

The continuity equation (4.3) and the energy laws (4.45)÷(4.50) correspond to the case where **all pumps are in operation**. In the case when **one of the pumps is off**, respectively when **two pumps are off**, the system of equations simplifies (one of the pumped flow values being zero, respectively two of the pumped flow values being zero).

The sum of the solutions (pumped flows) $Q_{F1} \div Q_{F3}$ calculated numerically (by solving the system of equations (4.45)÷(4.47) defining the operation of the plant) is checked in terms of a relative error ε_Q with respect to the corresponding measured value Q_T:

$$\varepsilon_Q = 100[Q_T - (Q_{F1} + Q_{F2} + Q_{F3})_{solutie}]/Q_T \quad [\%] \tag{4.52}$$

I emphasize that for a given experimental test, the system of equations (4.45)÷(4.47) solved numerically incorporates **4 measured values**: the relative pressures recorded at pressure transducers **TR1** and **TRa** (inserted into the system by differential pressure Δp (4.34)), respectively the volume of water V_T at the water meter **AT** and time t_T in which this volume is

recorded (entered into the system by total flow Q_T (4.2)). So the numerical results are definitely affected by inherent errors (measurement errors and preliminary calculation errors of the input data to the system). Pressure transducers have an accuracy of ± 0.03 bar (± 0.3 m.c.a.), so the differential pressure Δp can be determined with an accuracy of ± 0.6 m.c.a. The AT meter mounted on the DN40 pipeline has an accuracy of ± 0.05 litres [*Bmeters, 2021b*], so theoretically, the volume V_T can be measured with an accuracy of ± 0.05 litres; In the experimental stand, the volume value V_T is **displayed in litres, without decimals, on the PLC metering screen** (Figure 4.2), which reduces the accuracy of the measurement (it is possible to get a reading error both when resetting the meter and when reaching the desired volume). The timing of time t_T is also subject to a measurement error due to the human factor - due to the reaction time when starting the timer (simultaneously with resetting the water meter) and when stopping the timer (when the desired volume is reached) - a cumulative measurement error of a few tenths of a second is estimated (± 0.5 s can be allowed). It follows that, theoretically, the flow rate Q_T can be measured with an accuracy of ± 0.1 litres/s. Calculations have shown that the relative error values ε_Q (4.52) can also reach extreme values of order $\pm 8\%$.

The sum of the calculated values of the electrical powers absorbed by motors $P_{el1} \div P_{el3}$ is checked in terms of a **relative error** ε_{el} with respect to the **sum of the measured values of the electrical powers absorbed by motors** $P_{el_{mas1}} \div P_{el_{mas3}}$, with the relation:

$$\varepsilon_{et} = \frac{\left(P_{el_{mas1}} + P_{el_{mas2}} + P_{el_{mas3}}\right) - \left(P_{el_1} + P_{el_2} + P_{el_3}\right)_{calculate}}{P_{el_{mas1}} + P_{el_{mas2}} + P_{el_{mas3}}} 100 \quad [\%] \qquad (4.53)$$

The ε_{el}-error values are certainly affected by inherent errors - I stress that the measurement of electrical powers is not very precise: **the measured values are displayed in kW, with only two decimal places**, and the recorded values were in the range **0.11÷0.55 kW**.

4.2.2. Where the monitoring node is TR1 and the stand operates without end-users, with the VA valve partially closed and the V1-V3 valves in the normally open position

Here's how the experimental stand works:

- **no end-users -** with consumers' taps **C1÷C3** turned off, in which case the flow consumed is zero: $Q_{C1} = Q_{C2} = Q_{C3} = 0$;
- **with valve VA partially closed,** in which case the local hydraulic pressure drop coefficient ζ_{VA} has an **unknown value**, which has to be calculated;
- **with V1÷V3 valves in the normally open position,** in which case the local hydraulic head loss coefficients have the values in Table 4.1: $\zeta_{V1} = \zeta_{V2} = \zeta_{V3} = 0.4$.

In this case, the operation of the stand depends on **5 unknown quantities**, namely: the pumped flow rates $Q_1 \div Q_3$ and the local hydraulic head loss coefficients: ζ_{VR} at the regulating valve **VR** and ζ_{VA} at the valve **VA** - to determine their values, **5 equations are needed**.

Knowing the values of the pumped flow rates $Q_1 \div Q_3$, calculated as the solution of the system (4.45)÷(4.47), **the unknown values of the two local hydraulic head loss coefficients can be calculated, namely:** ζ_{VR} at the **VR control valve** and ζ_{VA} at the **VA valve**, **using two of the three functions** (4.48)÷(4.50). The solutions ζ_{VR} and ζ_{VA} for the system of two equations selected from the group of three (4.48)÷(4.50) can be obtained using the specialized function ***fsolve*** in MATLAB.

The parameters defining the energy and cavitation operation of P1÷P3 pumps can be determined according to the logic scheme shown in Figure 4.16. Finally, the relative errors ε_Q (4.52) and ε_{el} (4.53), resulting between the measured values and the calculated values for the pumped flow rates, respectively for the total electrical power absorbed in the pumping station, are calculated.

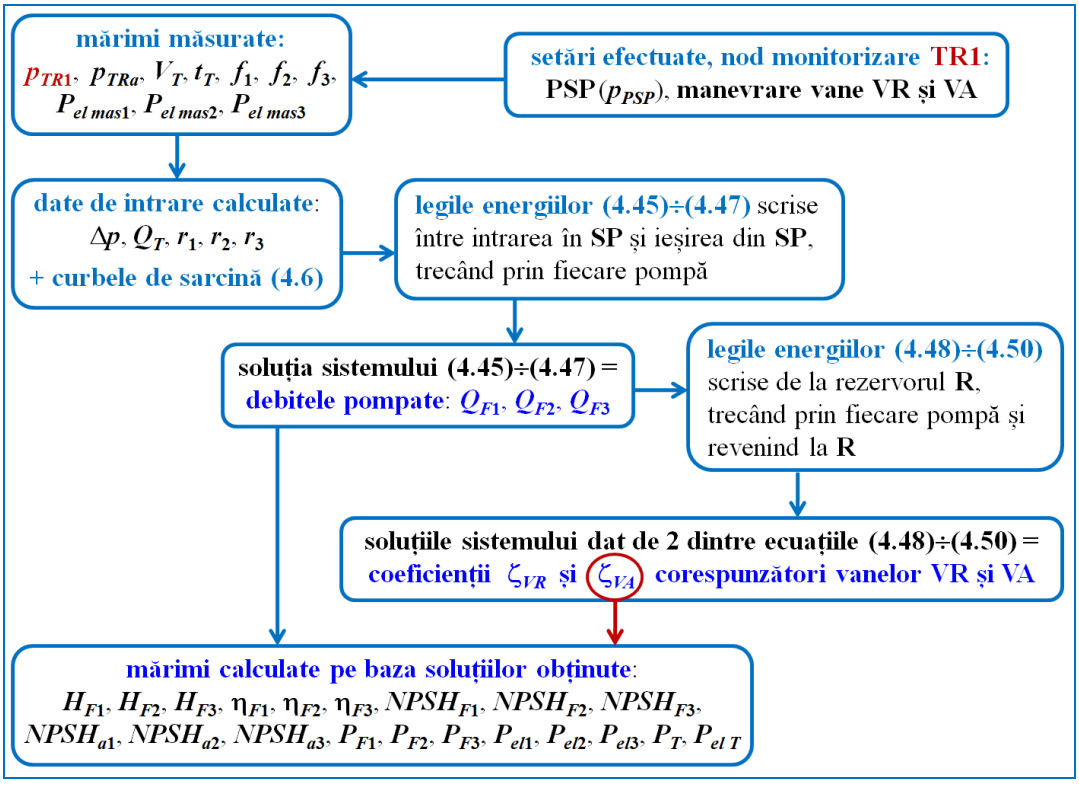

*Fig. 4.16. Logic diagram of solution determination - **TR1** monitoring node, operation without final consumers, with VA valve partially closed and V1÷V3 valves in normal open position*

4.2.3. If the stand operates without end-users, with the VA valve in the normally open position and the V1÷V3 valves partially closed

În cele ce urmează, standul experimental funcționează astfel:

- **no end-users -** with consumers' taps **C1÷C3** turned off, in which case the flow consumed is zero: $Q_{C1} = Q_{C2} = Q_{C3} = 0$;

- **with the VA valve** (valve located upstream of the suction line) in the **normally open position**, in which case the local hydraulic pressure drop coefficient has the value given in Table 4.1: $\zeta_{VA} = 0.4$;

- **with V1÷V3 valves** (valves located immediately upstream of the suction section of each pump) **partially closed, simultaneously or in turn (one or two out of three)**, in which case the local hydraulic pressure drop coefficients $\zeta_{V1}; \zeta_{V2}; \zeta_{V3}$ have **unknown values**, which must be calculated.

In this case, the operation of the stand depends on **7 unknown quantities**, namely: the pumped flow rates $Q_1 \div Q_3$ and the local hydraulic head loss coefficients: ζ_{VR} at the control valve **VR** and $\zeta_{V1} \div \zeta_{V3}$ at the valves **V1÷V3** - to determine their values, **7 equations are needed**. So, **in addition to the 6 laws of energies already written** - the $f_1 \div f_6$-functions defined by (4.45)÷(4.50), another law of energies must be added, for example **Bernoulli's relation written on the hydraulic discharge circuit**, between the node where the pressure transducer **TR1** is located and a point on the free surface of the reservoir R, as follows:

$$H_{hTR1} = H_{hR} + 0.5M_8Q_1^2 + M_9(Q_1 + Q_2)^2 + h_{lAT} + \left(M_{9r} + \sum_{j=10}^{14} M_j\right)Q_T^2 = 0 \qquad (4.54)$$

where the hydrodynamic loads at node **TR1** and at the free reservoir surface **R** are defined in (4.5); at the free reservoir surface **R**, the water velocity is assumed to be zero and the relative pressure is also zero, **R** being open at atmospheric pressure.

With these considerations, **Bernoulli's relation** (4.54) between **TR1** and **R** is rewritten in the form of the function $f_7 = 0$, as follows:

$$\begin{aligned} f_7 = &\left(M_{c8}Q_1^2 + \frac{p_{TR1}}{\rho g} + z_{TR1}\right) - z_R - 0.5M_8Q_1^2 - M_9(Q_1 + Q_2)^2 - \\ &- h_{lAT} - \left(M_{9r} + \sum_{j=10}^{14} M_j\right)Q_T^2 = 0 \end{aligned} \qquad (4.55)$$

where $M_{c8} = 0.0826/D_8^4$ is the kinetic modulus calculated with the diameter of the pipe with index $j = 8$, on which the pressure transducer **TR1** is located (the calculation is made under the assumption of *hydraulically short pipes*).

The system of **7 strongly nonlinear equations**, formed by the functions (4.45)÷(4.50) and (4.55), has **7 unknowns** ($Q_1 \div Q_3, \zeta_{VR}, \zeta_{V1} \div \zeta_{V3}$). The solution of the system of equations

$\{ f_1 = 0 ; ... ; \ f_7 = 0 \}$ can be obtained using the specialized function ***fsolve*** in MATLAB. Knowing the solution of the above system of equations, one **can calculate the parameters defining the energy and cavitation operation of the pumps P1÷P3**, according to the logic scheme illustrated in Figure 4.17. In this case too, the relative errors ε_Q (4.52) and ε_{el} (4.53) are calculated at the end.

When the **V1÷V3 valves are not operated simultaneously**, the system is simplified as follows:

- if only one pump suction valve **Vi** is operated partially closed, (where **i** takes a single value from the crowd {1; 2; 3}), and the other 2 valves **Vk** (where **k** ∈ {1; 2; 3} and **k ≠ i**), are in the normally open position, then the system reduces to **5 equations with 5 unknowns** ($Q_1 \div Q_3$, ζ_{VR}, ζ_{Vi}); for the 2 valves kept open, the value of the local hydraulic pressure drop coefficients ζ_{Vk} is taken as 0.4, as in Table 4.1;

- if **two valves Vi** (where **i** takes two values from the crowd {1; 2; 3}) are operated **(partially closed)**, and the third valve Vk (where **k** ∈ {1; 2; 3} and **k ≠ i**) is in the normally open position, then the system reduces to **6 equations with 6 unknowns** (pumped flows $Q_1 \div Q_3$, two coefficients ζ_{Vi} and the coefficient ζ_{VR}); for the valve kept open, the value of the coefficient ζ_{Vk} is taken as 0.4, as in Table 4.1.

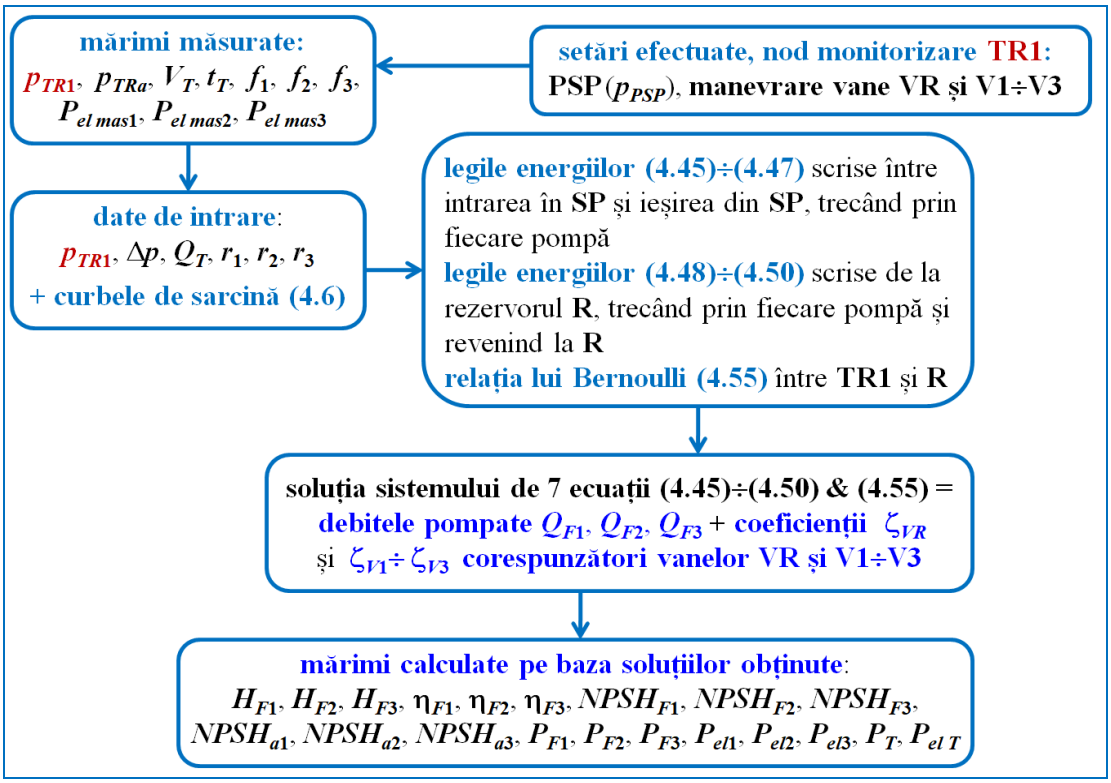

*Fig. 4.17. Logic diagram for determining the solutions - monitoring node **TR1**, operation without final consumers, with valve VA in the normally open position and with valves V1÷V3 partially closed*

4.2.4. Case where the monitoring node is TR1 and the stand operates without end-users, with the VA and V1÷V3 valves partially closed

În cele ce urmează, standul experimental funcționează astfel:

- **no end-users -** with consumers' taps **C1÷C3** turned off, in which case the flow consumed is zero: $Q_{C1} = Q_{C2} = Q_{C3} = 0$;
- **with valve VA partially closed,** in which case the local hydraulic pressure drop coefficient ζ_{VA} has an **unknown value**, which has to be calculated;
- **with partially closed V1÷V3 valves,** simultaneously or in turn (one or two out of three), in which case the $\zeta_{V1}; \zeta_{V2}; \zeta_{V3}$ coefficients have **unknown values**, which must be calculated.

In this case, the operation of the stand depends on **8 unknown quantities**, namely: pumped flow rates $Q_1 \div Q_3$ and local hydraulic head loss coefficients: ζ_{VR} at the **VR** control valve, ζ_{VA} at the **VA** valve and $\zeta_{V1} \div \zeta_{V3}$ at the valves **V1÷V3** - to determine their values, **8 equations are needed**. **In addition to the 7 energy laws already written** - the $f_1 \div f_7$ -functions defined by (4.45)÷(4.50) and (4.55), another energy law has to be added, for example **Bernoulli's relation** written on the **hydraulic suction circuit**, between a point on the free surface of the reservoir **R** and the node where the pressure transducer **TRa** is located, as follows:

$$H_{hR} = H_{hTRa} + (M_4 + M_5 + M_{6a})Q_T^2 + M_6(Q_1 + Q_2)^2 + 0.5M_7Q_1^2 = 0 \qquad (4.56)$$

where the hydrodynamic loads at the free surface of the reservoir **R** and at the node **TRa** are defined in (4.5). **Bernoulli's relation** (4.56) between **R** and **TRa** is rewritten as function $f_8 = 0$, as follows:

$$f_8 = z_R - \left(M_{c7}Q_1^2 + \frac{p_{TRa}}{\rho g} + z_{TRa} \right) - (M_4 + M_5 + M_{6a})Q_T^2 - M_6(Q_1 + Q_2)^2 - 0.5M_7Q_1^2 = 0 \quad (4.57)$$

where $M_{c7} = 0.0826 / D_7^4$ is the kinetic modulus calculated with the diameter of the pipe with index $j = 7$, on which the pressure transducer TRa is located.

The system of **8 strongly nonlinear equations** formed by the functions (4.45)÷(4.50), (4.55) and (4.57), has **8 unknowns** ($Q_1 \div Q_3, \zeta_{VR}, \zeta_{VA}, \zeta_{V1} \div \zeta_{V3}$). Solution of the equation system $\{ f_1 = 0;\ ...;\ f_8 = 0 \}$ an be obtained using the specialized MATLAB function ***fsolve***. Knowing the solution of the above system of equations, one can **calculate the parameters that define the energy and cavitation operation of the pumps P1÷P3**, according to the logic scheme illustrated in Figure 4.18. In this case too, the relative errors ε_Q (4.52) and ε_{el} (4.53) are calculated at the end.

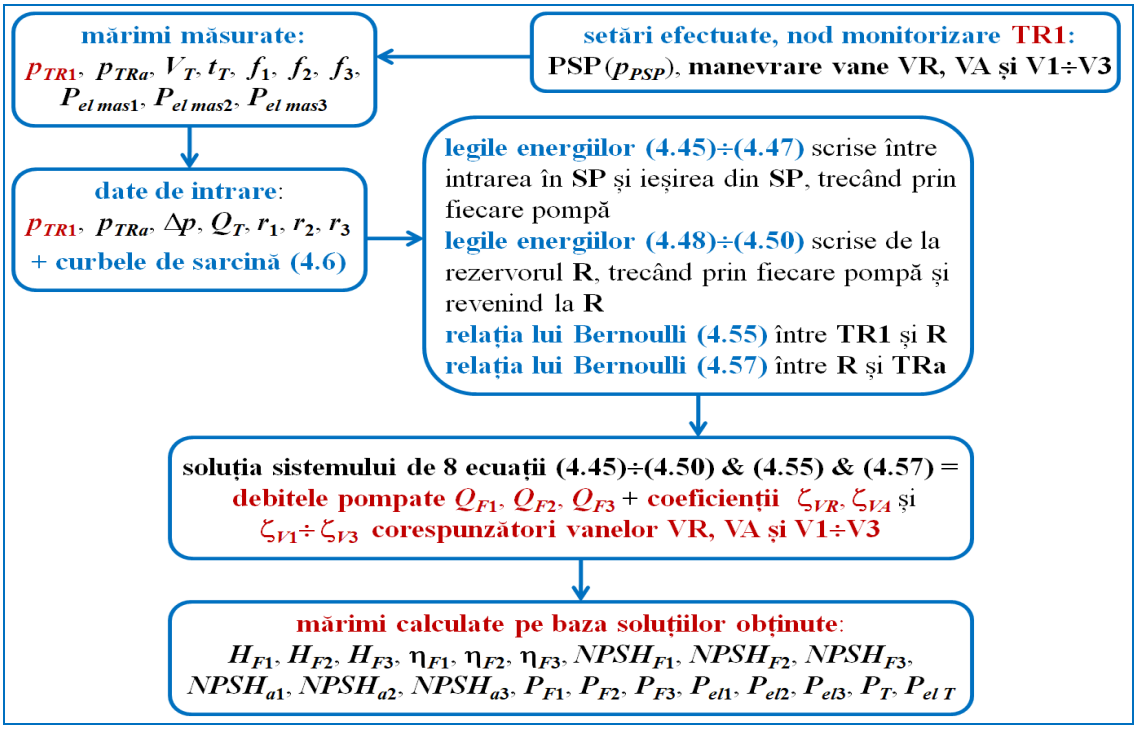

*Fig. 4.18. Logic diagram for determining the solutions - monitoring node **TR1**, operation without final consumers, with VA and V1÷V3 valves partially closed*

If the **V1÷V3 valves are not operated simultaneously**, the system is simplified as explained in subchapter 4.2.3, respectively reduced to **6 equations with 6 unknowns** if only one pump **suction valve is operated (partially closed)**, respectively reduced to **7 equations with 7 unknowns** if **two pump suction valves are partially closed**.

4.2.5. If the monitoring node is TR1 and the stand is working with end-users, with VA and V1÷V3 valves partially closed

Here's how the experimental stand works:

- **with final consumers** - **with consumer taps C1÷C3 partially closed**, in which case the consumed flow rates $Q_{C1} \div Q_{C3}$ are measured by the volumetric method using water meters **AC1÷AC3** and the local hydraulic head loss coefficients $\zeta_{C1}; \zeta_{C2}; \zeta_{C3}$ have **unknown values**, which have to be calculated;
- **with valve VA partially closed**, in which case the local hydraulic pressure drop coefficient ζ_{VA} has an unknown value, which has to be calculated;
- **with V1÷V3 valves partially closed, simultaneously or in turn (one or two out of three)**, in which case the $\zeta_{V1}; \zeta_{V2}; \zeta_{V3}$ coefficients have unknown values, which must be calculated.

For the **case of consumer operation**, **the continuity equation at tank R** is written as follows:

$$Q_T = Q_{C1} + Q_{C2} + Q_{C3} + Q_{14} \tag{4.58}$$

where Q_{C1}, Q_{C2} and Q_{C3} are the flows consumed in the end nodes (nodes $j = 29 \div 31$ in Figure 2.17) - these "consumed" flows are returned to the reservoir through a collecting gutter.

In this general case, where all **VR**, **VA**, **V1÷V3** valves and **C1÷C3** valves are operated within the stand, the operation of the stand depends on **11 unknown quantities**, namely: the pumped flow rates $Q_1 \div Q_3$ and the local hydraulic head loss coefficients, namely: ζ_{VR} at the **VR** control valve, ζ_{VA} at the **VA** valve $\zeta_{V1} \div \zeta_{V3}$ at the **V1÷V3** valves and $\zeta_{C1} \div \zeta_{C3}$ at the **C1÷C3** valves; to determine their values, **11 equations are needed.**

The $f_1 \div f_3$-functions previously defined by (4.45)÷(4.47) **remain valid** for operation with end consumers □ these functions represent 3 energy laws, written between **node 19** (SP inlet) and **node 24** (SP outlet), **passing through each pump P1÷P3.** Also, **Bernoulli's relation between R** and **TRa**, defined by the f_8-function (4.57), **remains valid**. On the other hand, the energy laws (4.48)÷(4.50) and (4.55), expressed by $f_4 \div f_7$-functions, **have to be rewritten taking into account the continuity equation** (4.58), in which the consumed flows $Q_{C1} \div Q_{C3}$ appear. This results in the following 4 new functions, denoted $f_9 \div f_{12}$ (these will replace the previous functions $f_4 \div f_7$):

- **energy laws from R,** passing through each pump **P1÷P3** and returning back to **R**:

$$\begin{aligned} f_4 \to f_9 = a \cdot r_1^2 - b \cdot Q_1^2 - \left(M_4 + M_5 + M_{6a} + M_{9r} + M_{10}\right) Q_T^2 - h_{l\,AT} - \\ - M_{11}\left(Q_T - Q_{C1}\right)^2 - M_{12}\left(Q_T - Q_{C1} - Q_{C2}\right)^2 - \\ - \left(M_{13} + M_{14}\right)\left(Q_T - Q_{C1} - Q_{C2} - Q_{C3}\right)^2 - \\ - \left(M_6 + M_9\right)\left(Q_1 + Q_2\right)^2 - \left(M_7 + M_1 + M_8\right) Q_1^2 = 0 \end{aligned} \tag{4.59}$$

$$\begin{aligned} f_5 \to f_{10} = a \cdot r_2^2 - b \cdot Q_2^2 - \left(M_4 + M_5 + M_{6a} + M_{9r} + M_{10}\right) Q_T^2 - h_{l\,AT} - \\ - M_{11}\left(Q_T - Q_{C1}\right)^2 - M_{12}\left(Q_T - Q_{C1} - Q_{C2}\right)^2 - \\ - \left(M_{13} + M_{14}\right)\left(Q_T - Q_{C1} - Q_{C2} - Q_{C3}\right)^2 - \\ - \left(M_6 + M_9\right)\left(Q_1 + Q_2\right)^2 - M_2 Q_2^2 = 0 \end{aligned} \tag{4.60}$$

$$\begin{aligned} f_6 \to f_{11} = a \cdot r_3^2 - b \cdot Q_3^2 - \left(M_4 + M_5 + M_{6a} + M_{9r} + M_{10}\right) Q_T^2 - h_{l\,AT} - \\ - M_{11}\left(Q_T - Q_{C1}\right)^2 - M_{12}\left(Q_T - Q_{C1} - Q_{C2}\right)^2 - \\ - \left(M_{13} + M_{14}\right)\left(Q_T - Q_{C1} - Q_{C2} - Q_{C3}\right)^2 - M_3 Q_3^2 = 0 \end{aligned} \tag{4.61}$$

- **Bernoulli's relation** between **TR1** and **R**:

$$f_7 \to f_{12} = \left(M_{c8} Q_1^2 + \frac{p_{TR1}}{\rho g} + z_{TR1} \right) - z_R - 0.5 M_8 Q_1^2 - M_9 (Q_1 + Q_2)^2 - \\ - (M_{9r} + M_{10}) Q_T^2 - h_{l\,AT} - M_{11} (Q_T - Q_{C1})^2 - \\ - M_{12} (Q_T - Q_{C1} - Q_{C2})^2 - (M_{13} + M_{14}) (Q_T - Q_{C1} - Q_{C2} - Q_{C3})^2 = 0 \tag{4.62}$$

In addition to the 8 laws of energies already written - the functions $f_1 \div f_3$, f_8 and $f_9 \div f_{12}$, defined by (4.45)÷(4.47), (4.57) and (4.59)÷(4.62), 3 more energy laws must be added **to get the total of 11 equations needed**. For example, **Bernoulli's relationships** written on the **hydraulic discharge circuit** between the node where the pressure transducer **TR1** is located and the orifice where the water jet exits from each consumer **C1÷C3** (nodes $j = 29 \div 31$) can be added as follows:

$$\begin{cases} H_{hTR1} = H_{h29} + 0.5 M_8 Q_1^2 + M_9 (Q_1 + Q_2)^2 + (M_{9r} + M_{10}) Q_T^2 + h_{l\,AT} + \\ \qquad + M_{15} Q_{C1}^2 + h_{l\,AC1} \\ H_{hTR1} = H_{h30} + 0.5 M_8 Q_1^2 + M_9 (Q_1 + Q_2)^2 + (M_{9r} + M_{10}) Q_T^2 + h_{l\,AT} + \\ \qquad + M_{11} (Q_T - Q_{C1})^2 + M_{16} Q_{C2}^2 + h_{l\,AC2} \\ H_{hTR1} = H_{h31} + 0.5 M_8 Q_1^2 + M_9 (Q_1 + Q_2)^2 + (M_{9r} + M_{10}) Q_T^2 + h_{l\,AT} + \\ \qquad + M_{11} (Q_T - Q_{C1})^2 + M_{12} (Q_T - Q_{C1} - Q_{C2})^2 + M_{17} Q_{C3}^2 + h_{l\,AC3} \end{cases} \tag{4.63}$$

where the hydrodynamic loads at node **TR1** and at the ports **C1÷C3** are defined in (4.5).

Because the water jets flow at atmospheric pressure, the relative pressure is zero immediately downstream of the $j = 29 \div 31$-port section. The local hydraulic head losses through the **AC1÷AC3** gauges, denoted $h_{l\,AC1} \div h_{l\,AC3}$, are described in terms of the flow rates consumed $Q_{C1} \div Q_{C3}$ by the polynomial regression curve (4.23). The hydraulic resistance modules $M_{15} \div M_{17}$ are defined by the relations (4.25), which also include the unknown coefficients $\zeta_{C1} \div \zeta_{C3}$ related to local hydraulic head losses at **C1÷C3** consumers.

The Bernoulli relations (4.63) between **TR1** and each consumer **C1÷C3** also take into account the continuity equation (4.58) fitted to the flow in $j = 25 \div 27$ index nodes (Figures 2.17 and 4.14). The relations (4.63) are rewritten as $f_{13} \div f_{15}$ functions , as follows**:**

$$f_{13} = \left(M_{c8} Q_1^2 + \frac{p_{TR1}}{\rho g} + z_{TR1} \right) - \left(M_{c15} Q_{C1}^2 + z_{29} \right) - 0.5 M_8 Q_1^2 - M_9 (Q_1 + Q_2)^2 - \\ - (M_{9r} + M_{10}) Q_T^2 - h_{l\,AT} - M_{15} Q_{C1}^2 - h_{l\,AC1} = 0 \tag{4.64}$$

$$f_{14}=\left(M_{c8}Q_1^2+\frac{p_{TR1}}{\rho g}+z_{TR1}\right)-\left(M_{c16}Q_{C2}^2+z_{30}\right)-0.5M_8Q_1^2-M_9\left(Q_1+Q_2\right)^2-$$
$$-\left(M_{9r}+M_{10}\right)Q_T^2-h_{l\,AT}-M_{11}\left(Q_T-Q_{C1}\right)^2-M_{16}Q_{C2}^2-h_{l\,AC2}=0 \qquad (4.65)$$

$$f_{15}=\left(M_{c8}Q_1^2+\frac{p_{TR1}}{\rho g}+z_{TR1}\right)-\left(M_{c17}Q_{C3}^2+z_{31}\right)-0.5M_8Q_1^2-M_9\left(Q_1+Q_2\right)^2-$$
$$-\left(M_{9r}+M_{10}\right)Q_T^2-h_{l\,AT}-M_{11}\left(Q_T-Q_{C1}\right)^2- \qquad (4.66)$$
$$-M_{12}\left(Q_T-Q_{C1}-Q_{C2}\right)^2-M_{17}Q_{C3}^2-h_{l\,AC3}=0$$

where $M_{c\,j}=0.0826/D_j^4$ is the kinetic modulus calculated with the diameter of the pipe with index $j=15\div17$, at the end of which the consumer under consideration is located (Figure 2.17).

The system of **11 strongly nonlinear equations**, formed by the functions (4.45)÷(4.47), (4.57), (4.59)÷(4.62) and (4.64)÷(4.66), has **11 unknowns** ($Q_1\div Q_3,\zeta_{VR},\zeta_{VA},\zeta_{V1}\div\zeta_{V3},\zeta_{C1}\div\zeta_{C3}$). The solution of the system of 11 equations can be obtained using the function ***fsolve*** in MATLAB..

Knowing the solution of the above system of equations, **one can calculate the parameters defining the energy and cavitation operation of P1÷P3 pumps** (as in subchapter 4.2.1), according to the logic scheme illustrated in Figure 4.19. The final result is the relative errors ε_Q (4.52) and ε_{el} (4.53).

The case described above is **the most general and complicated case** - practically all **VR**, **VA**, **V1÷V3** valves and **C1÷C3** taps are operated within the stand in some partially closed position. For **simpler cases, where the VA and V1÷V3 valves are not operated simultaneously**, the calculation will be done in a simplified way, following the corresponding methodology described in one of the subchapters 4.2.1÷4.2.4, by reducing the number of equations and the number of unknowns in the system of 11 equations attached to the operation with final consumers. If any of the **valves C1÷C3 is closed**, the system of 11 equations is reduced in the sense that the equation corresponding to the valve (end-user) kept closed is removed from (4.64)÷(4.66), i.e. the flow corresponding to the closed valve is cancelled from both the continuity equation (4.58) and the energy laws (4.59)÷(4.62)

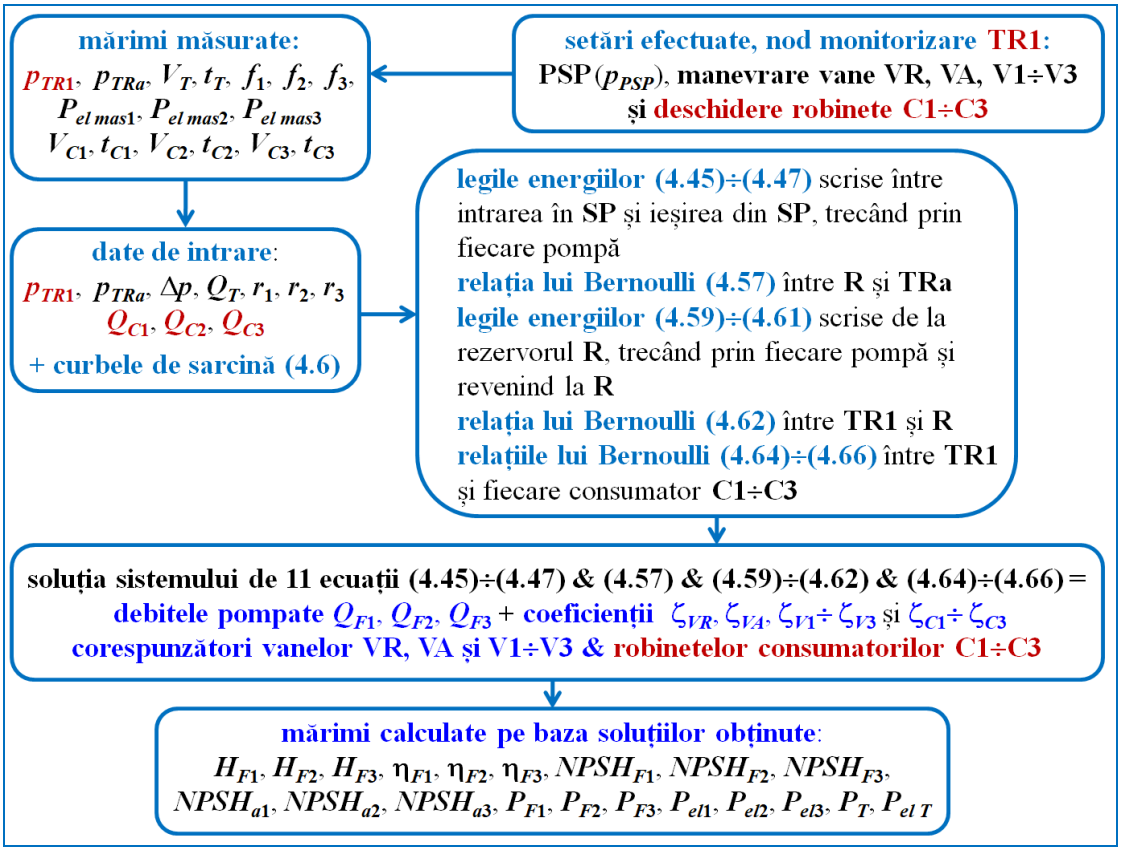

*Fig. 4.19. Logic diagram for determining the solutions - monitoring node **TR1**, operation with end consumers, with VA and V1÷V3 valves partially closed*

5. Experimental study of the energy and cavitation operation of pumps in the pumping station, without consumers, with prescribed pressure (PSP) at the transducer TR1 in the pumping station

5.1. Types of experimental tests performed

In order to study the energetic and cavitational operation of the pumps, we carried out several series of experiments, **modifying the conditions on the hydraulic suction circuit**, at different stages of the experimental stand, as follows. The pumps were tested both individually and coupled in parallel. The hydraulic installation was operated without consumers. **All measured and calculated data are inserted in APPENDIX A, consisting of Annexes A1÷A7.**

① **between september 2018 and september 2019**, the stand was controlled by the "**Megacontrol**" automatic control system (Figure 2.7), the stand was **equipped with Danfoss [1]frequency converters** (Figure 2.8); the control was carried out on the basis of the relative pressure values p_{TR1} recorded by the **TR1** transducer mounted on the delivery bus of the pumping station (Figures 2. 6 and 2.17); the pumped flow rate was regulated through the **VR** valve mounted on the delivery pipe with index $j = 14$; the tests were carried out **without final consumers**; in this configuration, we carried out **4 test campaigns**:

(A1; A2) for the first 2 test campaigns, carried out in **September 2018 (**see **Appendices A1 and A2) we installed a small diameter suction line - a DN40 pipe** (denoted by $j = 5$ in the diagram in Figure 2.17) with inner diameter $D_5 = 29$ mm and length $L_5 = 13.44$ m; the **VA** valve on the suction pipe with $j = 4$ (at the outlet of the tank) was kept in a fully open position; these were the only tests in which, during cavitations, we also measured the vibration velocity v_v [mm/s] on the pipes next to the suction flange of each pump (on suction pipes with index j = 1a÷3a in Figure 2. 17); the pumps were **operated in parallel coupled on "automatic" mode**, according to the algorithm implemented in the automation, so one, two or all 3 pumps were operated, depending on the required total flow rate Q_T (**according to the position of the regulating valve VR**) so that the prescribed pressure (Pressure Set Point, noted p_{PSP}) was maintained (reached);

---

[3] The experimental stand was designed/built in compliance with the standards in force [*ANSI 9.6.6., 2016; ISO 5198, 1987; ISO 5199, 2002; ISO 9906, 2012; ISO 9908, 1993; STAS 8804/8-1992*]. The measuring instruments were installed/used according to standards [*IEC 62828-1, 2017; IEC 62828-2, 2017; ISO 4064-5, 2014; ISO 20816-1, 2016; NML 003-05, 2005*].

(A3; A4) for the third and fourth test campaigns, carried out between **July and September 2019 (see Appendices A3 and A4),** we used a **large diameter suction line - a DN63 pipe** (*j = 5* in Figure 2.17), with internal diameter $D_5 = 45.8$ mm and length $L_5 = 13.44$ m; the pumps were operated **individually**, by settings imposed by means of buttons directly on the frequency converters; only one pump was tested for cavitation **(flow being regulated with VR valve)**, and the other 2 pumps were switched off (by permutations, all pumps were tested individually); except for 2 tests performed with pump P2 at variable speed ("automatic" mode), the rest of the tests of the running pumps (P1, or P2, or P3) were performed at constant speed ("manual" mode), equal to the rated speed; the cavitational regime was established either by **partially closing the VA valve on the suction line** with j = 4 (at the outlet of the reservoir) or by **partially closing the valve at the inlet of the pump on the suction line** with the index j = 1a (valve **V1**), or 1b (valve **V2**), or 1c (valve **V3**), as appropriate

② from July to November 2020, the stand was controlled by Mitsubishi Electric **PLC** FX5U-32M (Figure 3.4), the stand was equipped with **Mitsubishi frequency converters** (Figure 3.6); the control was based on the relative pressure values p_{TR1} recorded by the **TR1** transducer mounted on the delivery bus of the pumping station (Figures 2.6 and 2. 17); the **large diameter suction line - DN63 pipe** (*j = 5* in figure 2.17) with internal diameter $D_5 = 45.8$ mm and length $L_5 = 13.44$ m was used; the pumped flow rate was regulated by the **VR** valve mounted on the discharge line with index *j = 14*; the tests were carried out **without final consumers**; also in this configuration we carried out 2 test campaigns (fifth and sixth):

(A5; A6) for the fifth test campaign, carried out in July 2020 (Annexes A5 and A6), we carried out 2 sets of tests:

- first, the pumps were operated **individually**, through settings imposed in "manual" mode (Figure 3.15) (see Appendix A5); only one pump was tested in cavitating mode, and the other 2 pumps were kept closed (through permutations, all pumps were tested individually); the tests were carried out **by partially closing the VR valve on the reservoir**, then the **VR** valve was held still and **the suction valve on the operating pump (as appropriate, V1:V3) was gradually closed**; after completing this type of test, **we vented the pumps** (when pumps operate in cavitation, air vapour accumulates behind the mechanical seal);

- next, pump P2 was first tested in "automatic" mode (variable speed) and pumps P1 and P3 were switched off; **then 2 pumps (pumps P1 and P2) were tested in parallel**, both in "automatic" mode, and pump P3 was switched off; finally, **all 3 pumps were tested in parallel**, in "automatic" mode **(Appendix A6)**; the tests were carried out by **partially closing the VR valve on the tank,** then the **VR** valve was held stationary **and the V1:V3 valves on the** suction side of the operating pump/pumps (one, two or three valves as appropriate) were gradually closed;

(A7) for the sixth test campaign, carried out in **November 2020** (see **Appendix A7**), the **3 pumps were tested in parallel**, in "automatic" mode, **by partially closing the VR and VA valves** (the position of these valves was changed alternately).

Depending on the level of cavitation achieved, after 6÷20 points of operation in cavitation mode, the tested pumps were vented to evacuate the air accumulated behind the mechanical seal of each pump.

7. Conclusions

7.1. General conclusions on the results obtained

The PhD thesis "Experimental studies on the energy and cavitation performance of parallel coupled variable speed centrifugal pumps" contributes to the improvement of pumping station operation. The topic is of great interest in drinking water supply systems as well as in other hydraulic networks/systems in power plants and other industrial or irrigation purposes.

Pumping systems are one of the largest "energy consumers" in the world: about 20% of the energy produced worldwide is used to drive electric motors in pumping stations [*Oikonomou et al, 2018; Dadar et al, 2021*]; worldwide, between 25% and 50% of the energy consumed in industry corresponds to pumping in various hydraulic plants and systems [*Ross, 2023*]. As a result, reducing electricity consumption for pumping by improving the operation of pumps remains a highly topical desideratum: improving the operation of pumping stations contributes both to reducing electricity consumption and thus CO2 emissions and to protecting water resources [*Świętochowska & Bartkowska, 2022*].

The chosen topic is a "classic" one, but it is open (being incompletely studied) and timely in the context of current efforts related to pumping efficiency. I have identified the topicality of the topic and the opportunity to study it in my professional activity of more than 16 years in energy engineering, of which the last 7 years in the field of pumping stations. The problems existing *in situ* in the operation of pumping stations justify the study undertaken.

In order to justify the importance of the chosen topic, in the introductory part of the thesis, I presented in detail a case study corresponding to the Seimenii Mici irrigation pumping station (north of Cernavodă) - a modern, semi-buried pumping station, commissioned in 2015 and completely destroyed (flooded) in 2017, due to inadequate design and ignorance of the operating staff. When the pumps were dismantled, it turned out that the impellers of the 4 pumps had blades seriously damaged by cavitational erosion (they had portions with multiple caverns and even perforated portions), less than a year after their commissioning!

For the study of the energetic and cavitational operation of pumps, in this thesis I designed, built and commissioned an experimental stand in the Hydraulic Machines Laboratory (room ELa 022) of the Department of Hydraulics, Hydraulic Machines and Environmental Engineering, UPB. The main components of the stand were obtained through sponsorship from the companies KSB, Multigama Tech, Multigama Service and Valrom. The core component of the stand is the pump station (SP) with 3 variable speed pumps coupled in parallel. During the study, we used two different automation and control systems, each with a different type of frequency converter.

I would like to remind you that I have realized this experimental stand and carried out all the experimental test campaigns in collaboration with my colleague, PhD student Eng. Remus Alexandru Mădulărea, who also completed his PhD thesis [*Mădulărea, 2023*] under the supervision of Professor Sanda-Carmen Georgescu. The two PhD theses were carried out in parallel and complemented each other, so that each thesis contains different sets of experimental tests, as appropriate, with related modelling and/or numerical calculations.

In order to test the pumps in cavitating mode, we installed suction manifolds with different diameters (DN40 and DN63) and partially closed some valves on the suction circuit. **The pumping station is equipped with insufficient measuring devices (like most urban pumping stations)**, so that the recorded data available are only the relative pressure on the discharge and suction pipelines in the SP, the speed of the pumps via frequency converters and the electrical power absorbed by each drive motor. A water meter is installed at the outlet of the SP, allowing the total volume of water to be metered. In the absence of flow meters inside the pumping station, the flow rate pumped with each pump is determined on the **basis of the characteristic curves provided by the manufacturer and similarity relations**.

The control of the pumps is given according to the pressure prescribed in the automation system (Pressure Set Point - PSP), pressure that the system tries to reach and/or maintain at the chosen monitoring point, depending on the required water flow rate (regulated by a valve marked VR, located on the delivery line, away from the SP). Two pressure monitoring points have been fixed in the experimental stand: one point on the delivery line of the pumping station (at the pressure transducer marked TR1) and another point also on the delivery line, but at a distance from the SP (at the pressure transducer marked TR2). The pressure transducer TR2 is mounted immediately downstream of the 3 end consumers C1÷C3 (3 taps), which simulates the variable water consumption in the system. When the consumer taps (at least one of the 3 taps) are open, the pumped water flow can be regulated by both types of valves: the main regulating valve noted VR and the taps C1÷C3. The automation system controls the operation of the pumps (starting/switching on and varying their speed) so that the pressure measured with TR1 (or TR2) reaches the prescribed pressure (PSP) for the required flow rate in the system.

Based on a system of nonlinear equations, based on the continuity equation in nodes, the law of energies between system nodes and similarity relations, energy operating points were calculated for all pumps in operation. For each pump, the calculation of the values of the NPSH required by the pump and the NPSH available in the plant for each value of the pumped flow rate allowed the assessment of the cavitational regime of the pumps.

During the experimental trials to study the cavitational functioning of the pumps, tests were carried out without cavitations and with developed cavitations, respectively; some cases of incipient cavitations were also identified. **Developed cavitation was confirmed not only by NPSH calculations, but also by its specific noise and vibrations near the pump inlet.**

Incipient cavitation occurred without any visible drop in pumping head. When cavitations developed, the pumping head drop increased sharply from almost zero to 13.6%, then increased sharply to 65.3% simultaneously with the increase in flow. It should be pointed out that in the experiments performed for parallel coupled pumps, **fully developed cavitation started well below the 3% limit indicated in the literature**. The 3% limit is however only indicated for one pump in operation !!! - I have not identified studies for pumps coupled in parallel). **So pumps cavitate more when coupled in parallel, than when operating in isolation.**

From a mathematical point of view, the systems of nonlinear equations describing the operation of the system and the numerical solutions obtained show that these control methods are equivalent [**Mădulărea, Ciuc et al, 2019**]. **Experiments did not confirm this equivalence - the results obtained in the thesis showed that the "classical" control method is better than the "remote" control method**, in the sense that **the "classical" method (TR1) ensures pump operation with lower power consumption than the "remote" method (TR2).** However, we have identified the advantages and disadvantages of both control methods. The experimental trials provide enough useful data to debunk a myth that pumping stations work better if they are remotely controlled. In the experimental stand, we observed an increase in instabilities and a

fluctuation in the pressure recorded by the TR2 pressure transducer (for the same flow rate value, the TR1 pressure transducer recorded a stable, constant relative pressure value).

7.2. Original contributions

This PhD thesis contains the following original contributions:

- a bibliographic study in which 95 papers were analysed on the basis of 10 criteria of interest - as a result of this study, it was found that the topic addressed in this PhD thesis is not covered in these papers on the part of the cavitation operation of parallel coupled pumps, i.e. the topic is insufficiently covered on the part of the energy operation of parallel coupled pumps controlled on the basis of a method or strategy for regulating their operation; Moreover, none of the identified works deals simultaneously with both aspects of parallel coupled pump operation, i.e. energy and cavitation operation;

- design, construction and commissioning of an experimental stand, with a pumping group and 3 final consumers - the experimental stand allows to carry out energy and cavitation tests of 3 multistage centrifugal pumps, driven with variable speed, coupled in parallel in a pumping station framed in a closed circuit hydraulic installation, under conditions of variable water demand at the consumers;

- equipping the experimental stand with measuring devices (water meters and pressure transducers) and an automation and control panel with HMI (*Human Machine Interface*);

- stand control - was designed in the thesis to allow the operation of the pumps in the pumping station to be controlled (start/stop and speed variation) according to the pressure level recorded in one of the two monitoring nodes provided on the delivery line, namely: a node located at the outlet of the pumping station (TR1) and a node (TR2) located at a distance from the pumping station, immediately downstream of the final consumers;

- study of the energetic and cavitational operation of pumps coupled in parallel with variable speed - **the results obtained are new and original** (no studies on such tests have been identified); these tests were carried out without consumers and the pumping station was controlled by the "classical" method (TR1);

- highlighting the influence of the suction circuit on the proper operation of a pumping station feeding a water supply network - we have analysed the problems that the energy and cavitation operation of variable speed turbopumps poses in the operation of pumping stations, both in individual operation and especially in parallel operation of pumps;

- study of the energy operation of parallel coupled variable speed pumps controlled by two control methods: "classical" (TR1) and "remote" (TR2) - **the results are new and original; all experimental tests carried out for the TR2 monitoring node are a novelty in the scientific literature**; the study showed that the "classical" method provides lower energy consumption (no experimental studies were found to confirm this result);

- the study of the energy operation of parallel coupled, variable speed, alternately driven pumps (in tandem TR1/TR2) - **this study is a novelty in the international scientific literature.** The results of these tests and conclusions were presented on 7 July 2022 ***[Ciuc et al, 2022a]*** at the 14th International Hydroinformatics Conference - HIC 2022 [https://hic2022.utcb.ro/]. From the information so far, from the literature study undertaken in the thesis and from the discussions held at the HIC 2022 conference with renowned Italian specialists (from Politehnica of Bari, Federico II University of Naples and "G. d'Annunzio" University of Chieti Pescara), **it has been confirmed that there are no experimental studies conducted in the laboratory on the operation of remotely controlled pumping stations available in the literature** (it does not mean that such experimental studies do not exist, just that if they do, the data are not available/accessible). The discussions held confirmed **that both the test methodology** (proposed and used in the thesis) **and the results obtained in this thesis are new and original in the scientific literature**, and therefore represent an important contribution of the thesis. From this point of view, in my opinion and that of the co-authors, the scientific article ***[Ciuc et al, 2022a]*** has high potential for citation after publication in a journal.

7.3. Research perspectives

The present PhD thesis has opened up new research directions in the field of cavitation testing of parallel coupled pumps (with constant speed, but especially with variable speed), respectively in the control of a pumping station by an automation and control system. In the following, I list some of the research perspectives, which can be continued on the same experimental stand:

- it is possible to extend all cavitational tests with "remote" control of the pumps, choosing as monitoring node, the node where the TR2 pressure transducer is already located (in the thesis, these tests were controlled strictly by the "classical" method with the TR1 pressure transducer);

- all cavitational tests with variable water flow imposed on final consumers can be extended (in the thesis, these tests were performed without consumers);

- all energy tests of pumps with both control methods ("classical" - TR1 and "remote" - TR2) can be extended to verify the conclusion obtained in this thesis; the results obtained are novel and further study is needed;

- the experimental stand can be equipped with flow meters (to reduce errors in determining flow rates using the volumetric method related to water meters); the experimental stand can be equipped with vibration transducers (very useful for detecting cavitations) - in any variant of upgrading the equipment of the stand, the experimental tests can be resumed.

Bibliographical references

Studies (books, scientific articles, theses, projects and reports)

1. **[Al-Arabi, 2010]**
   Al-Arabi A.A.B., **2010**, *Effect of sand concentration ratio on centrifugal pump performance at various working temperatures*, Proceedings 7th International Conference on Heat Transfer, Fluid Mechanics and Thermodynamics, 19-21 July, Antalya, Turkey, https://repository.up.ac.za/bitstream/handle/2263/44909/AlArabi_Effect_2015.pdf?sequence=1&isAllowed=y
2. **[Al-Arabi & Alsalmi, 2017]**
   Al-Arabi A.A.B., Alsalmi A.M., **2017**, *Cavitation in centrifugal pumps connected in series and parallel*, Journal of Engineering Research and Applied Sciences, 4th edition, vol. 1, Hoon, Libya
3. **[Al-Arabi & Selim, 2009]**
   Al-Arabi A.A.B., Selim S.M.A., **2009**, *Reality of cavitation inception in centrifugal pumps*, Proceedings 8th International Conference on Sustainable Energy Technologies – SET2008, 31 Aug. - 3 Sept., Aachen, Germany
4. **[Al-Hashmi, 2008]**
   Al-Hashmi S., **2008**, *Monitoring pumping systems using vibration signal analysis*, Proceedings 9th International Conference on Computational Structures Technology, Civil-Comp Press, Stirlingshire, UK, paper 101, doi:10.4203/ccp.88.101
5. **[Al-Hashmi et al, 2004]**
   Al-Hashmi S., Gu F., Li Y., Ball A.D., Fen T., Lui K., **2004**, *Cavitation detection of a centrifugal pump using instantaneous angular speed*, Proceedings ASME 7th Biennial Conference on Engineering Systems Design and Analysis – ESDA2004, 58255, 185-190
6. **[Al-Obaidi, 2019]**
   Al-Obaidi A.R., **2019**, *Experimental investigation of the effect of suction valve opening on the performance and detection of cavitation in the centrifugal pump based on acoustic analysis*, Archives of Acoustics, 44(1), 59-69, doi:10.24425/aoa.2019.126352
7. **[Anton Alin et al, 2019]**
   Anton Alin, Mos D., Muntean S., Draghici I., **2019**, *Software solution for efficiency assessment of the hydraulic pumps in service*, 2019 International Conference on Energy and Environment – CIEM, 17-18 Oct., Timisoara, Romania, IEEE Conf. Publications, 374-378, doi:10.1109/CIEM46456.2019.8937705
8. **[Azizi et al, 2018]**
   Azizi R., Hajnayeb A., Ghanbarzadeh A., Changizian M., **2018**, *Cavitation severity detection in centrifugal pumps*, in: Advances in technical diagnostics, Timofiejczuk A., Łazarz B., Chaari F., Burdzik R. (eds), Proceedings ICDT 2016 – Applied Condition Monitoring, vol. 10, Springer, https://doi.org/10.1007/978-3-319-62042-8_4
9. **[Berardi et al, 2015a]**
   Berardi L., Laucelli D., Ugarelli R., Giustolisi O., **2015**, *Leakage management: Planning remote real time controlled pressure reduction in Oppegård Municipality*, Procedia Engineering, 119, 72-81

10. **[Berardi et al, 2015b]**
Berardi L., Laucelli D., Ugarelli R., Giustolisi O., **2015**, *Hydraulic system modelling: background leakage model calibration in Oppegård Municipality*, Procedia Engineering, 119, 633-642
11. **[Berardi et al, 2018]**
Berardi L., Simone A., Laucelli D., Ugarelli R.M., Giustolisi O., **2018**, *Relevance of hydraulic modelling in planning and operating real-time pressure control: case of Oppegård municipality*, Journal of Hydroinformatics, 20(3), 535-550
12. **[Birajdar et al, 2009]**
Birajdar R., Patil R., Khanzode K., **2009**, *Vibration and noise in centrifugal pumps - sources and diagnosis methods*, Proceedings 3rd International Conference on Integrity, Reliability and Failure, 20-24 July, Porto, Portugal, S1163_P0437
13. **[Borges, 2012]**
Borges G., **2012**, *Irrigation system evaluation and pump efficiency*, Agriculture Systems Management California Polytechnic State University, San Luis Obispo, CA, USA
14. **[Brennen, 1994]**
Brennen C.E., **1994**, *Hydrodynamics of pumps*, Concepts NREC, White River Junction, VT, USA, https://authors.library.caltech.edu/25019/2/HydroPmp.pdf
15. **[Brennen, 2016]**
Brennen C.E., **2016**, *On the dynamics of a cavitating pump*, IOP Conference Series Earth and Environmental Science, 49(5), 052018
16. **[Brennen & Braisted, 1980]**
Brennen C.E., Braisted D.M., **1980**, *Stability of hydraulic systems with focus on cavitating pumps*, IAHR Symposium 1980, Tokyo
17. **[Briceño et al, 2019]**
Briceño C., Iglesias P., Martinez J., **2019**, *Influence of the regulation mode in the selection of the number of Fixed Speed Drives (FSD) and Variable Speed Drives (VSD) pumps in water pumping stations*, Proceedings 4th International Electronic Conference on Water Sciences, doi:10.3390/ECWS-4-06445
18. **[Briceño-León et al, 2021]**
Briceño-León C.X., Iglesias-Rey P.L., Martinez-Solano F.J., Mora-Melia D., Fuertes-Miquel V.S., **2021**, *Use of fixed and variable speed pumps in water distribution networks with different control strategies*, Water, 13(4), 479, https://doi.org/10.3390/w13040479 & *Supplementary materials* (6 pages): https://www.mdpi.com/2073-4441/13/4/479/s1
19. **[Brogan et al, 2016]**
Brogan A., Gopalakrishnan V., Sturtevant K., Valigosky Z., Kissock K., **2016**, *Improving variable-speed pumping control to maximize savings*, ASHRAE Transactions, 122(2), 141-148, https://www.ers-inc.com/wp-content/uploads/2017/03/Improving-Variable-Speed-Pumping-Control.pdf
20. **[Burchiu et al, 2006]**
Burchiu V., Gheorghiu L., Dudău Al., **2006**, *Ghidul utilizatorului de pompe*, vol. 1&2, Editura ATLAS Press, Bucuresti
21. **[Byeon et al, 2015]**

Byeon S., Choi G., Maeng S., Gourbesville P., **2015**, *Sustainable water distribution strategy with smart water grid*, Sustainability, 7, 4240-4259, doi:10.3390/su7044240

22. **[Capponi et al, 2014]**
Capponi C., Ferrante M., Pedroni M., Brunone B., Meniconi S., Zaghini M., Leoni F., **2014**, *Real data analysis and efficiency of the TEA Mantova Casale (Italy) variable-speed pumping station*, Procedia Engineering, 70, 248-255
23. **[Călinoiu, 2009]**
Călinoiu C., **2009**, *Senzori si traductoare*, vol. 1, Editura Tehnică, București
24. **[Chini et al, 2005]**
Chini S.F., Rahimzadeh H., Bahrami M., **2005**, *Cavitation detection of a centrifugal pump using noise spectrum*, Proceedings of IDETC/CIE 2005, 24-28 Sept., Long Beach, California, USA, DETC2005-84363
25. **[Chudina, 2003]**
Chudina M., **2003**, *Noise as an indicator of cavitation in a centrifugal pump*, Acoustical Physics, 49(4), 463-474
26. **[Cimorelli et al, 2020]**
Cimorelli L., Covelli C., Molino B., Pianese D., **2020**, *Optimal regulation of pumping station in water distribution networks using constant and variable speed pumps: A technical and economical comparison*, Energies, 13(10), 2530; https://doi.org/10.3390/en13102530
27. **[Ciuc, 2014]**
Ciuc P.-O., **2014**, *Punerea în funcțiune a unui Stand de pompe KSB cu turație variabilă – Studiul experimental aferent funcționării standului*, Proiect de diplomă, Facultatea de Energetică, UPB
28. **[Ciuc, 2016]**
Ciuc P.-O., **2016**, *Studiul experimental și numeric al funcționării unui Stand KSB cu 3 pompe cu turație variabilă cuplate în paralel*, Proiect de disertație, Facultatea de Energetică, UPB
29. **[Ciuc et al, 2019a]**
Ciuc P.-O., Mădulărea R.A., Georgescu A.-M., Diminescu M.A., Georgescu S.-C., **2019**, *Experimental test rig designed to analyse pumping station operation controlled by pressure at different key points*, E3S Web of Conferences (WOS:000468021200047), 85, 06001, https://doi.org/10.1051/e3sconf/20198506001
30. **[Ciuc et al, 2019b]**
Ciuc P.-O., Mădulărea R.A., Georgescu A.-M., Georgescu S.-C., Dunca G., Bucur D.M., **2019**, *Cavitation influence on the operation of a pumping station rig with variable speed pumps*, 2019 International Conference on Energy and Environment – CIEM, 17-18 Oct., Timisoara, Romania, IEEE Conf. Publications (WOS:000630902700051), 239-243, doi:10.1109/CIEM46456.2019.8937656, https://ieeexplore.ieee.org/document/8937656
31. **[Ciuc et al, 2022a]**
Ciuc P.-O., Mădulărea R. A., Georgescu A.-M., Georgescu S.-C., **2022**, *Experimental investigations on classical versus remote control of variable speed driven pumps operating in parallel*, 14th International Conference on Hydroinformatics – HIC 2022, 4-8 July 2022,

Bucharest, Book of Abstracts, Session 5A – Digital Transformation of Urban Water Systems, paper ID 101

32. **[Ciuc et al, 2022b]**
Ciuc P.-O., Mădulărea R. A., Pîrăianu V.-F., Georgescu A.-M., Georgescu S.-C., **2022**, *Duty points dropdown due to cavitation in variable speed driven pumps operating in parallel*, 14th International Conference on Hydroinformatics – HIC 2022, 4-8 July 2022, Bucharest, Book of Abstracts, Session 2D – Hydraulic and Hydrological Modeling, paper ID 100 (selected for the *Special Issue: HIC 2022*, in *Journal of Hydroinformatics*, editors A.-M. Georgescu, S.-C. Georgescu, G. Freni, P. Gourbesville)

33. **[Cowan et al, 2013]**
Cowan D., Liebner T., Bradshaw S., **2013**, *Influence of impeller suction specific speed on vibration performance*, Proceedings 29th International Pump Users Symposium, 1-3 Oct., Houston, Texas, USA

34. **[Dadar et al, 2021]**
Dadar S., Đurin B., Alamatian E., Plantak L., **2021**, *Impact of the pumping regime on electricity cost savings in urban water supply system*, Water, volume 13, 1141, https://doi.org/10.3390/w13091141

35. **[Darweesh, 2018]**
Darweesh M.S., **2018**, *Assessment of variable speed pumps in water distribution systems considering water leakage and transient operations*, Journal of Water Supply: Research and Technology – Aqua, 67(1), 99-108, https://doi.org/10.2166/aqua.2017.086

36. **[de Abreu Costa et al, 2018]**
De Abreu Costa J.N., Holanda de Castro M.A., Magalhães Costa L.H., Costa Barbosa J.M., **2018**, *New formula proposal for the determination of variable speed pumps efficiency*, Brazilian Journal of Water Resources, 23(44), https://doi.org/10.1590/2318-0331. 231820180003

37. **[Dong et al, 2019]**
Dong L., Zhao Y., Dai C., **2019**, *Detection of inception cavitation in centrifugal pump by fluid-borne noise diagnostic*, Shock and Vibration, Hindawi, vol. 2019, paper 9641478, https://doi.org/10.1155/2019/9641478

38. **[Drăghici et al, 2017]**
Drăghici I.A., Atănăsoaiei C., Bosioc A.I., Muntean S., Anton L.E., **2017**, *Experimental analysis of the global performances for a pump with symmetrical suction elbow at two speeds*, Energy Procedia, 112, 225-231

39. **[Drăghici et al, 2016]**
Drăghici I.A., Muntean S., Bosioc A.I. , Ginga G., Anton L.E., **2016**, *Unsteady pressure field analysis at pump inlet equipped with a symmetrical suction elbow*, Proceedings of the Romanian Academy – Series A: Mathematics, Physics, Technical Sciences, Information Science, 17(3), 237-244

40. **[Drăghici, 1971]**
Drăghici N.N., **1971**, *Conducte pentru transportul fluidelor*, Editura Tehnică, București

41. **[Dunca et al, 2008]**

Dunca G., Isbășoiu E.C., Călinoiu C., Bucur D.M., Ghergu C., **2008**, *Vibrations level analyse during pumping station Gâlceag operation*, UPB Sci. Bull, D, 70(4), 181-190

42. **[Dunca, Ciuc et al, 2017]**
Dunca G., Pîrăianu V.-F., Roman R., **Ciuc P.-O.**, Georgescu S.-C., **2017**, *Experimental versus EPANET simulation of variable speed driven pumps operation*, Energy Procedia (WOS:000404848300013), 112, 100-107, https://doi.org/10.1016/j.egypro.2017.03.1070

43. **[Eaton et al, 2022]**
Eaton J.W., Bateman D., Hauberg S., Wehbring R., **2022**, *GNU Octave. A high-level interactive language for numerical computations*, 7th edition for Octave 7.2.0. (released in July 2022), https://docs.octave.org/octave.pdf

44. **[Fu et al, 2015]**
Fu Y., Yuan J., Yuan S., Pace G., d'Agostino L., Huang P., Li X., **2015**, *Numerical and experimental analysis of flow phenomena in a centrifugal pump operating under low flow rates*, Journal of Fluids Engineering, 137(1), 011102-1, https://doi.org/10.1115/1.4027142

45. **[Georgescu A.-M., 2017]**
Georgescu A.-M., **2017**, *Analiza problemei de vibrații apărute în urma retehnologizării unei stații de pompare*, capitolul 3.2 în *Cercetări aplicate de Ingineria fluidelor*, Teza de abilitare, Universitatea Tehnică de Construcții București

46. **[Georgescu A.-M. et al, 2014a]**
Georgescu A.-M., Cosoiu C.-I., Perju S., Georgescu S.-C., Hasegan L., Anton A., **2014**, *Estimation of the efficiency for variable speed pumps in EPANET compared with experimental data*, Procedia Engineering, 89, 1404-1411, doi:10.1016/j.proeng.2014.11.466, http://www.sciencedirect.com/science/article/pii/S1877705814025818

47. **[Georgescu A.-M. & Georgescu S.-C., 2007]**
Georgescu A.-M., Georgescu S.-C., **2007**, *Hidraulica reţelelor de conducte şi Maşini hidraulice*, Editura Printech, Bucureşti

48. **[Georgescu A.-M. et al, 2014b]**
Georgescu A.-M., Georgescu S.-C., Coșoiu C. I., Alboiu N. I., Hlevca D., **2014**, *Probleme de Maşini hidraulice*, Editura Printech, Bucureşti

49. **[Georgescu A.-M. et al, 2015]**
Georgescu A.-M., Georgescu S.-C., Cosoiu C. I., Hasegan L., Anton A., Bucur D. M., **2015**, *EPANET simulation of control methods for centrifugal pumps operating under variable system demand*, Procedia Engineering, 119, 1012-1019, doi:10.1016/j.proeng.2015.08.995

50. **[Georgescu A.-M. et al, 2007]**
Georgescu A.-M., Georgescu S.-C., Petrovici T., Culcea M., **2007**, *Pumping stations operating parameters upon a variable demand, determined numerically for the water distribution network of Oradea*, UPB Sci. Bull, Series C: Electrical Engineering, 69(4), 643-650

51. **[Georgescu A.-M. et al (Ciuc), 2018]**
Georgescu A.-M., Mădulărea R.A., **Ciuc P.-O.**, Georgescu S.-C., **2018**, *Decision support for a centre pivot irrigation system based on numerical modelling*, Proceedings 13th International Conference on Hydroinformatics – HIC 2018, EPiC Series in Engineering

(ISSN: 2516-2330), G. La Loggia, G. Freni, V. Puleo and M. De Marchis (eds.), vol. 3, 764-771, https://easychair.org/publications/paper/lHPR, https://doi.org/10.29007/frqh

52. **[Georgescu A.-M. et al, 2014c]**
Georgescu A.-M., Perju S., Georgescu S.-C., Anton A., **2014**, *Numerical model of a district water distribution system in Bucharest*, Procedia Engineering, 70, 707-714, doi:10.1016/j.proeng.2014.02.077, http://www.sciencedirect.com/science/article/pii/S1877705814000794

53. **[Georgescu A.-M. et al, 2017]**
Georgescu A.-M., Perju S., Madularea R. A., Georgescu S.-C., **2017**, *Energy consumption due to pipe background leakage in a district water distribution system in Bucharest*, 8th International Conf. on Energy and Environment – CIEM, 19-20 Oct., Bucharest, IEEE Conf. Publications (WOS:000427610300053), 251-254, doi:10.1109/CIEM.2017.8120785, http://ieeexplore.ieee.org/document/8120785/

54. **[Georgescu S.-C. et al (Ciuc), 2017a]**
Georgescu S.-C., Bucur D. M., Dunca G., Georgescu A.-M., Nicolae A. A., **Ciuc P.-O.**, **2017**, *Hydraulic balancing of the cooling water system of a Pumped Storage Power Plant*, 8th International Conf. on Energy and Environment – CIEM, 19-20 Oct., Bucharest, IEEE Conf. Publications (WOS:000427610300052), 246-250, doi:10.1109/CIEM.2017.8120766, http://ieeexplore.ieee.org/document/8120766/

55. **[Georgescu S.-C. & Georgescu A.-M., 2014a]**
Georgescu S.-C., Georgescu A.-M., **2014**, *Calculul rețelelor hidraulice cu GNU Octave,* Editura Printech, București

56. **[Georgescu S.-C. & Georgescu A.-M., 2014b]**
Georgescu S.-C., Georgescu A.-M., **2014**, *Manual de EPANET*, Editura Printech, București

57. **[Georgescu S.-C. & Georgescu A.-M., 2015]**
Georgescu S.-C., Georgescu A.-M., **2015**, *Pumping station scheduling for water distribution networks in EPANET*, UPB Sci. Bull, Series D: Mechanical Engineering, 77(2), 235-246

58. **[Georgescu S.-C. et al, 2005]**
Georgescu S.-C., Georgescu A.-M., Dunca G., **2005**, *Staţii de pompare. Încadrarea turbopompelor în sisteme hidraulice*, Editura Printech, Bucureşti

59. **[Georgescu S.-C. et al (Ciuc), 2017b]**
Georgescu S.-C., Georgescu A.-M., Mădulărea R.A., **Ciuc P.-O.**, **2017**, *Raport asupra Staţiei de Pompare care alimentează sistemul de irigaţii Seimenii Mici (SP Seimeni)*, Raport nr. 1/27.10.2017, Beneficiar Valrom Industrie

60. **[Georgescu S.-C. et al, 2015]**
Georgescu S.-C., Georgescu A.-M., Madularea R. A., Piraianu V.-F., Anton A., Dunca G., **2015**, *Numerical model of a medium-sized municipal water distribution system located in Romania*, Procedia Engineering, 119, 660-668, doi:10.1016/j.proeng.2015.08.919)

61. **[Georgescu S.-C. et al, 2010]**
Georgescu S.-C., Popa R., Georgescu A.-M., **2010**, *Pumping stations scheduling for a water supply system with multiple tanks*, UPB Sci. Bull, Series D: Mechanical Engineering, 72(3), 129-140

62. **[Germanopoulos, 1985]**
Germanopoulos G., **1985**, *A technical note on the inclusion of pressure dependent demand and leakage terms in water supply network models*, Civil Engineering Systems, 2(3), 171-179
63. **[Giustolisi et al, 2016]**
Giustolisi O., Berardi L., Laucelli D., Savić D., Kapelan Z., **2016**, *Operational and tactical management of water and energy resources in pressurized systems: Competition at WDSA 2014*, Journal of Water Resources Planning and Management, 142(5), https://doi.org/10.1061/(ASCE)WR.1943-5452.0000583
64. **[Giustolisi et al, 2011]**
Giustolisi O., Savić D.A., Berardi L., Laucelli D., **2011**, *An Excel based solution to bring water distribution network analysis closer to users*, Proceedings 11th International Conference on Computing and Control for the Water Industry – CCWI 2011, 3, 805-810
65. **[Giustolisi et al, 2008]**
Giustolisi O., Savić D., Kapelan Z., **2008**, *Pressure-driven demand and leakage simulation for water distribution networks*, Journal of Hydraulic Engineering, 134(5), 626-635
66. **[Giustolisi & Todini, 2009]**
Giustolisi O., Todini E., **2009**, *Pipe hydraulic resistance correction in WDN analysis*, Urban Water Journal, 6(1), 39-52, https://doi.org/10.1080/15730620802541623
67. **[Giustolisi & Walski, 2012]**
Giustolisi O., Walski T.M., **2012**, *Demand components in Water Distribution Network Analysis*, Journal of Water Resources Planning and Management**,** 138(4), 356-367, https://doi.org/10.1061/(ASCE)WR.1943-5452.0000187
68. **[Gomes et al, 2011]**
Gomes R., Sá Marques A., Sousa J., **2011**, *Estimation of the benefits yielded by pressure management in water distribution systems*, Urban Water Journal, 8(2), 65-77, doi:10.1080/1573062X.2010.542820
69. **[Guo et al, 2021]**
Guo M., Zou H., Chen B., Zuo Z., Liu S., **2021**, *Experimental performance of a pump and the related vortices in a pump intake of a model pump station*, Journal of Physics: Conference Series, 1909(1), 012045
70. **[Guo et al, 2020]**
Guo W., Perera J.C., Cox D., Nimbalkar S.U., Wenning T., Thirumaran K., Levine E., **2020**, *Variable-Speed Pump efficiency calculation for fluid flow systems with and without static head*, US Department of Energy, https://www.osti.gov/servlets/purl/1649114
71. **[Gupta et al, 2013]**
Gupta S., Chouksey V.K., Srivastava M., **2013**, *Online detection of cavitation phenomenon in a centrifugal pump using audible sound*, ITSI Transactions on Electrical and Electronics Engineering, 1(5), 103-107
72. **[Horowitz et al, 2006]**
Horowitz F.B., Lipták B.G., Bain S., **2006**, *Pump controls*, chapter 8.34, pp. 2084-2109, in *Process control and optimization*, vol. II, B.G. Lipták (ed.), *Instrument Engineers'*

Handbook, 4th edition, CRC Press, Taylor & Francis Group, http://twanclik.free.fr/electricity/IEPOPDF/1081ch8_34.pdf

73. **[Iamandi et al, 2002]**
Iamandi C., Petrescu V., Damian R., Sandu L., Anton A., **2002**, *Hidraulica instalaţiilor. Calculul sistemelor hidraulice*, vol. II, Editura Tehnică, Bucureşti

74. **[Iamandi et al, 1985]**
Iamandi C., Petrescu V., Sandu L., Damian R., Anton A., Degeratu M., **1985**, *Hidraulica instalaţiilor. Elemente de calcul şi aplicaţii*, Editura Tehnică, Bucureşti

75. **[Isbăşoiu et al, 2009]**
Isbăşoiu E.C., Bucur D.M., Dunca G., Ghergu C.M., Tănase N.O., **2009**, *Încercarea maşinilor hidraulice*, Editura Politehnica Press, București

76. **[Isbăşoiu & Georgescu, 1995]**
Isbăşoiu E. C., Georgescu S.-C., **1995**, *Mecanica Fluidelor*, Editura Tehnică, Bucureşti

77. **[Jensen & Dayton, 2000]**
Jensen J., Dayton K., **2000**, *Detecting cavitation in centrifugal pumps. Experimental results of the Pump Laboratory*, ORBIT, Second Quarter, 26-30

78. **[Jones & Sanks, 2008]**
Jones G.M., Sanks R.L., **2008**, *Pumps: Intake design, selection, and installation*, chapter 12 in: *Pumping station design*, Jones G.M., Sanks R.L., Tchobanoglous G., Bosserman II B.E. (eds) 3rd ed., Butterworth-Heinemann, Burlington, MA, USA

79. **[Kaya & Ayder, 2017]**
Kaya M., Ayder E., **2017**, *Prediction of cavitation performance of radial flow pumps*, Journal of Applied Fluid Mechanics, 10(5), 1397-1408

80. **[Kotb & Abdulaziz, 2015]**
Kotb A., Abdulaziz A. M., **2015**, *Cavitation detection in variable speed pump by analyzing the acoustic and vibration spectrums*, Engineering, 7, 706-716, http://dx.doi.org/10.4236/ eng.2015.710062

81. **[Lamaddalena & Khila, 2012]**
Lamaddalena N., Khila S., **2012**, *Energy saving with variable speed pumps in on-demand irrigation systems*, Irrigation Science, 30, 157-166, doi: 10.1007/s00271-011-0271-7

82. **[Laucelli et al, 2016]**
Laucelli D., Berardi L., Ugarelli R., Simone A., Giustolisi O., **2016**, *Supporting real-time pressure control in Oppegård Municipality with WDNetXL*, Procedia Engineering, 154, 71-79

83. **[Lee et al, 2015]**
Lee S.W., Sarp S., Jeon D.J., Kim J.H., **2015**, *Smart water grid: the future water management platform*, Desalination and Water Treatment, 55(2), 339-346, doi: 10.1080/19443994.2014.917887

84. **[Li & Baggett, 2007]**
Li G., Baggett C.C., **2007**, *Real-time operation optimization of variable-speed pumping stations in water distribution systems by adaptive discharge pressure control*, Proceedings World Environmental and Water Resources Congress 2007: Restoring Our Natural Habitat, ASCE

85. **[Loucks & van Beek, 2017]**

Loucks D.P., van Beek E., **2017**, *Urban water systems*, chapter 12, pp. 527-565, in *Water resource systems planning and management. An introduction to methods, models, and applications*, D.P. Loucks, E. van Beek (eds.), Springer

86. **[Mahaffey & van Vuuren, 2014]**
Mahaffey R.M., van Vuuren S.J., **2014**, *Review of pump suction, reducer selection: Eccentric or concentric reducers*, Journal of the South African Institution of Civil Engineering, 56(3), 65-76, paper 1070

87. **[Maksimovic & Masry, 2009]**
Maksimovic Č., Masry E. N., **2009**, *Potentials for improvement of energy efficiency for new design of water distribution systems*, Proceedings Water Distribution Systems Analysis – WDSA 2008, https://doi.org/10.1061/41024(340)26

88. **[Marchi et al, 2012]**
Marchi A., Simpson A.R., Ertugrul N., **2012**, *Assessing variable speed pump efficiency in water distribution systems*, Drinking Water Engineering and Science, 5, 15-21, https://doi.org/10.5194/dwes-5-15-2012

89. **[Mădulărea, 2023]**
Mădulărea R.A., **2023**, *Studii experimentale și numerice asupra funcționării energetice a pompelor centrifuge cu turație variabilă, cuplate în paralel*, Teză de doctorat, Universitatea POLITEHNICA din București (*în pregătire*)

90. **[Mădulărea, Ciuc et al, 2019]**
Mădulărea R.A., **Ciuc P.-O.**, Georgescu A.-M., Georgescu S.-C., **2019**, *Speed factors computed for pumping schedules in water distribution networks: DDA versus PDA formulations*, E3S Web of Conferences (WOS:000468021200048), 85, 06002, https://doi.org/10.1051/e3sconf/20198506002

91. **[Menke et al, 2016]**
Menke R., Abraham E., Stoianov I., **2016**, *Modeling variable speed pumps for optimal pump scheduling*, Proceedings World Environmental and Water Resources Congress 2016, 199-209, ASCE

92. **[Mishra et al, 2020]**
Mishra B.K., Chakraborty S., Kumar P., Saraswat C., **2020**, *Urban water demand management*, pp. 41-57, in *Sustainable Solutions for Urban Water Security*, Water Science and Technology Library, vol. 93, Springer, doi: 10.1007/978-3-030-53110-2_3

93. **[Moradi-Jalal et al, 2003]**
Moradi-Jalal M., Marino M.A., Asce H.M., Afshar A., **2003**, *Optimal design and operation of irrigation pumping stations*, Journal of Irrigation and Drainage Engineering, 129(3)

94. **[Mousmoulis et al, 2019]**
Mousmoulis G., Yiakopoulos C., Kassanos I., Antoniadis I., Anagnostopoulos J., **2019,** *Vibration and acoustic emission monitoring of a centrifugal pump under cavitating operating conditions*, IOP Conference Series Earth and Environmental Science, 405, 012003

95. **[Muranho et al, 2014]**

Muranho J., Ferreira A., Sousa J., Gomes A., Sá Marques A., **2014**, *Pressure-dependent demand and leakage modelling with an EPANET extension – WaterNetGen*, Procedia Engineering, 89, 632-639, https://doi.org/10.1016/j.proeng.2014.11.488

96. **[Neagoe et al, 2019]**
Neagoe A., Tică E. I., Georgescu S.-C., Petrovici T., **2019**, *Informatică aplicată: Manual de GNU Octave*, Editura Politehnica Press, Bucureşti

97. **[Ng & Brennen, 1978]**
Ng S.L., Brennen C.E., **1978**, *Experiments on the dynamic behavior of cavitating pumps*, Journal of Fluids Engineering, 100(2), 166-176

98. **[Oikonomou et al, 2018]**
Oikonomou K., Parvania M., Khatami R., **2018**, *Optimal demand response scheduling for water distribution systems*, IEEE Trans. Ind. Inform., 14, 5112-5122

99. **[Page et al, 2017]**
Page P.R., Abu-Mahfouz A.M., Mothetha M.L., **2017**, *Pressure management of water distribution systems via the remote real-time control of variable speed pumps*, Journal of Water Resources Planning and Management, 143(8), 04017045, http://ascelibrary.org/doi/full/10.1061/(ASCE)WR.1943-5452.0000807

100. **[Page et al, 2019]**
Page P.R., Zulu S'b., Mothetha M.L., **2019**, *Remote real-time pressure control via a variable speed pump in a specific water distribution system*, Journal of Water Supply: Research and Technology – Aqua, 68(1), 20-28, doi:10.2166/aqua.2018.074

101. **[Pîrăianu et al (Ciuc), 2021]**
Pîrăianu V.-F., Drăgoi C., **Ciuc P.-O.**, Mădulărea R. A., Georgescu A.-M., Georgescu S.-C., **2021**, *Dry fountains of UPB: Operation modelling and power consumption assessment*, UPB Scientific Bulletin, Series C: Electrical Engineering and Computer Science (WOS:000741473700029), 83(4), pp. 363-378, https://www.scientificbulletin.upb.ro/rev_docs_arhiva/rez5e3_690095.pdf

102. **[Pîrăianu et al, 2016]**
Pîrăianu V.-F., Dumitran G.E., Vuță L.I., Drăgoi C., **2016**, *Improving efficiency of a water supply system based on energy tariffs*, Proceedings International Multidisciplinary Scientific GeoConference SGEM, vol I, 459-464, https://sgem.org/sgemlib/spip.php?article7779&lang=en

103. **[Pothof & Clemens, 2011]**
Pothof I.W.M., Clemens F., **2011**, *Experimental study of air-water flow in downward sloping pipes*, International Journal of Multiphase Flow, 37(3), 278-292

104. **[Pothof & Clemens, 2012]**
Pothof I.W.M., Clemens F.H.L.R., **2012**, *Air pocket removal from downward sloping pipes*, Proceedings 9th International Conference on Urban Drainage Modelling, Belgrade, Serbia

105. **[Pothof & Karney, 2012]**
Pothof I.W.M., Karney B., **2012**, *Guidelines for transient analysis in water transmission and distribution systems*, chapter 1, pp. 1-21, in *Water Supply System Analysis*, A. Ostfeld (ed.), http://dx.doi.org/10.5772/53944

106. **[Ross, 2023]**

Ross B., **2023**, *Pumping systems – low hanging fruit in saving energy*, 12 p., Armstrong Ltd. – White Papers, https://armstrongfluidtechnology.com/en/resources-and-tools/education-and-training/white-papers

107. **[Rossman, 2000]**
Rossman L.A., **2000**, *EPANET 2 Users Manual*, US Environmental Protection Agency, EPA/600/R-00/057, Cincinnati, OH, https://nepis.epa.gov/Adobe/PDF/P1007WWU.pdf

108. **[Rossman et al, 2020]**
Rossman L.A., Woo H., Tryby M., Shang F., Janke R., Haxton T., **2020**, *EPANET 2.2 User Manual*, US Environmental Protection Agency, EPA/600/R-20/133, Cincinnati, OH, https://cfpub.epa.gov/si/si_public_record_Report.cfm?dirEntryId=348882&Lab=CESER

109. **[Salvadori et al, 2012]**
Salvadori S., Cappelletti A., Martelli F., Nicchio A., Carbonino L., Piva A., **2012**, *Numerical prediction of cavitation in pumps*, Proceedings 15th International Conference on Fluid Flow Technologies – CMFF'2012, 4-7 Sept., Budapest, Hungary

110. **[Salvadori et al, 2015]**
Salvadori S., Cappelletti A., Montomoli F., Nicchio A., Martelli F., **2015**, *Experimental and numerical evaluation of the $NPSH_r$ curve of an industrial centrifugal pump*, Proceedings 11th European Conference on Turbomachinery Fluid Dynamics & Thermodynamics – ETC11, 23-27 March, Madrid, Spain, https://aerospace-europe.eu/media/books/ETC2015-011.pdf

111. **[Sethi & Di Molfetta, 2019]**
Sethi R., Di Molfetta A., **2019**, *Optimization of a water supply system*, chapter 6, in *Groundwater Engineering*, Springer, 127-136

112. **[Shankar et al, 2021]**
Shankar V.K.A., Subramaniam U., Elavarasan R.M., Raju K., Shanmugam P., **2021**, *Sensorless parameter estimation of VFD based cascade centrifugal pumping system using automatic pump curve adaption method*, Energy Reports, 7, 453-466, https://doi.org/10.1016/j.egyr.2021.01.002,
https://www.sciencedirect.com/science/article/pii/S235248472 1000032

113. **[Shi, 2013]**
Shi Y., **2013**, *Pump controller design for variable primary flow configuration systems*, MSc Thesis, Architectural Engineering – Dissertations and Student Research, 25, University of Nebraska, Lincoln, USA, https://digitalcommons.unl.edu/archengdiss/25/

114. **[Sloteman, 2007]**
Sloteman D.P., **2007**, *Cavitation in high energy pumps – Detection and assessment of damage potential*, Proceedings 23rd International Pump Users Symposium, 29-38, Texas A&M University, Turbomachinery Laboratories, https://doi.org/10.21423/R1VH53, http://oaktrust.library.tamu.edu/bitstream/handle/1969.1/163945/ch06-sloteman.pdf?sequence=1&isAllowed=y

115. **[Sreedhar et al, 2017]**
Sreedhar B.K., Albert S.K., Pandit A.B., **2017**, *Cavitation damage: Theory and measurements – A review*, Wear, volumes 372-373, 177-196

116. **[Swamee & Jain, 1976]**

Swamee P.K., Jain A. K., **1976**, *Explicit equations for pipe flow problems*, Journal of Hydraulic Engineering Division, 102(5), 657-664

117. **[Swamee & Sharma, 2008]**
Swamee P.K., Sharma A. K., **2008**, *Design of water supply pipe networks*, Wiley-Interscience, John Wiley & Sons Inc., New Jersey

118. **[Świętochowska & Bartkowska, 2022]**
Świętochowska M., Izabela Bartkowska I., **2022**, *Optimization of energy consumption in the pumping station supplying two zones of the water supply system*, Energies, 15(1), 310; https://doi.org/10.3390/en15010310

119. **[Tanyimboh & Templeman, 2004]**
Tanyimboh T.T., Templeman A.B., **2004**, *A new nodal outflow function for water distribution networks*, Proceedings 4th International Conf. Engineering Computational Technology, B.H.V. Topping, C.A. Mota Soares (eds.), Civil-Comp Press, Stirling, UK, paper 64

120. **[Thornton & Lambert, 2006]**
Thornton J., Lambert A., **2006**, *Managing pressures to reduce new breaks*, IWA Water21, December, 24-26

121. **[Todini, 2011]**
Todini E., **2011**, *Extending the global gradient algorithm to unsteady flow extended period simulations of water distribution systems*, Journal of Hydroinformatics, 13(2), 167-180

122. **[Todini et al, 2007]**
Todini E., Tryby M.E., Wu Z.Y., Walski T.M., **2007**, *Direct computation of variable speed pumps for water distribution system analysis*, in *Water Management Challenges in Global Change*, B. Ulanicki, K. Vairavamoorthy, D. Butler, P.L.M. Bounds, F.A. Memon (eds.), Taylor and Francis, Balkema, 411-418

123. **[Trifunović, 2006]**
Trifunović N., **2006**, *Introduction to urban water distribution*, Taylor & Francis Group, London, UK

124. **[Van Bennekom et al, 2001]**
Van Bennekom A., Berndt F., Rassool M.N., **2001**, *Pump impeller failures – a compendium of case studies*, Engineering Failure Analysis, 8, 145-156

125. **[Zhang L. & Zhuan, 2019]**
Zhang L., Zhuan X., **2019**, *Optimization on the VFDs' operation for pump units*, Water Resources Management, 33, 355-368, https://doi.org/10.1007/s11269-018-2106-2

126. **[Zhang Z. et al, 2020]**
Zhang Z., Liu H., Wang Y., **2020,** *Experimental and numerical study on the free surface vortex of a mixed flow pump device model*, Journal of Physics: Conference Series, vol. 1600, 012082, doi:10.1088/1742-6596/1600/1/012082

127. **[Wagner et al, 1988]**
Wagner J.M., Shamir U., Marks D.H., **1988**, *Water distribution reliability: Simulation methods*, Journal of Water Resources Planning and Management, 114(3), 276-294

128. **[Wu et al, 2009]**

Wu Z.Y., Tryby M., Todini E., Walski T.M., **2009**, *Modeling variable-speed pump operations for target hydraulic characteristics*, Journal AWWA, https://doi.org/10.1002/j.1551-8833.2009.tb09823.x

Standards

129. **[ANSI 9.6.6., 2016]**
*** **ANSI/HI 9.6.6.-2016**, *American National Standard for rotodynamic pumps for pump piping*, American National Standards Institute, Inc., published by Hydraulic Institute, Parsippany, New Jersey, USA
130. **[IEC 62828-1, 2017]**
*** **IEC 62828-1:2017**, *Reference conditions and procedures for testing industrial and process measurement transmitters – Part 1: General procedures for all types of transmitters*, TC 65, Industrial-process measurement, control and automation/ SC 65B, Measurement and control devices
131. **[IEC 62828-2, 2017]**
*** **IEC 62828-2:2017**, *Reference conditions and procedures for testing industrial and process measurement transmitters – Part 2: Specific procedures for pressure transmitters*, TC 65/ SC 65B
132. **[ISO 4064-5, 2014]**
*** **ISO 4064-5:2014**, *Water meters for cold potable water and hot water – Part 5: Installation requirements*, ISO/TC 30, Measurement of fluid flow in closed conduits/ SC 7, Volume methods including water meters
133. **[ISO 5198, 1987]**
*** **ISO 5198:1987**, *Centrifugal, mixed flow and axial pumps – Code for hydraulic performance tests – Precision grade*, ISO/TC 115, Pumps
134. **[ISO 5199, 2002]**
*** **EN ISO 5199:2002**, *Technical specifications for centrifugal pumps- Class II*, second edition, ISO/TC 115, Pumps/ SC 1, Dimensions and technical specifications of pumps
135. **[ISO 9905, 1998]**
*** **BS EN ISO 9905:1998,** *Technical specifications for centrifugal pumps – Class I*, BSI, ISO/TC 115/ SC 1
136. **[ISO 9906, 2012]**
*** **ISO 9906:2012**, *Rotodynamic pumps – Hydraulic performance acceptance tests – Grades 1, 2 and 3*, ISO/TC 115, Pumps/ SC 2, Methods of measurement and testing
137. **[ISO 9908, 1993]**
*** **ISO 9908:1993**, *Technical specifications for centrifugal pumps – Class III*, ISO/TC 115/ SC 1
138. **[ISO 10816-3, 2009]**
*** **ISO 10816-3:2009**, *Mechanical vibration – Evaluation of machine vibration by measurements on non-rotating parts – Part 3: Industrial machines with nominal power above 15 kW and nominal speeds between 120 r/min and 15000 r/min when measured in situ*, ISO/TC 108, Mechanical vibration, shock and condition monitoring/ SC 2,

Measurement and evaluation of mechanical vibration and shock as applied to machines, vehicles and structures

139. **[ISO 20816-1, 2016]**
*** **ISO 20816-1:2016,** *Mechanical vibration – Measurement and evaluation of machine vibration – Part 1: General guidelines***,** ISO/TC 108/ SC 2

140. **[NML 003-05, 2005]**
*** **NML 003-05**, 1 iunie **2005**, *Norma de metrologie legală "Contoare de apă"*, Biroul Român de Metrologie Legală [Monitorul Oficial, partea I, 664 bis, 26.07.2005]

141. **[SR 1343-1, 2006]**
*** **SR 1343-1:2006**, *Alimentări cu apă – Determinarea cantităţilor de apă potabilă pentru localităţi urbane şi rurale*, Asociația de Standardizare din România (ASRO)

142. **[STAS 8804/8-1992]**
*** **STAS 8804/8-1992**, *Fitinguri din oțel nealiat și aliat, pentru sudare cap la cap. Reducții – Dimensiuni*, ASRO, http://www.uprucctr.com/pdf/13.pdf

Brochures / technical books & equipment / software user manuals

143. **[Aversa – DP Pumps, 2019]**
*** **Aversa – DP Pumps**, **2019**, *Products range/ Double suction pumps/ NDS SIRET*, Aversa – DP Pumps s.r.l., România, http://aversadppumps.com/index.php/productslist/double-suction-pumps/22-nds-siret

144. **[Bmeters, 2021a]**
*** **Bmeters**, **2021**, *REED pulse emitter devices (GSD8)*, http://www.watergas.it/grk_files/uploads/b_meters/downloads/sistemi_lettura_remoto_bmeters.pdf

145. **[Bmeters, 2021b]**
*** **Bmeters**, **2021**, *Water meters*, Bmeters Srl, Italy, https://www.bmeters.com/en/products/gmb-i/

146. **[Danfoss, 2012]**
*** **Danfoss**, **2012**, *VLT® Micro Drive FC 51 Operating Instructions*, https://www.danfoss.com/en/about-danfoss/our-businesses/drives/

147. **[DP Pumps, 2012]**
*** **DP Pumps**, **2012**, *Hydro-Unit Utility Line – Installation and operating instructions. Series HU Utility MC(MF): HU-2-DPVME6/4-B-DPC-DOL*, The Netherlands, https://www.dp-pumps.com/image/file/Installation%20&%20operating%20instructions%20Hydro-Unit%20Utility%20Line.pdf

148. **[DP Pumps, 2013a]**
*** **DP Pumps**, **2013**, *Motor specifications – Motor DMC 0.37kW 230/400V 2P 71B IP55 Pos. 800*, The Netherlands

149. **[DP Pumps, 2013b]**
*** **DP Pumps**, **2013**, *Pump technical specifications, hydraulic performance, dimensions – Vertical centrifugal pump, suction and discharge connections in-line: DPV 2/3 B~Oval G 1~0.37kW 230/400V~50Hz 2P~IEC 71B~~Fixed Ca SiC EPDM*, The Netherlands

150. **[Flowserve, 2016]**

*** **Flowserve, 2016**, *Worthington LNN, LNNV and LNNC centrifugal pumps – User instructions (Installation. Operation. Maintenance)*, https://www.flowserve.com/sites/default/files/2016-07/71569074-e.pdf

151. **[FLYGT, 2017]**

*** **FLYGT**, **2017**, *Pump cavitation and how to avoid it* (white paper), Cavitation, June 2017, Xylem Inc., https://www.xylem.com/siteassets/support/tekniska-rapporter/white-papers-pdf/cavitation-white-paper.pdf

152. **[KSB, 2015]**

*** **KSB**, **2015**, *Data sheet, Performance curve, Installation plan & Connection plan – Low-pressure centrifugal pump Etanorm, ETN 125-100-315 GGXAA10GD616002B*, Multigama Tech srl, București – reprezentanţa KSB în România şi Republica Moldova

153. **[KSB, 2016]**

*** **KSB**, **2016**, *Data sheet, Performance curve, Installation plan & Connection plan – Omega V 300-300 B GB P M*, Multigama Tech srl, București – reprezentanţa KSB în România şi Republica Moldova

154. **[MATLAB, 2022]**

*** **MATLAB**, **2022**, *Documentation/ Optimization toolbox/ Systems of nonlinear equations/ fsolve*, The MathWorks, https://www.mathworks.com/help/optim/ug/fsolve.html

155. **[Mitsubishi Electric, 2021]**

*** **Mitsubishi Electric**, **2021**, *Drive products/ Inverters-FREQROL*, https://www.mitsubishielectric.com/fa/products/drv/inv/index.html

156. **[PompeMC, 2018]**

*** **PompeMC Trading Plus**, **2018**, *Ce este un convertizor de frecvență sau un soft starter*, https://pompemc.ro/ce-este-un-convertizor-de-frecventa-sau-soft-starter/

157. **[Pressure Loss, 2022]**

*** **Coastal Pipco**, **2022**, *Pressure loss through water meters*, Oxnard, California, USA, https://www.coastalpipco.com/i/chart21.pdf

158. **[Seimeni, 2015]**

*** **Documentație tehnică** – *Sistem irigații Seimenii Mici, județul Constanța*, **2015**, Proiect[2] nr. 255/01.13, ALLPLAN Proiect srl, Constanța

159. **[VALROM Industrie, 2018]**

*** **VALROM Industrie**, **2018**, *Carte tehnică – Sistem de instalații sanitare și de încălzire (PPR)*, https://valrom.ro/wp-content/uploads/2021/02/Carte_tehnica_RandomKIT_2018_RO.pdf

160. **[VMI, 2011]**

*** **VMI**, **2011**, *Viber X1™, Manualul utilizatorului – Vibrometru portabil, ver. 1.4*, Vibration Measurement Instruments – VMI International AB, Linköping, Sweden

161. **[*Water Facility Design Guidelines*, 2021]**

[4] Beneficiary Land & Buildings Real Estate, Bucharest. The documentation is confidential and has been provided by VALROM Industrie srl

*** **Water Facility Design Guidelines**, **2021**, in *Guidelines and Standards Book*, City of San Diego – Public Utilities Department, Sand Diego, CA, USA, https://www.sandiego.gov/sites/default/files/legacy/water/pdf/cip/book2.pdf